

University of Nottingham
UK | CHINA | MALAYSIA

Establishing and Utilising *In Vitro* Lung Models to Demonstrate Peptide Mediated Non-Viral Delivery

Lauren J. Smith

Thesis submitted to the University of Nottingham for the Degree of Doctor of Philosophy

March 2022

Word Count:43704

Abstract

Despite their success as gene therapy delivery systems, viral vectors have some unresolved issues; pathogenicity, immunogenicity, and off target effects can be detrimental and sometimes even oncogenic. Commercialised vectors can also still come with a higher price point.

An alternative method that might aid in reducing both the negative biological effects and could prove more cost effective is non-viral gene therapy delivery systems. Many are utilised for a variety of diseases currently in research, with varying levels of success. The main focus of this project was to investigate the efficiency of a peptide-based delivery system mediated by the process of Glycosaminoglycan enhanced transduction (GET). This cell penetrating peptide (cell penetrating peptide) contains enhanced peptide domains that allow for interaction with heparan sulphate cell surface sugars, aiding in cell entry. The overall molecule charge also allows binding with double stranded DNA (dsDNA), compacting into a nanoparticle (NP) which can enter the nucleus and allow for transient expression of chosen genes on modified plasmids.

This PhD project combines the novel Glycosaminoglycan enhanced transduction peptide non-viral delivery system (GET system) with two *in vitro* lung based models, in an attempt to test non-viral delivery without excessive animal use, and to determine this particular non-viral delivery methods efficiency *in vitro*. The lung models used were murine precision cut lung slices (PCLS), which utilises *ex vivo* tissue; and human cell Air liquid interface (ALI)

cultures, which utilise lung cell lines *in vitro*. The lung was focussed on due to the potential for non-viral delivery to this organ, particularly in the context of genetic lung disorders such as Cystic Fibrosis (CF).

Within this project, peptide mediated delivery of reporter and enhanced luciferase plasmids to an *in vitro* lung model was demonstrated using the GET non-viral system; air liquid Interface cultures were also attempted to further demonstrate peptide mediated non-viral delivery in a human relevant in vitro model.

The demonstration of GET non-viral delivery to an *in vitro* lung model could potentially provide an alternative non-viral methods in the future, for correction of mutations such as the ΔF508 mutation found in 70% of cystic fibrosis patients, or in any other genetic diseases where the mutation is monogenic.
Adding to the body of research on non-viral delivery methods is key to improving non-viral delivery systems; further research can potentially provide more useful information as to the genetic diseases they may be utilised to successfully treat.

COVID-19 Impact Statement

From March 2020, Due to the COVID-19 Pandemic, the University of Nottingham labs closed. I was 6 months into the second year of my PhD, and I had to discard everything I was working on and stay home.

Delayed return post lockdown

I was allowed to return to the Biodiscovery institute (BDI) around mid-September 2020. I lost around 7 months of experimental hands-on time within the laboratory; I believe that due to the time in which my PhD this occurred, in the second year of my studies, this affected the volume of results I was able to collect. I tried my best to mitigate this by planning experiments in advance and being selective about which experiments I did to achieve the best outputs and create figures for my final write-up. I also considered earlier first year work I had already completed and decided to include some of this work.

No Desk or seated Access

Upon initial return to work, restrictions on seated areas affected general ability to carry out work; individuals who worked within BDI were not allowed to use their previous desk space and were informed to only come in for necessary lab work. Whilst understandable due to the situation, this made any experiment with a timecourse or larger gaps difficult. I tried my best to mitigate this by carrying out a large amount of my data processing and desk work at home.

Unable to obtain relevant training

Before COVID-19 first lockdown, I had arranged for training at the NMRC on SEM and was hoping to organise other types of training to help me learn techniques to aid in the completion of my thesis. Unfortunately, this situation prevented me from accessing the NMRC as a new user, and I never got to learn this technique or use any equipment. It was also difficult to learn any new techniques in the lab and interface directly with individuals. Unfortunately, this was something I was unable to mitigate, and I was not able to include any SEM work within my PhD. When some restrictions were lifted, I was able to be trained and inducted onto the SLIM department confocal microscope, and I was able to obtain some immunofluorescence data.

No initial weekend access

Initially no weekend access was permitted to BDI, and it took some time for this policy to be changed. This made my cell culture and cell experimentation difficult, as I would not normally go further than a weekend without observing samples and changing media due to the small volumes in the experiments. Even when allowed in for weekend work, a new system meant individuals had to reapply for weekend access every single week by a set time, so missing this deadline meant access was revoked for that weekend. I tried my best to mitigate this by checking my samples daily and carrying out regular media changes within the week and making sure I always reapplied for my access every week within good time.

Availability of bookable spaces

Whilst BDI tried to accommodate all individuals needing to work in the building outside of lab time by making desk and office spaces bookable from around November/December 2021, social distancing and taped off areas meant there wasn't enough space for everyone to use when needed. I found it difficult to find anywhere to book to use in between experiments the majority of the time, as many individuals would simply block book whatever space they already had. This made general working within the BDI as a building difficult. I tried my best to mitigate this by carrying out the majority of my writing and data processing from home.

Reduced capacity Lab spaces

The main lab in which I carried out my work, like many spaces in university, had to run at reduced capacity. A lab that had 7 hoods was reduced to 3 initially, with room capacity also restricted to 3/4 people at any one time. This was eventually lifted to 4 hoods, however the division I was a part of had multiple lab groups and many members, so many individuals needed these hoods. This made getting lab work done difficult for everyone. I tried my best to mitigate this by working later in the day when the lab was in less demand (after 4-5pm).

Plasticware and consumable shortages

There were issues with obtaining the right consumables, particularly plasticware. On many occasions, stocks of multiple types of plasticware were missing. Suppliers and internal stores were usually unable to give indication to

end users when there may be any new consumables, making experimental planning difficult. I tried my best to mitigate this by checking what plasticware was available before a new experiment was started, and within our lab group we began to re-use white luminescence plates for the platereader after soaking and disinfection.

Broken equipment within Division

The plate reader had ongoing issues after we returned to work from September 2020. Around early/mid 2021, it eventually became unusable and was taken out of use awaiting an engineer to come and resolve the issue. The issue was still not completely resolved by the time I left. whilst the division was at one point provided with use of some alternate plate readers that belonged to another group in a different building, this still had some impact on my experimental planning and general ability to obtain results that relied on plate reading use during this time. I found this difficult to mitigate due to the timing, as I did not have much time left until my funding ended in September 2021.

I understand that the University has had to react to an ever changing and often confusing situation with little to no notice, which has been difficult for everyone, staff and students alike. I have tried my best to adapt to the ongoing situation and mitigate difficulties to complete my work as best I could. I hope, given the circumstances, the impact COVID and its ongoing effects have had on my PhD will be considered when my work is examined.

Acknowledgments

I would like to formally acknowledge The EPSRC and MRC funding councils, as the funders of this PhD program. I would also like to formally acknowledge The Regenerative Medicine CDT (Centre for Doctoral Training), for accepting me as a student onto their program in 2017.

I formally acknowledge my Supervisory team; Prof. Felicity Rose, Dr. Amanda Tatler, Dr. James Dixon.

I would also like to acknowledge old friends and mentors; my first supervisor, Dr. Simon Streeter. He was the first person I told when I got my PhD place, and the first person I always went to for help and guidance; his support knew no bounds. Equally, Dr. Jonathan Chamberlain, a model PhD student and source of knowledge during my undergraduate and master's projects, whose thesis set the bar I aspired to reach with my own. I would not be the researcher I am today without these mentors.

I would like to thank my uncle, Dr. Rodney Smith; an established scientist, who gave me that first opportunity to dip my toe into the scientific world - for which I will be forever grateful.

I would like to acknowledge and thank my new team lead and colleague in my new full time role as an Organ on chip scientist at UKHSA; Dr. Kevin Bewley, and Dr. Naomi Coombes. They have watched me write up around my full time job, and have been empathetic, understanding, and supportive throughout this process. They have been great colleagues since I started in October 2021, and I really appreciate the support they have shown me.

And to my family;

To my other half, Matthias Mayer. My biggest fan, my best friend. I know I would have given up long ago on this endeavour, if not for you being here with me. Thank you for never giving up on me. Here's to moving on to bigger and better things, always together.

To my brother, Will, who despite being hundreds or thousands of miles away in the employ of her majesty's Royal Navy, always seems to find the time to call me and see how I am (and to ask if I'm a doctor yet...)

To my Mum and Dad, Mandy and Laurence, who spent my life telling me 'You can' and 'you will'. Their love and support has always been limitless, and despite how much I struggled with this PhD, they always believed I could do it, even when I did not.

This has been an arduous and almost impossible journey at times, far more difficult than I ever expected. My family, your pride in me has always motivated me to keep trying and keep going. Whether you read this whole thing, or this one page, it doesn't matter. I hope at least I did you proud. Thank you.

CONTENTS

1. Chapter 1: Introduction 1

1.1 Gene therapy 1

1.2 Development of Gene Therapies 1

1.2.1 Current state of genetic therapy testing 4

1.2.2 Current therapy delivery approaches 6

1.3 Methods of Gene Delivery 10

1.3.1 Viral based Systems 10

1.3.2 Adenoviruses 13

1.3.3 Adeno-associated Viruses (AAV) 14

1.3.4 Lentiviruses 16

1.4 Non-viral based Systems 20

1.4.1 Lipids 20

1.4.2 Polymers 21

1.4.3 Dendrimers 22

1.4.4 Nanoparticle systems 24

1.4.4.1 Lipid nanoparticles 25

1.4.5 Cell Penetrating Peptides 26

1.4.5.1 Glycosaminoglycan-binding Enhanced Transduction (GET) 27

1.5 Potential Models for lung genetic therapy testing 31

1.5.1 Lung ex vivo Models 32

1.5.1.1 PCLS 32

1.5.2 Lung in vitro models 35

1.5.2.1 Air liquid interface model (ALI) 35

1.5.2.2 Lung on Chip (LOC) 38

1.5.2.3 Lung Spheroid and Organoid Cultures 41

1.6 Aims and Objectives 43

2. Chapter 2: Materials and Methods 45

2.1 Immortalised Human Bronchial Epithelial cells (iHBECs) 45

2.1.1 Thawing 45

2.1.2 Media preparation 46
2.1.2.1 KSFM 46
2.1.2.2 PneumaCult™ 46
2.1.3 iHBEC culture 47
2.1.4 Transwell culture at the air liquid interface (ALI) 48
2.1.5 Transepithelial/Transendothelial electrical resistance (TEER) 51
2.1.6 Immunofluorescence 53
2.1.6.1 Antibodies 53
2.1.6.2 Transwell preparation and staining 55
2.1.6.3 Confocal microscopy 57
2.1.7 Plate preparation for bacterial culture and vector generation 57
2.1.8 Bacterial Transformation 58
2.1.9 Vector preparation 58
2.1.9.1 Vector sequences 59
2.1.10 Transwell culture transfection 62
2.2 Precision cut lung slices (PCLS) 62
2.2.1 Animals 62
2.2.2 Agarose preparation 63
2.2.3 PCLS Generation & storage 63
2.2.4 General culture 66
2.2.5 PCLS Assay timeline 66
2.2.6 PCLS Viability assay 67
2.2.7 PCLS Transfections 69
2.2.7.1 Luciferase expression assay for transfection efficiency 69
2.2.7.2 Centrifugation of transfections 70
2.2.8 LiveDead assay 70
2.2.9 Wax embedding of samples 71
2.2.10 Microtome of wax embedded samples 71
2.2.11 Immunohistochemistry 71
2.2.12 Statistical Methods 72
2.2.13 Gelatin PCLS 72

2.2.13.1 Gelatin preparation 72
2.2.13.2 Gelatin perfusion 73
2.2.13.3 Storage 73
2.2.13.4 Thawing and General culture 73
2.2.13.5 LiveDead assay 74
3. Chapter 3: Utilising Precision Cut Lung Slices (PCLS) as an in vitro model in which to demonstrate non -viral delivery 75
3.1 Introduction 75
3.2 Demonstration of transfection in PCLS 76
3.3 PCLS viability compared pre and post transfection 78
3.4 Visual qualitative analysis of PCLS viability post transfection 81
3.5 Utilisation of enhanced plasmid 85
3.5.1 Variation of Plasmid Concentration 85
3.5.2 Serial Delivery 89
3.6 Use of serum in PCLS culture 93
3.6.1 Effects of absence of serum from culture 93
3.6.2 Effects of selective presence of serum 98
3.7 Physical force to aid transfection permeation 102
3.8 Discussion 104
3.8.1 Transfection efficiency within the model 104
3.8.2 Viability of tissues 106
3.8.3 Effect of variation in plasmid concentration 108
3.8.4 Effect of serial delivery 110
3.8.5 Significance of Serum in PCLS culture 112
3.8.5.1 Effect of Selective use of serum 114
3.8.6 Effect of Physical force on transfection and expression 116
4. Chapter 4: Investigating Gelatin as an alternate perfusion material to improve the in vitro PCLS Model 119
4.1 Introduction 119
4.1.1 Gelatin PCLS behaviour in culture 121
4.1.2 Livedead assay for visual qualitative analysis 125

4.1.3 Visual confirmation of slice reduction pre and post incubation 127

4.1.4 Viability and expression from initial transfection experiments 127

4.2 Discussion 131

4.2.1 Effect on temperature changes on Gelatin PCLS integrity 131

4.2.2 Viability of Gelatin PCLS post structure loss 133

4.2.3 Initial investigation of transfective ability comparative to agarose PCLS and agarose-based conditions 134

5. Chapter 5: Establishing an in vitro Air Liquid Interface model (ALI) for demonstration of non-viral delivery 136

5.1 Introduction 136

5.2 Initial transfection of iHBECs 137

5.3 Initial transwell cultures 140

5.3.1 Transepithelial/Transendothelial electrical resistance (TEER) of initial layers 142

5.3.2 Immunofluorescence with initial markers 145

5.3.2.1 P63 for basal cell identification 145

5.3.2.2 αTubulin for ciliated cell identification 145

5.3.2.3 Comparative timepoints to determine presence of specific cell types 149

5.3.2.4 Immunofluorescence confirmation with Confocal Microscopy 151

5.3.3 Transepithelial/Transendothelial electrical resistance (TEER) of adapted cultures 153

5.3.3.1 Collagen coated transwells comparative to non-collagen coated transwells 153

..... 154

5.3.4 Immunofluorescence of adapted cultures 155

5.3.4.1 ZO-1 for Identification of Tight junction formation 155

5.3.4.2 MUC5AC for identification of Mucin secretion 155

5.4 Initial transfection of Transwell cultures 159

5.5 Discussion 161

5.5.1 Cell type and cell population age 162

5.5.2 Initial transwell Iterations 164

5.5.3 TEER readings for confirmation of layer development 164

5.5.3.1 Comparisons of non-coated and collagen coated plasticware..... 165
5.5.4 Choice of markers for immunofluorescence..... 166
5.5.5 Initial GET peptide delivery to potentially established ALI cultures ... 171
6. Conclusions and Future Outlook 172
7. *References* 177

List of Abbreviations

HIV – Human Immunodeficiency virus

ADA-SCID – Adenosine deaminase - severe combined immunodeficiency

AAV – Adeno-Associated Virus

ZFN – Zinc Finger Nuclease

CRISPR - clustered regularly interspaced short palindromic repeats

Cas9 - CRISPR-associated protein 9

DNA – Deoxyribonucleic Acid

RNA – Ribonucleic Acid

Ds, ds – double stranded

Ss, ss – single stranded

CAR-T – Chimeric Antigen Receptor T-cell Therapy

NILV- Non-Integrating Lentiviral Vector

LV – Lentivirus

NP - Nanoparticle

LNPs – Lipid Nanoparticles

MNPs – Magnetic nanoparticles

GET – Glycosaminoglycan enhanced transduction

CF – Cystic Fibrosis

CFTR - Cystic fibrosis transmembrane conductance regulator

UKCFGTC - UK Cystic Fibrosis Gene Therapy Consortium

CPP – Cell Penetrating Peptide

PTD – peptide transduction Domain

PEI – Polyethyleneimine

LOC – Lung on Chip

OoaC – Organ on a Chip

GFP – Green Fluorescent Protein

PCLS – Precision Cut Lung Slices

HBSS – Hanks Balanced Salt Solution

PBS – Phosphate Buffered Saline

DMEM – Dulbecco's Modified Eagle Medium

KSFM – Keratinocyte Serum Free Medium

EX-BM – Expansion Basal Medium

ALI – BM – Air Liquid Interface Basal Medium

ALI – Air Liquid Interface

PET Membrane – Polyethylene terephthalate Membrane

SFM – Serum Free Medium

GM – Growth Medium

iHBEC – immortalised Human Bronchial Epithelial cells

TEER – Transepithelial/Transendothelial electrical resistance

IF – Immunofluorescence

IHC – Immunohistochemistry

H&E – Haemotoxylin and Eosin

List of Tables

Table 1 *Dilutions of Antibodies used throughout Immunofluorescence (IF) experiments*

List of Figures

Figure 1.1	*Schematic of Zinc Finger Nucleases*
Figure 1.2	*Schematic of CRISPR/Cas9*
Figure 1.3	*Outline of the Viral life cycle*
Figure 1.4	*GET peptide interaction with Plasmid DNA*
Figure 1.5	*Air Liquid Interface (ALI) culture*
Figure 1.6	*Lung-On-Chip (LOC) Model*
Figure 2.1	*Transwell culture at the Air Liquid Interface (ALI)*
Figure 2.2	*Transepithelial/Transendothelial electrical resistance (TEER)*
Figure 2.3	*Transwell preparation and staining*
Figure 2.4	*PMV-GLuc 2 Gaussia Luciferase plasmid map*
Figure 2.5	*Enhanced luciferase plasmid maps*
Figure 2.6	*Precision Cut Lung Slice (PCLS) Method of Generation and storage*
Figure 2.7	*PCLS Assay Timeline*
Figure 3.1	*Demonstration of Transfection and subsequent expression in PCLS*

Figure 3.2	*Demonstration of Viability in PCLS, up to 2 weeks post transfection*
Figure 3.3	*Livedead of PCLS before and after transfection*
Figure 3.4	*Haematoxylin and Eosin (H&E) staining of Untransfected and Transfected PCLS*
Figure 3.5	*Comparison of DNA plasmid concentration variation on Expression in PCLS*
Figure 3.6	*Viability of PCLS samples at differing plasmid concentrations over time*
Figure 3.7	*Expression profiles of PCLS Undergoing Serial Delivery every 2 days and every 3 days*
Figure 3.8	*Viability of PCLS samples undergoing serial delivery*
Figure 3.9	*Comparison of expression profiles of PCLS in Growth Media and Serum Free Media (SFM)*
Figure 3.10	*Comparison of Viability of PCLS in Growth Media (growth medium) and Serum Free Media (SFM)*
Figure 3.11	*Expression and Viability Profiles of Selective Serum use in PCLS Culture*
Figure 3.12	*Expression Profiles of Selective Serum use in PCLS Culture*
Figure 3.13	*Expression and Viability of PCLS with and without Centrifugation (RCF)*

Figure 4.1	*Gelatin PCLS pre and post incubation at 37ºC*
Figure 4.2	*Visible cell disaggregation post incubation of Gelatin PCLS*
Figure 4.3	*Livedead staining of Gelatin PCLS samples, 24 hours Post incubation*
Figure 4.4	*Appearance of Gelatin PCLS within transwells, pre and post incubation*
Figure 4.5	*Viability and expression profiles of Initial Gelatin PCLS comparative to agarose PCLS and varying agarose 'glue' conditions*
Figure 5.1	*Initial proof of transfection in iHBEC monolayers*
Figure 5.2	*Initial imaging of developing transwell samples*
Figure 5.3	*Initial TEER readings of early transwell samples*
Figure 5.4	*Initial Immunofluorescence using P63 Marker*
Figure 5.5	*Initial Immunofluorescence using αTubulin Marker*
Figure 5.6	*Comparative immunofluorescence over time using αTubulin*
Figure 5.7	*Attempt at visualisation of immunofluorescence of P63, αTubulin, and FOXI1 markers with Confocal Microscopy*
Figure 5.8	*TEER readings of Transwell samples after introduction of collagen coated transwells and Air liquid Interface media system*
Figure 5.9	*Immunofluorescence using ZO-1 Marker*

Figure 5.10 *Immunofluorescence using MUC5AC Marker*

Figure 5.11 *Initial Transfection attempt of iHBEC transwell cultures*

1. *Chapter 1: Introduction*

1.1 Gene therapy

Gene therapy is defined as ‘using genes to treat or prevent disease’. Genetic therapy and genetic engineering enables us to edit and alter the genetics of an organism, which allows for the development of tested gene therapies which can be used to treat a variety of genetic based disease states.

1.2 Development of Gene Therapies

Gene therapy, or transference of genetic material utilising a transfection mechanism, was first demonstrated in 1971, with the utilisation of irradiated herpes simplex virus to deliver a thymidine Kinase active gene to a Eukaryotic cell line (Munyon, Kraiselburd, Davis, & Mann, 1971), and correction of the genetic disorder Galactosemia in isolated patient human fibroblasts with bacteriophage transduction of a corrective gene (Merril, Geier, & Petricciani, 1971). Gene therapy was first described in the context of treatment for human genetic diseases in 1972 by Friedmann and Roblin (Freidmann & Roblin, 1972) and outlined the possibilities as well as the potential hazards of utilising such genetic manipulation in humans. From here, gene therapy research progressed to a multitude of animal studies throughout the 1980s, with both successful and unsuccessful studies carried out in humans; one unpublished small trial in 1980 involved 2 patients who

were treated with recombinant DNA for potential correction of beta Thalassemia, which was an issue at the time due to unethical practice (U.S. Congress, Office of Technology Assessment, 1984). Another later study in 1990 in which children with ADA-SCID, a severe combined immunodeficiency, were successfully treated using retroviral mediated gene transfer of the Adenosine Deaminase (ADA) gene. This study helped to demonstrate that gene corrections could be successfully integrated to produce gene expression, and patients had improved immunity and ADA expression that could still be observed up to 4 years post trial (Blaese, Culver, Miller, & French Anderson, 1996). However, transience of expression and presence of corrective genes in newly generated cells within patients still posed an issue.

The early 1990s saw the first cancer gene therapy, demonstrated initially in a rat Glioblastoma model that later progressed to a human gene therapy trial (Trojan, Johnson, Rudin, Ilan, & Tykocinski, 1993); (Trojan, et al., 2012). It was around this time that human gene therapy trials were focussed on severe combined immune deficiencies; treatments demonstrated some efficacy, using a variety of methods including retroviruses, genetically modified stem cells, and combination of both (Cavazzana-Calvo, 2000); (Aiuti, 2002). Issues arose in the early 2000s, as a minor number of treated patients in an SCID gene therapy clinical trial resulted in T lymphocyte proliferation, leading to a leukemic – like condition; however, in most other patients, they demonstrated successful genetic uptake in the short term (Hacein-Bey-Abina, 2003).

After unfortunate deaths in late 1990s gene therapy trials, such as the death of Jesse Gelsinger after administration of an Adeno-associated viral treatment (Thomas, Ehrhardt, & Kay, 2003), gene therapy was set back.

The 2000s saw some defining research demonstrated in animal models as opposed to human trials, including the first genetic correction of sickle cell disease in a transgenic mouse model (Pawliuk, 2001), targeting of brain tumours with non-viral DNA complexes, which enabled DNA to cross the blood brain barrier in rats (Zhang, Boado, & Pardridge, 2003), and lentiviral vector delivery of miRNAs in mice to stabilise gene transfer in immunocompetent mice (Brown, Venneri, Zingale, Sergi, & Naldini, 2006). Correction of red/green colour blindness was also demonstrated in primates, by utilising an AAV to deliver the functional Human form of the L-opsin gene (Mancuso, et al., 2009).

In the late 2000s, human clinical gene therapy trials demonstrated more ethical and successful outcomes, including delivery of lentiviral HIV-1 vector with a genetically modified CD4 T cell population to specifically target an HIV envelope protein (Levine, et al., 2006), treatment of metastatic melanoma utilising retroviral vector to confer a T cell receptor gene, which enabled lymphocyte populations in tumour recognition and targeting (Morgan, et al., 2006), and use of an AAV to deliver the functional Gene RPE65 to patients with Leber's congenital amaurosis (LCA), an early childhood disease which causes retinal degeneration and eventual blindness. A follow up study also

demonstrated not only safety in utilisation of an AAV, but effectiveness of treatment past 18 months (Vander, 2009); (Simonelli, et al., 2010).

1.2.1 Current state of genetic therapy testing

In the last decade, a multitude of research and clinical trials have come to a close, giving a much clearer picture of the success and longevity of potential gene therapy treatments. Disease states such as Beta Thalassemia (Cavazzana-Calvo, et al., 2010), Achromatopsia (Komáromy, et al., 2010), Cystic Fibrosis (Perry, Penny-Dimri, Aslam, Lee, & Southern, 2017), Hemophilia (Nathwani, et al., 2011), ADA-SCID, as well as a multitude of cancers, including Leukaemia (Porter, Levine, Kalos, Bagg, & June, 2011) have been investigated either with animal models or have been taken to full length human clinical trials. Larger scale efforts that focus on non-viral delivery agents include work by the UKCFGTC, who have focussed on non-viral gene therapy delivery to cystic fibrosis patients (Alton, et al., 2013).

Most significantly, the progression to human clinical trials that involve 'in body' gene editing, where patients are delivered a therapy that can edit and correct *in situ*, rather than a viral or non-viral system delivering the genetic material. This has benefit over other gene therapies as transience of expression no longer becomes an issue, as genome edits would ensure all new cells had the corrected genetics. However, there is still some small risk of unwanted off target effects.

These types of treatments usually contain a Zinc Finger Nuclease (ZFN) (Figure 1.1) or CRISPR/Cas9 component (Figure 1.2), to allow for intricate and highly accurate editing, which can minimalize the risks associated with other treatments, such as viral based gene therapy. Two currently in progress clinical trials of this nature include a small-scale trial utilising CRISPR for correction of Leber Congenital Amaurosis (Editas Medicine, Inc., 2019), and another small-scale trial utilising ZFNs for correction of Hunter Syndrome (Sangamo Therapeutics, 2017).

Another key gene therapy advancement is the use of chimeric antigen receptor T cells (CAR-T). Useful in cancer research and immunotherapy work, the process involves genetically engineering the T cells of a patient with chimeric antigen receptors that allow for both antigen-binding and T cell activation. The result is a T cell population with the ability to internally target cancerous cells (Kuwana, et al., 1987). CAR-T can utilise either patients' own T cell population (autologous) or can come from a healthy donor (allogenic). Integration of the CAR gene is achieved using viral methods such as γ-retroviral and lentiviral vectors (Zhang, Zhao, & Huang, 2020); (Jin, et al., 2016) or by gene editing with CRISPR/Cas9 (Eyquem, et al., 2017). Due to the use of immune cells, CAR-T has proven most effective against blood borne and immune based cancers, and even in some immune disorders (Mougiakakos, et al., 2021). However, solid tissue tumours have proven more difficult to target (Lim & June, 2017). Clinical trial data has demonstrated use of CAR-T to target specific leukaemia's (Lee, et al., 2015); (Jacoby, et al., 2022), multiple lymphomas (Makita, Yoshimura, & Tobinai,

2017); (Shah, et al., 2020), and myeloma (Alabanza, et al., 2022); (Cohen, et al., 2022).

1.2.2 Current therapy delivery approaches

More than one method of delivery exists for current gene therapies. The key difference in gene therapy approaches is whether the manipulation takes place *ex vivo* or *in vivo*; in vivo involves direct intracellular targeting within the patient, whereas *ex vivo* involves removal of the material, usually cells, from the patient (or a donor) to allow for editing and manipulation. After this, the edited cells are used to treat the patient and become the delivered therapy (Keeler, ElMallah, & Flotte, 2017); (Tajer, Pike-Overzet, Sagrario, Havenga, & Staal, 2019).

The delivery method is chosen dependent on the specific physical area or disease being targeted. More exposed organs such as the eye and skeletal muscle can be delivered to *in vivo* as they are easier to reach, and the focus of the therapy is on a single organ or system. More difficult to reach or more complex systems, such as the lymphatic or immune systems that circulate throughout the body, are usually edited *ex vivo* with removal of the patients stem cells, B- or T-cells. This method is particularly useful in cases of lymphatic or blood bound cancers such as leukaemia (Kalos, et al., 2011); (Kochenderfer, et al., 2010).

A notable *ex vivo* method is CAR-T therapy (Chimeric antigen receptor T cell therapy), which involves removing a patients T-Cells (or taking these cells from a suitable donor) and editing them to include a synthetic receptor. The receptor then allows the T-Cells to recognize and target tumour cells (Mhaidly & Verhoeyen, 2019). Generation of CAR-T as a therapy, despite its effectiveness, has both a complex production process and is expensive. Recently however, CAR-T has been implemented using multiple *in vivo* methods. Utilising synthesised nanocarriers or viral vectors for delivery of gene editing

tools and CAR genes can allow for in situ generation of autologous CAR-T cells inside the host (Xin, et al., 2022); (Huckaby, et al., 2021); (Parayath, Stephan, Koehne, Nelson, & Stephan, 2020).

There are currently many approved cellular gene therapy products which are ready for use in patients; these products utilise both *ex vivo* and *in vivo* delivery approaches. Some of the applications of approved products include direct treatment of mutation associated retinal dystrophy (FDA, 2022); (Irigoyen, et al., 2022), and repair of cartilage knee defects using autologous chondrocytes cultured on collagen membranes to generate a cellularised scaffold (FDA, 2021); (Carey, Remmers, & Flanigan, 2020).

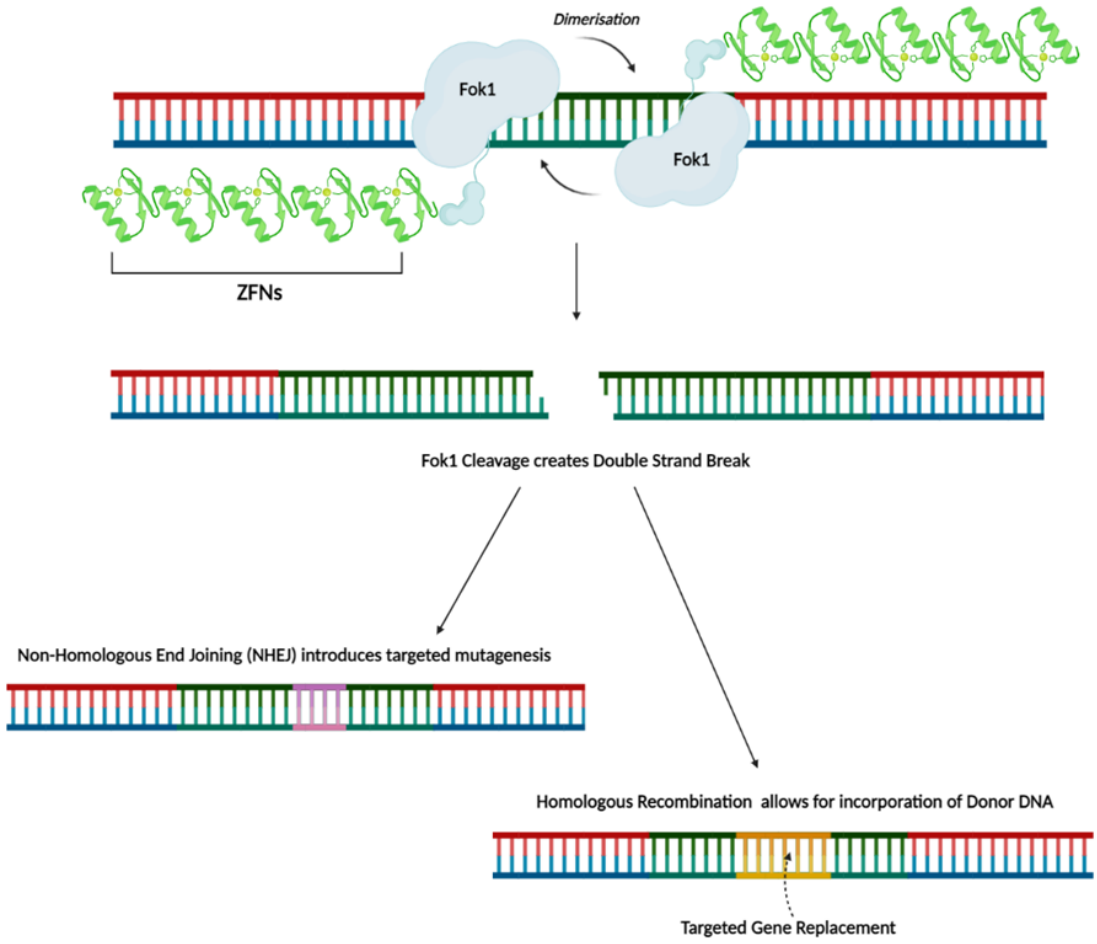


Figure 1.1 Schematic of Zinc Finger Nucleases *Zinc Finger Nucleases are composed of a DNA binding domain (Zinc Finger Repeats) and a catalytic domain (Fok1). ZFNs can bind to DNA, dependent on their prespecified target sequence. Dimerisation of the Fok1 Domains cleaves DNA, resulting in a double stranded break. This allows for either non-Homologous end joining to occur, introducing targeted mutations, or specified Donor DNA to be incorporated at the break during homologous recombination. This allows for highly specific genetic editing to be carried out. Figure rendered in Biorender.*

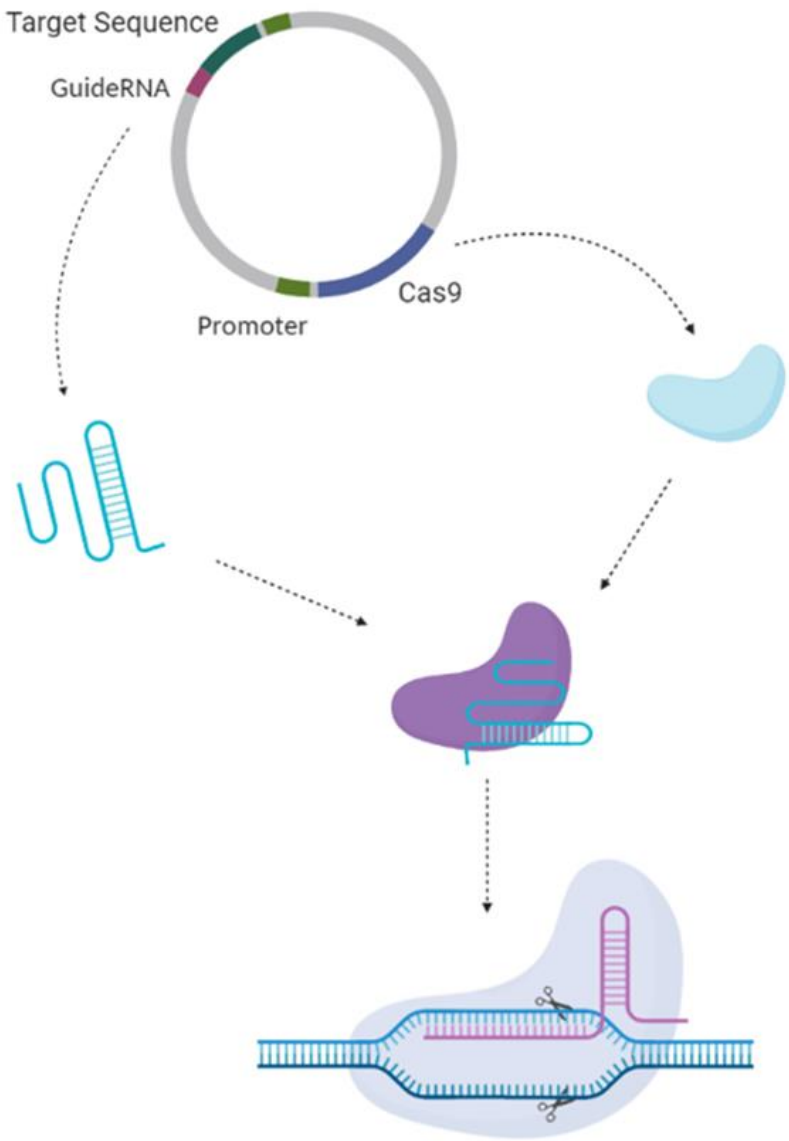


Figure 1.2 Schematic of CRISPR/Cas9 *An engineered expression plasmid containing the target sequence can be transfected into any chosen cell type. Inactive Cas9 is transcribed and translated as the single stranded GuideRNA is transcribed. Binding of GuideRNA and Inactive Cas9 induces conformational changes to form Active Cas9, which identifies and binds the targeted sequence using its protospacer adjacent motif (PAM) sequence.Figure rendered in Biorender.*

1.3 Methods of Gene Delivery

Genetic information can reach the nucleus in a variety of ways, which can be broadly classified into viral and non-viral; viral systems utilise specific viral mechanisms to effectively deliver the required vector, with non-viral systems instead utilising chemical properties to escort the vector across the cell membrane. Whilst being efficient, viral systems have the disadvantage of potential off target effects, which can lead to development of oncogene activation and cancer formation, alongside other health complications (Thomas, Ehrhardt, & Kay, 2003); (Baum, et al., 2003). Although in some cases not as effective, non-viral systems avoid this issue entirely. However, both viral and non-viral systems have proven their efficacy in a multitude of research, with some even demonstrating success at clinical trial level.

1.3.1 Viral based Systems

Viral based systems include any delivery system that involves the use of part of or a whole virus. Viral systems can be particularly effective as they take advantage of the viral replication cycle, and when modified to include the required gene, can ensure successful entry of the genetic material into the host cells (Dimmock, Easton, & Leppard, 2016). All natural viral infections are dependent on successful entry to host cells, followed by replication utilising host cell machinery, and shedding of new virus to infect surrounding cells (Figure 1.3). Some viruses can also become latent within a cell and reactivate infection after initial entry. Viral infections can be either lytic or

lysogenic. In lytic infection, replication is rapid, and host cells are lysed when the cycle is complete to enable viruses to enter and infect other host cells (Dimmock, Easton, & Leppard, 2016). In lysogenic infection, viruses can be present without harming the host cells for many years, integrating their DNA directly into the host cell DNA and only replicating as new host cells are formed. They can also be triggered to release virions from the host cell to aid in further infection (Howard-Varona, Hargreaves, Abedon, & Sullivan, 2017). Many natural viruses have been utilised for scientific research, and at the clinical trial level as potential gene therapy vectors.

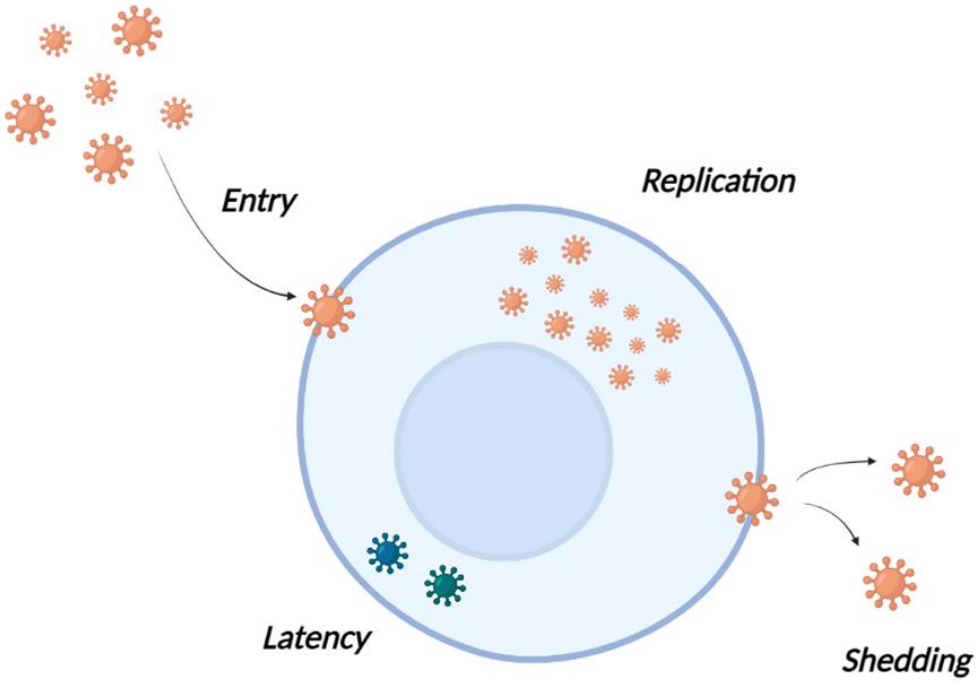


Figure 1.3 Outline of the Viral life cycle *The process of viral invasion of host cells involves 4 basic stages; entry, replication, viral shedding and viral latency. Whilst latent, virions can evade host immunity by 'hiding' within cells they have in infected. Figure rendered in Biorender.*

1.3.2 Adenoviruses

Originally isolated from human adenoids, adenoviruses are capable of human infection, and can be genetically manipulated for gene delivery use. They are around 90 – 100 nm in size, 150 MDa, making them one of the largest known viruses with no envelope, and contain double stranded DNA. Classified within the viral family adenoviridae, a multitude of individual adenoviruses (or serotypes) exist, which are capable of infection of many vertebrate hosts (Rowe, Huebner, Gilmore, Parrott, & Ward, 1953); (Reddy, Natchiar, Stewart, & Nemerow, 2010).

Adenovirus strains can be the cause of mild disease states such as tonsillitis, conjunctivitis, gastroenteritis, and ear infections (Ruuskanen, Mertsola, & Meurman, 1988) ; (Chu & Pavan-Langston, 1979); (Jones, et al., 2007); (Murrah, et al., 2015) but can cause more severe illnesses including encephalitis, meningitis, and severe pneumonia in children (Straussberg, Harel, Levy, & Amir, 2001); (Souer, Woulters, de Saint-Georges, Content, & Depierreux, 1991); (Yu, et al., 2016).

Adenoviruses have emerged as a gene delivery vector of choice, being utilised in disease state clinical trials (Wold & Toth, 2014), including most notably cystic fibrosis (Boucher, et al., 1994). Research with adenovirus serotypes demonstrates high transduction efficiency, most likely due to ease of human infection and high availability of multiple serotypes for use in trials (Crystal, 2014); (Breyer, et al., 2001). However, there have been

complications in some research, specifically related to adenoviral immunogenicity (Wold & Toth, 2014).

More recently, adenoviral vectors have been utilised outside of a gene therapy context. Recombinant adenoviral vectors were used in viral based COVID-19 vaccines to deliver transgenes for SARs-Cov-2 stabilised spike protein (Folegatti, et al., 2020). Many other vaccines also utilised various recombinant adenoviral vectors, and after *in vivo* animal and small scale clinical trials, some were initially approved for use and distributed throughout the population; these included the Oxford–AstraZeneca COVID-19 vaccine (Hassan, et al., 2020), the Janssen COVID-19 vaccine (Sadoff, Struyf, & Douoguih, 2021), BioNTech, Moderna (Basheeruddin Asdaq, et al., 2022), and Gam-COVID-Vac (ClinicalTrials.gov Identifier: NCT04436471, 2020). Whilst not used for the purposes of gene editing, use of a viral vector in vaccine generation can be useful to highlight immune response of the chosen vector.

1.3.3 Adeno-associated Viruses (AAV)

Adeno-associated viruses (AAV) are significantly small viruses (20 nm) from the *Parvoviridae* family, genus *Dependoparvovirus.* Due to their small size, reduced mild immune response, and lack of pathogenicity (Naso, Tomkowicz, Perry, & Strohl, 2017); (Wu, Yang, & Colosi, 2010) they present as a promising vector for gene therapy development. AAVs were first discovered in 1965, when they were observed as particles genetically distinct

from simian adenovirus in culture (Atchinson, Casto , & Hammon, 1965). Key to their use as a reliable gene therapy vector is their predictability comparative to other viral vectors, which is in part due to their stable integration of the host genome. Wild type AAVs have been shown to interact and integrate at the AAVS1 site on chromosome 19 in a site-specific manner (Kotin, et al., 1990); (Samulski, et al., 1992).

Current AAV research has highlighted associated adenoviruses as potential gene therapy vectors for multiple disease states. Recent animal model work has demonstrated some success with AAV vectors; Use of specific AAVs 8 and 9 demonstrated targeted delivery of GFP to inner ear cell populations in a guinea pig hearing loss model, highlighting the potential for AAV clinical translation to genetically target and improve hearing impairment (Wang, et al., 2022). A combination of AAVs 2 and 8 was used for delivery of GFP and acid α-glucosidase (GAA) in a mouse model of Pompe disease, establishing an effective dose for recovery of GAA deficiency (Han, Gheorghiu, Li, Kang, & Koeberl, 2022). Another mouse model also focussed on Laron syndrome, where the body is unable to utilise growth hormone (GH) and thus results in dwarfism in mammals; here, an AAV was used to deliver murine growth hormone receptor (GHR) and improved GH uptake (Sia, et al., 2022).

Further work has also demonstrated targeted AAV9 delivery in mice *in vivo* and in human cardiomyocytes *in vitro* for ischemic cardiomyopathy (Martinez, et al., 2022) and there has also been use of AAV8 within small scale clinical trials for Tay Sachs Disease (Flotte, et al., 2022). AAVs have

also recently been used in combination gene delivery; they have been utilised as the delivery vector for CRISPR editing tools to more efficiently generate CAR-T therapies (Ding, Chao, & Gao, 2022).

1.3.4 Lentiviruses

Lentiviruses are larger, enveloped viruses usually around 80 – 100 nm, from the viral family *Retroviridae.* Alongside gammaretroviruses, they are a subtype of the retrovirus (Milone & O'Doherty, 2018) and investigated in research as a potential gene therapy vector. They are widespread in humans and several other mammalian species; the most commonly known lentivirus is human immunodeficiency virus (HIV) (Cockrell & Kafri, 2007).

Each enveloped virion contains single stranded RNA and proteins such as reverse transcriptase and integrase within the capsid, which enables utilisation of host cell machinery to copy the viral RNA template and integration of the viral genome with the host cell, allowing for continued viral replication (Milone & O'Doherty, 2018).

Lentiviruses present an attractive potential gene therapy vector due to their endogenous ability, where they integrate their genome directly into the host cells. This means all future progeny cells inherit the mutation. They are also able to infect non-dividing cells, and can integrate a large amount of genetic information (Yamashita & Emerman, 2004). These features could be key to reducing the issue of transience with gene therapy vectors and enabling the required mutation to reach all cells.

Current lentiviral research has demonstrated the wide potential usage and utility of lentiviral vectors, including demonstration of prostate cancer cell death utilising lentiviral bound trastuzumab (Zhang, et al., 2009), and correction of haemophilia A in a mouse model (Shi, et al., 2007). Other research has also demonstrated transference of the insulin gene into a diabetic rat model (Oh, Li, & Kim, 2006), lentiviral potential gene therapy application in chronic granulomatous disease (Barde, et al., 2011), and even *in utero* lentiviral delivery for prevention of arthritis within a mouse model (Roybal, Endo, Radu, Zoltick, & Flake, 2011).

Much lentiviral research has been within *in vitro* and early-stage animal models; however, some lentiviral vectors have reached clinical trial stages for specific disease states. Recent and ongoing trials include an HIV-1 trial established in 2003 with ongoing patient monitoring, which has reported no adverse events or mal effects for patients up to 8 years post-administration of treatment (McGarrity, et al., 2013). Another clinical trial, for β-Thalassemia, a genetic blood disorder characterised by reduced levels of functional haemoglobin leading to reduced oxygen availability in the patient, initially demonstrated initial success in 2010 (Cavazzana-Calvo, et al., 2010). Following trials modified and improved on the initial lentiviral vector that was used (Thompson, et al., 2018), which also led to success for some patients in the form of future blood transfusion-independence (Thompson, et al., 2018); (Marktel, et al., 2019). However, further patient monitoring over time may be required to truly confirm if individuals would require no further specific treatment.

There have also been small scale clinical trials for other genetic disease states, including metachromatic leukodystrophy (Sessa, et al., 2016), Wiskott-Aldrich syndrome (Aiuti, et al., 2013), and for cancer immunotherapy applications in specific cancers like leukaemia (Maude, et al., 2014), all with varying levels of success.

The integrative ability of the lentivirus can be both an advantage and an issue; there is the potential for insertional mutagenesis around the integration site, oncogene activation, or tumorigenesis due to inactivation of tumour suppressing genes (Schlimgen, et al., 2016); (Themis, et al., 2005). To prevent potential off target effects, lentiviruses can be modified to produce non-integrating lentiviruses (NILVs) (Gurumoorthy, et al., 2022). Integration efficiency can be reduced with either targeted mutations to the retroviral integrase (IN) enzyme, or to the integrase attachment site (Engelman, et al., 1995); (Zhu, Dobard, & Chow, 2004).

Non-integrating lentiviruses (NILVs) have been used in a variety of research. Early research has utilised HIV-based lentiviral vectors for targeted delivery by mutating integration sites to make these vectors non-integrating and demonstrated delivery in *in vitro* muscle (Apolonia, et al., 2007). Other work has demonstrated specific targeting of B cells positive for Epstein Barr virus (Flynn, Zacharias, Zhou, Cannon, & Philpott, 2011), and localised targeted transgene delivery using a NILV to improve regeneration of retinal epithelial pigment (RPE) cells within a macular degeneration mouse model (Kampik, et al., 2017). Non-Integrating Lentiviral vectors can also be modified with the use of a S/MAR site (scaffold/matrix attachment region), to overcome loss of

genomic material post-cell division, and thus aid in prolonged expression (Verghese, Goloviznina, Skinner, Lipps, & Kurre, 2014); (Xu, et al., 2016).

More recently, they have been used in combination therapy, where a non-integrating lentiviral vector was the delivery system for CRISPR/Cas9 gene editing components to target and correct the haemoglobin-Beta gene mutation that causes sickle cell disease (Uchida, et al., 2021). Non-integrating viral vectors have also been useful in generating CAR-T cells; recent research demonstrated use of an NILV with a scaffold attachment matrix region site (S/MAR) to successfully deliver the CAR transgene to cells *in vitro*. They also demonstrated NILVs gene editing capability by delivering green fluorescence protein (GFP) *in vitro* (Jin, et al., 2016). Research such as this demonstrates the potential for safe non- integrated engineering using viral vectors, without loss of cellular uptake or expression.

Despite their merits, all viral based gene therapy viral vectors still have the potential to introduce recombination events and cause unwanted off target effects; this key safety issue, alongside financial cost, presents some barriers for larger scale commercialisation and widespread use of viral vectors for gene therapy.

1.4 Non-viral based Systems

Non-viral based delivery systems include any system not dependent on utilisation of natural viral mechanisms or structures. Key advantages to non-viral delivery over viral based methods include their lack of immunogenicity, and minimal toxicity (Sainz-Ramos, et al., 2021). Non-viral delivery methods include physical methods, such as injections, electroporation or similar poration methods (hydro, sono or photo) and an array of chemical-based methods (Nayerossadat, Maedeh, & Ali, 2012); (Mali, 2013). Chemical methods can be grouped broadly into polymers, dendrimers, lipids (Jones, Chen, Ravikrishnan, Rane, & Pfeifer, 2013), nanoparticles (Singh, Prateeksha, Gupta, Chen, & Atanasov, 2017); (Wong, et al., 2017) and peptides (Hadianamrei & Zhao, 2022).

1.4.1 Lipids

Lipids, specifically cationic lipids, can be utilised for genetic and small cargo delivery through the formation of liposomes or lipoplexes (Junquera & Aicart, 2016); (Liu, et al., 2020). Liposomes form as spherical structures, due to the hydrophilic head and hydrophobic tail regions. This formation causes hydrophobic areas to move away from aqueous solutions, leaving only the hydrophilic areas exposed on the outside of the structure and establishing a phospholipid bilayer (Cevc & Richardsen, 1999). The overall positive charge of liposomes makes them ideal for binding and encapsulating negatively

charged molecules such as nucleic acids, including DNA, RNA, and siRNA (Bozzuto & Molinari, 2015); (Wu & McMillan, 2009); (Vitor, Bergami-Santos, Barbuto, & de la Torre, 2013). When bound to nucleic acids, the resulting complexes are usually referred to as lipoplexes; when the liposome encapsulates the nucleic acid, the resulting lipoplex enables intracellular delivery of the cargo via cell membrane fusion (Almofti, et al., 2003); (Tarahovsky, Koynova, & MacDonald, 2004).

1.4.2 Polymers

A variety of polymers can be utilised in non-viral gene delivery; these macromolecules are usually easy to manufacture and can be tailored to meet specific delivery and cargo requirements, enabling production of effective polymeric nanoparticle systems.

When electrostatic interaction between the polymer and cargo molecule occurs, polyplexes are formed; polyplexes are functionally similar to lipoplexes, instead involving a chosen polymer binding nucleic acid material to form the polymer-DNA complex. Electrostatic interactions allow for polyplex formation due to use of positively charge cationic polymers (Rai, Alwani, & Badea, 2019); (Midoux, Breuzard, Gomez, & Pichon, 2008); (Sirianni, et al., 2022). These nanoscale particles can then enter the cell and deliver the chosen cargo.

The most commonly used polymers in gene and drug delivery research include the commercial agent Polyethyleneimine (PEI) (Lungwitz, Breunig, Blunk, & Göpferich, 2005); (Song, et al., 2012) and chitosan (Santos-

Carballal, Fernández Fernández, & Goycoolea, 2018); (Wong, et al., 2006), as well as polyspermine (Hosseinkhani, Azzam, Tabata, & Domb, 2004), cyclodextrin, PLGA (Barichello, Morishita, Takayama, & Nagai, 1999); (Makadia & Siegel, 2011), PLA (Rancan, et al., 2009), and Poly(L-lysine) (Trubetskoy, Torchilin, Kennel, & Huang, 1992); (Martinez-Fong, et al., 1999). These polymers are used both independently and can be combined to further improve targeted delivery and cargo uptake.

Polymeric nanoparticles demonstrate delivery of a range of cargos to multiple sites both *in vitro* and *in vivo*; PLGA modified with PEG and alendronate demonstrated nanoparticle absorption to hydroxyapatite (HA), as a potential model for targeted drug delivery to bone (Choi & Kim, 2007). Hybrid polymer work compared PEGylations of PAMAM and PEI as potential tumour targeting delivery systems, including a peptide targeting ligand to target glucose-regulated protein-78 kDa (GRP-78) (Wood, et al.). Other hybrid polymer work has also demonstrated the mucus penetrating potential of PLGA-PEG nanoparticles to highlight their potential for mucosal drug delivery (Xu, et al., 2013), and utilised Chitosan-PEI coated in hyaluronic acid (HA) to deliver siRNAs for Aquaporin-2 (AQP2) to reduce lesions in endometriosis rat models (Zhao, et al., 2016).

1.4.3 Dendrimers

Dendrimers are molecules with a uniform branching polymeric structure. Multiple individual dendrons form around a focal point to make a 3D, spherical dendrimer molecule. Due to their method of formation and

structure, many properties of dendrimers can be modified and are controllable, including their toxicity and water solubility.

Current research has so far utilised dendrimers for drug delivery, specifically across the blood brain barrier (BBB). Dendrimer facilitated delivery in brain has been demonstrated *in vivo*, with a rabbit model for Cerebral palsy (Kannan, et al., 2012), a murine model for Rett syndrome (Nance, et al., 2017), and a canine model for Hypothermic Circulatory Arrest (HCA) brain injury (Mishra, et al., 2014). In each model, specific therapeutics were complexed with dendrimers, and targeted delivery to neurons or microglial cells was achieved.

Alongside this research, dendrimers have also been utilised as a genetic non-viral delivery system. Initial work utilising dendrimers for genetic delivery to murine lung proved unsuccessful (Rudolph, Lausier, Naundorf, Muller, & Rosenecker, 2000), however, later work demonstrated dendrimers as effective carriers of siRNA to HIV-infected lymphocytes (Weber, et al., 2008) and as a non-viral method for therapeutic delivery in HIV infection (Gonzalo, et al., 2010). Further work also modified dendrimers for application in targeted transgene delivery to human retinal pigment epithelial cells (Mastorakos, et al., 2015) and targeted Atoh1 gene delivery to a rat cochlea model for demonstration of dendrimers nanocarrier capabilities (Wu, et al., 2013).

More recent advancements have demonstrated dendrimers as a potential gene therapy delivery system in cancer. Research has used complexation with alternate polymers such as PEI to improve plasmid delivery to specific

cancer cells (Neves, et al., 2021) and duplexing with CRISPR/cas9 machinery to create a targeted genome editing system for specific cancers such as colorectal cancer (Wan, et al., 2021).

1.4.4 Nanoparticle systems

Nanoparticle systems have proven useful particularly in drug delivery, and are able to deliver a variety of potentially therapeutic agents (Rizvi & Saleh, 2018). They have the key feature of tunability, allowing for the particles properties to be controlled and changed as needed (Fay, et al., 2017). There is also some research supporting the ability of some nanoparticle systems to cross the blood brain barrier effectively (Ayub & Wetting, 2022). Nanoparticle systems can utilise organic or inorganic materials, providing delivery options for multiple applications. Similar to other delivery methods, side effects can occur, dependent on the material used; nanotoxicity and bioaccumulation have been observed in some systems (Khanna, Ong, Bay, & Baeg, 2015).

Nanoparticle systems are also useful in the context of gene delivery, and can utilise a variety of materials, including metals and silica. Inorganic nanoparticles, including gold (Abashkin, et al., 2021) and silica (Slita, Egorova, Casals, Kiselev, & Rosenholm, 2018); (Zhu, et al., 2021) have demonstrated genetic delivery capability (Sousa de Almeida, et al., 2022). Coated iron oxide particles have also been tested to determine potential toxicity *in vitro* (Magdolenova, et al., 2015) and have demonstrating successful gene delivery *in vitro* (Xiao, Castro, Rodrigues, Shi, & Tomas, 2015).

1.4.4.1 Lipid nanoparticles

Lipids can be effectively adapted into lipid nanoparticle systems, referred to as solid lipid nanoparticles (SLNs), and have demonstrated some effective drug transport capabilities (Lim & Kim, 2002); (Lee, Lim, & Kim, 2007). They have proven most useful for encapsulating and targeted delivery of a variety of nucleic acids (Pedersen, Hansen, Heydenreich, Kristensen, & Poulsen, 2006); (Hayes, et al., 2006); (Montana, et al., 2007).

Lipid nanoparticles can be modified to improve their intracellular delivery; choice of material during formulation is important, as this can affect packaging and delivery capabilities. For example, PEG is a widely used coating material for nanoparticle delivery, due to its minimal toxicity, hydrophilic nature, and the stability it can provide to nanoparticles during circulation; however, PEGylation can inhibit intracellular delivery, and there is some evidence it may also inhibit endosomal escape (Hatakeyama, et al., 2007); (Masuda, et al., 2009); (Moore, Sheppard, & Sakiyama-Elbert, 2009); (Chan, et al., 2012).

Lipid nanoparticle systems (LNPs) have some demonstrable delivery *in vitro*, such as in HeLa cells (Severino, et al., 2015), alveolar macrophages (Yu, Liu, Liu, Zhang, & Xu, 2010), and T lymphocytes (Ramishetti, et al., 2015), as well as *in vivo* within mouse models (Delgado, et al., 2012).

There has also been successful demonstration of lipid based nanoparticle delivery in a breast cancer cell line and associated xenograft model (Piao, et

al., 2013), and a clinical trial has also demonstrated successful delivery of siRNAs to target VEGF and kinesin spindle protein (KSP) in cancer patients utilising a targeted LNP (Tabernero, et al., 2013).

Some of the most recent work with lipid nanoparticles has focussed on vaccine delivery; lipid nanoparticles were used to transport RNA based vaccines BNT162b1 and BNT162b2 (Pfizer) coding for spike glycoprotein (S) of SARS-CoV-2 (Vogel, et al., 2021). Issues arose with the choice of nanoparticle coating; PEGylation appeared to trigger allergic reactions within small numbers of the population, with some individual cases being severe (Klimek, et al., 2021). However, there was some evidence to suggest PEG combined with the deliverable vaccine was eliciting a reaction, as opposed to PEG as an individual ingredient (Troelnikov, et al., 2021).

1.4.5 Cell Penetrating Peptides

Also known as peptide transduction domains (PTDs), cell penetrating peptides are small peptide chains found in current natural systems, such as transactivating transcription factor (TAT) used by the HIV-1 virus (Vives, Brodin, & Lebleu, 1997); (Tünnemann, et al., 2006). The properties of a cell penetrating peptide can be exploited, and they can be synthetised and utilised as a mechanism for genetic delivery *in vitro* (Milletti , 2012). Cell penetrating peptides can translocate the cell membrane, making them an ideal carrier for functional molecules of potential therapies (Madani, Lindberg, Langel, Futaki, & Graslund, 2011); (Trabulo, Cardoso, Mano, & De

Lima, 2010). They are able to facilitate cellular uptake of a variety of molecules in sizes ranging from nanoparticles to larger plasmid DNA (Derakhshankhah & Jafari, 2018). They are usually small peptides that interact with their cargo either chemically with covalent bonds, or through non-covalent interaction (Reissmann, 2014).

cell penetrating peptides can enter a cell through 3 main mechanisms: endocytosis-mediated entry, forming a transitory structure, or direct penetration of the membrane (Opalinska & Gewirtz, 2002). The most common method, endocytosis translocation, involves folding of the plasma membrane and the cell 'ingests' the cell penetrating peptide and its cargo (Duchardt, Fotin-Mleczek, Schwarz, Fischer, & Brock, 2007); (Lundin, et al., 2008). This process can be clathrin or calveolin dependent, or completely independent of both (Mayor & Pagano, 2007). Direct membrane penetration is reliant on electrostatic interactions and positively charged side chains such as arginine being present on the cell penetrating peptide , which facilitates entry through transient pore formation (Hu, Sinha, & Patel, 2015); (Hu & Patel, 2016). cell penetrating peptide Translocation of the membrane via a transitory structure can be mediated by formation of structures such as inverted micelles (Plénat, et al., 2004); (Deshayes, et al., 2004).

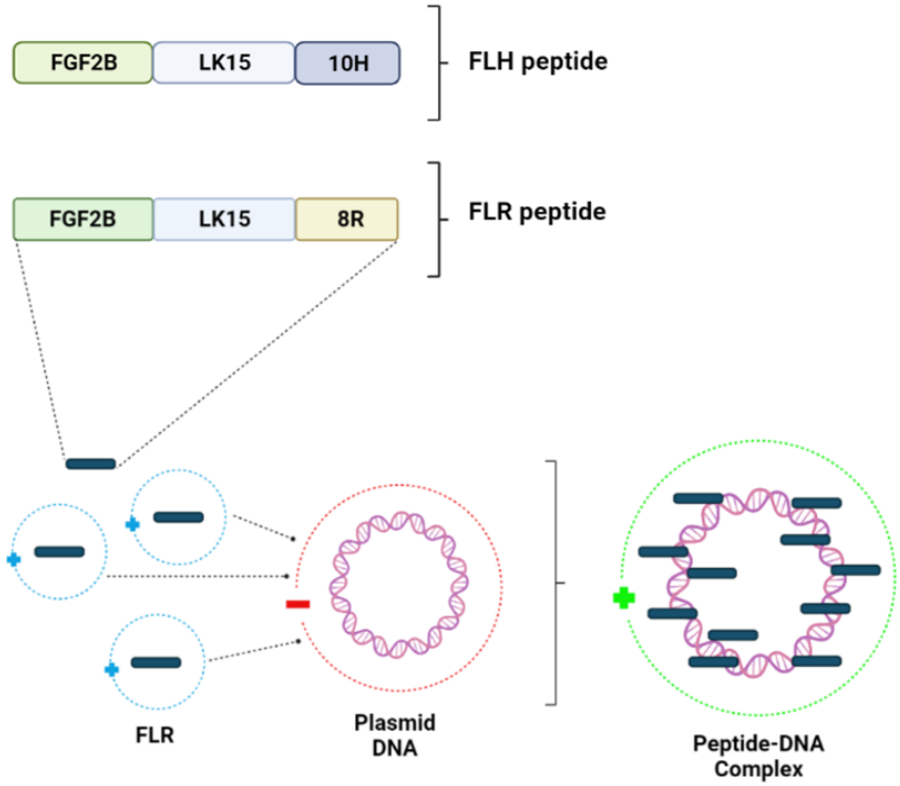
1.4.5.1 Glycosaminoglycan-binding Enhanced Transduction (GET)

The GET non-viral peptide is a novel delivery system that utilises Glycosaminoglycan binding enhanced transduction (GET). It involves small peptides that can bind plasmid DNA, or any similar macromolecular cargo, for delivery into cells by forming a nanoparticle able to penetrate the cell membrane (Figure 1.4 A). Specific peptide domains used enable cell surface heparan sugar targeting and intracellular transduction (Osman, et al., 2018). Previous work within the Dixon lab group work has demonstrated the GET systems ability to deliver reporter plasmids, proteins, transcription factors and magnetic nanoparticles to a variety of cell types, showing high transfection levels with minimal toxicity (Dixon, et al., 2016); (Abu-Awwad, Thiagarajan, & Dixon, 2017).

The peptide has 3 domains, with each enabling different functions. FLR consists of FGF2B, a 16-residue heparan sulphate-GAG binding peptide derived from the fibroblast growth factor 2 (FGF2) protein; LK15, an amphiphilic pan-nucleic acid interaction region, which aids in improved DNA condensation and intracellular trafficking; and octa-arginine (8R), a cell penetrating peptide (cell penetrating peptide) which aids in efficient cell entry (Osman, et al., 2018). The enhanced FLH peptide differs, in its substitution of the 8-chain arginine cell penetrating peptide with a 10-chain histidine (Figure 1.4 B). This method of non-viral delivery does not appear to affect viability when utilised *in vitro* (Abu-Awwad, Thiagarajan, & Dixon, 2017); (Dixon, et al., 2016), and can produce high transfection levels in cells upon delivery of plasmid DNA (Osman, et al., 2018). The modification of FLR into FLH improves endosomal escape by causing osmotic imbalance and

triggering endosomal swelling, allowing release of any cargos trapped within vesicles (Power, Cavanagh, Dixon, Curtin, & O'Brien, 2022).

A



B

Abbreviation	Full name	Amino Acid Sequence
F	FGF2B	TYRSRKYTSWYVALKR
L	LK15	KLLKLLLKLLLKLLK
R	8R	RRRRRRRR
H	10H	HHHHHHHHHH

Figure 1.4 GET peptide interaction with Plasmid DNA *(A) The GET peptide is referred to as FLR, due to its 3 specific Domains. FLR can interact with the plasmid DNA due to its positive charge, which is attracted to the negative charge of the phosphate backbone of the plasmid. The resulting complex has a slight overall positive charge, which further aids in cell entry. (B) Each peptide domain has a specific amino acid sequence. Individual figure components rendered in Biorender.*

1.5 Potential Models for lung genetic therapy testing

Multiple model types exist in which lung based gene therapy vectors could be tested; these range from full scale animal models, down to *ex vivo* and *in vitro* based models, with initial research carried out on lung cell monolayers.

Animal models, whilst considered a key research stage to enable progression to clinical trials and eventually product commercialisation, do not always accurately mirror the internal human environment or human reactions to specific treatments. Whilst accurately maintaining the 3D structures and particularly intact immune responses of a living mammal, it is becoming more evident that they provide a less than accurate picture of how a treatment or delivery system may behave in a human lung (Miller & Spence, 2017); (Evans & Lee, 2020). Animal models usually also come with significant animal wastage, and in some larger scale animal trials, increased financial cost. This presents an argument for improving and utilising more *ex vivo* and *in vitro* lung models (Nichols, Niles, Vega, & Cortiella, 2013); (Cidem, Bradbury, Traini, & Ong, 2020).

Ex vivo lung models usually involve excision of specific tissues which can be utilised experimentally for research, which can aid in reduction of the high levels of wastage seen in animal model use. *In vitro* models are more 'lab based'; samples can be either removed and used as primary material in its current state, or cells can be isolated from disaggregated primary tissue. This also aids in prevention of animal wastage, particularly in the case of human

cell based *in vitro* models. A useful *ex vivo* model is the precision cut lung slice (Rosales Gerpe, et al., 2018); (Bryson, et al., 2020); (Viana, O'Kane, & Schroeder, 2021) which uses animal or human lung explant tissue to produce thin slices of lung that maintain the cell localisation of *in vivo* without the use of a whole animal model (Hirn, et al., 2014); (Wu, Van Dijk, Bos, Kistemaker, & Gosens, 2019); (Lauenstein, et al., 2014).

However, advancements in *in vitro* lung modelling allow for cell differentiation to create more accurate organ structure-mimicking environments (Mainardi, Occhetta, & Rasponi, 2022); (Petrosyan, Cravedi, & Villani, 2019). Some models are now incorporating physical and mechanical pressures to maintain specific cell phenotypes, and aid in preservation of developing 3D structures similar to those observed *in vivo* (Huh, et al., 2010)*;* (Kim & Ingber, 2013)*;* (Si, et al., 2021).

1.5.1 Lung ex vivo Models

1.5.1.1 PCLS

Precision cut lung slices (PCLS) are emerging as an investigative *ex vivo* tool with multiple applications; they have most prominently been used in airway-based research (Held, Martin, & Uhlig, 1999); (Li, et al., 2020). They can be easily generated, with the most common method being agarose perfusion of either animal lung sets immediately post sacrifice, or agarose injection of donated human lung tissue (Sanderson, 2011). Once cooled, agarose provides a non-toxic support structure to hold open the lung tissue, allowing for accurate slicing into precision cut lung slices. Utilisation of lung

tissue in this way allows for generation of multiple samples, increasing the number of experiments that can be carried out from a single lung set or tissue sample. They can also be generated from a variety of species, with previous research utilising sheep (Lambermont, et al., 2014), mouse (Akram, et al., 2019), pig (Krimmling & Schwegmann-Weßels, 2017), guinea pig (Ressmeyer, et al., 2006) and marmoset monkey (Seehase, et al., 2012), alongside work utilising human tissue (Lauenstein, et al., 2014). Human tissue is the best host tissue from which to generate PCLS, as it is the most anatomically accurate, thus ensuring results produced are more significant and translatable.

A key advantage of PCLS is their preservation of physical lung structures and cell localisation, which allows for clear visualisation of airways; observation of more than 40 cell types has been achieved *in vitro*, which is comparable to the *in vivo* environment (Wu, Van Dijk, Bos, Kistemaker, & Gosens, 2019). These factors combined establish them as a potential alternative to larger scale *in vivo* animal studies.

PCLS research has investigated immune response (Henjakovic, et al., 2008), cytotoxicity (Krabbe, et al., 2018); (Neuhaus, et al., 2017), disease modelling (Banerjee, Huckuntod, Mills, Kurten, & Pechous, 2019), and delivery of therapeutic molecules (Nassimi, et al., 2010). Human and murine lung tissue are the most commonly used for PCLS generation, and have provided a useful platform for investigating pulmonary fibrosis (Alsafadi, et al., 2017), COPD (Maarsingh, et al., 2019), effects of gaseous contaminants (Switalla, et al., 2010), and Asthma (Kim, et al., 2015).

Due to their versatility and ease of application for a multitude of studies, PCLS present as a model system for demonstration for gene delivery. For example, delivery using adenoviral and lentiviral systems has shown successful transfection of PCLS generated from murine and ovine tumour bearing tissue alongside unaffected tissue, to investigate selectivity of oncolytic viruses (Rosales Gerpe, et al., 2018). Other similar studies also demonstrate the use of PCLS for viral investigation, including antiviral use against influenza (Liu, et al., 2015); (Wu, et al., 2010), and as a model for oncolytic viral delivery (Diallo, Roy, Abdelbary, De Silva, & Bell, 2011).

1.5.2 Lung in vitro models

1.5.2.1 Air liquid interface model (ALI)

Air liquid interface culture (ALI) is a method used to elevate standard lung cell culture for investigative research (Jiang, Schaefer, & Chu, 2018). ALI has been utilised in a variety of studies, including inflammation (Hu, et al., 2020), nanoparticle delivery (Lenz, et al., 2009); (Brandenberger, et al., 2010) aerosolization drug delivery (Lenz, et al., 2014); (Ong, et al., 2016); (Schmid, et al., 2017) disease state modelling (Munis, Hyde, & Gill, 2020) and environmental toxicity (Upadhyay & Palmberg, 2018), with a specific focus on cigarette smoke exposure (Ishikawa & Ito, 2017); (Cao, Muskhelishvili, Latendresse, Richter, & Heflich, 2017); (Duffney, et al., 2018).

Standard lung cell culture is traditionally carried out in well plates or flasks, to maintain constant nutrient supply and prevent cells from drying, cultures are usually fully submerged. For general proof of concept or in studies where cell phenotype and function is not relevant to the experimental outcome, this is a cost effective and useful culture method.

However, a key feature of *in vivo* lung is its mucosal barrier; lung epithelial cells, whilst in a well-regulated humid environment, are never completely submerged in liquid *in vivo*. Culturing lung cells on transwells (Figure 1.5 A) introduces an Air Liquid interface (ALI), where the cells are supplied with media and fed nutrients from below the membrane they are seeded on and

exposed to the air at their apical (upper) surface (Choe, Tomei, & Swartz, 2006). This method can prove useful when trying to reproduce the mucociliary phenotype observed in *in vivo* epithelial airways (Hill & Button, 2012).

A variety of lung cell types can be utilised for transwell ALI culture, depending on the focus of the study. The lung cells are seeded at a specific density onto 96, 24 or 12 well transwell inserts, and traditionally cultured submerged for the first 3 – 5 days until full confluence is reached (Huang, et al., 2017); (Cozens, et al., 2018). After this initial submersion, all media is removed from the apical chamber and the confluent cell layer is exposed to the air (Figure 1.5 B); (Gras, et al., 2017). Media is maintained in the well beneath the transwell (the basal chamber) to supply the cell layer with nutrients and specific supplements that can aid in driving differentiation of specific cell types (Lee, Petris, Hynds, & O'Callaghan, 2020) The exposure of the cell layer to the air is key in triggering differentiation and development of the multiple cell types observed in the lung *in vivo* (Figure 1.5 C) (Leung, Wadsworth, Yang, & Dorscheid, 2020); (Michi & Proud, 2021).

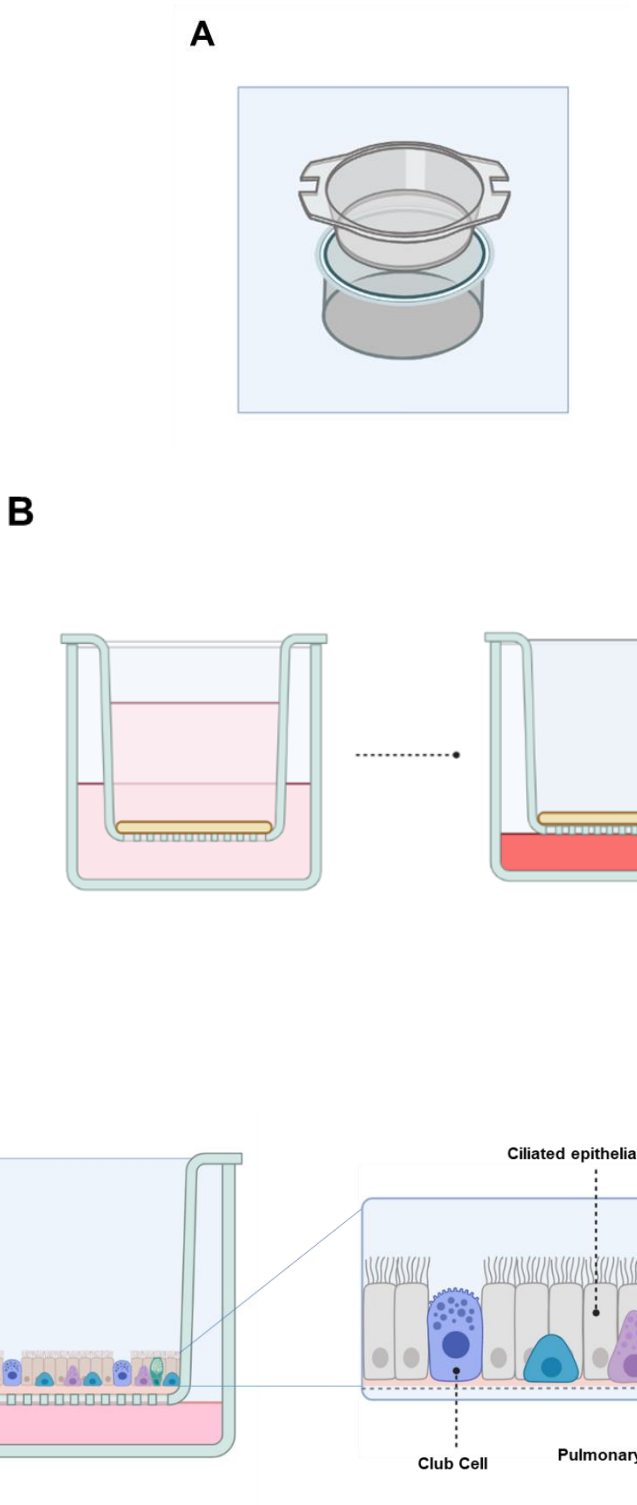


Figure 1.5 Air Liquid Interface (ALI) culture *(A) plastic transwell inserts fit within wells, to allow for suspension of membranes over media. (B) lung cells are seeded onto the membrane, and completely submerged during expansion. Once confluent, specialised differentiation media is put into the basal chamber and the apical surface is exposed to the air (C) around 21 to 28 days, mucociliary phenotype can be observed and an epithelial layer, similar to in vivo, should be present. Figure rendered in Biorender.*

1.5.2.2 Lung on Chip (LOC)

Lung on chip (LOC) is a type of *in vitro* experimental model used for research in a similar method to tissue explants and other cell-based models. Invented and realised in 2010 by Don Ingber and Dongeun Huh (Huh, et al., 2010), the development of chip technology allowed for expansion into multiple organs, including internal structures of the kidney (Petrosyan, Cravedi, & Villani, 2019); (Jang & Suh, 2010), heart, (Agarwal, Goss, Cho, McCain, & Parker, 2013), brain (Moreno, et al., 2015) and gut (Kim & Ingber, 2013). Current research is experimenting with multiple chip types, with the eventual aim to link organ chips directly and create a closed interacting system (Luni, Serena, & Elvassore, 2014); (Iravaidya & Shuler, 2004); (Zhang, Zhao, Abdul Rahim, van Noort, & Yu, 2009).

The lung on chip mimics the internal 3D organ environment, but on a significantly smaller scale. The microchip device contains a small microfluidic tube divided internally by a flexible membrane; on each side of the membrane, lung epithelial and lung endothelial cells are seeded (Benam, et al., 2017). Lung cells are chosen dependent on the area of lung the model will mimic; both Alveolar and upper airway models are now possible (Jain, et al., 2018); (Si, et al., 2021). Cells are seeded and grown on the upward facing surface of the membrane, with lung endothelial cells on the other side. Similar to a transwell, this allows for the apical surface to be exposed to air to allow for differentiation, and the lower surface can be fed media and nutrients. Cells are fed media via chambers on the device (Figure 1.6) and cultured to allow cell differentiation and development of either an alveolar

layer, or an airway epithelial layer presenting a mucociliary phenotype. The device design adds an advantage over more static models such as transwells as the membrane can be mechanically flexed to mimic the *in vivo* breathing movement of the lung. Flow rate of media can also be moderated and controlled with specialised equipment (Stucki, et al., 2018).

If a patient's cells were utilised in such a chip system, this could pave the way for a more personalised type of medicine for the individual for any organ. Devices such as these could also potentially replace extensive animal testing, providing a more cost effective, accurate and a more ethical method for new treatments, toxicity studies, and even drug trials. The most recent organ on a chip (OoaC) research has utilised organ chip devices to identify candidate antiviral therapeutics and prophylactics in the small airway (Si, et al., 2021), modelling leaky gut barriers in the colon (Apostolou, et al., 2021), modelling osteoarthritis with cartilage on chip (Mainardi, Occhetta, & Rasponi, 2022), and even utilising multiple organ chips to mimic immunocompetency for evaluating T-cell bispecific antibodies (TCBs) targeting antigens on tumours (Kerns, et al., 2021).

The most recent lung on chip work has now recapitulated the cystic fibrosis lung on an airway on chip, to aid in investigation of this lung specific genetic disorder (Plebani, et al., 2021).

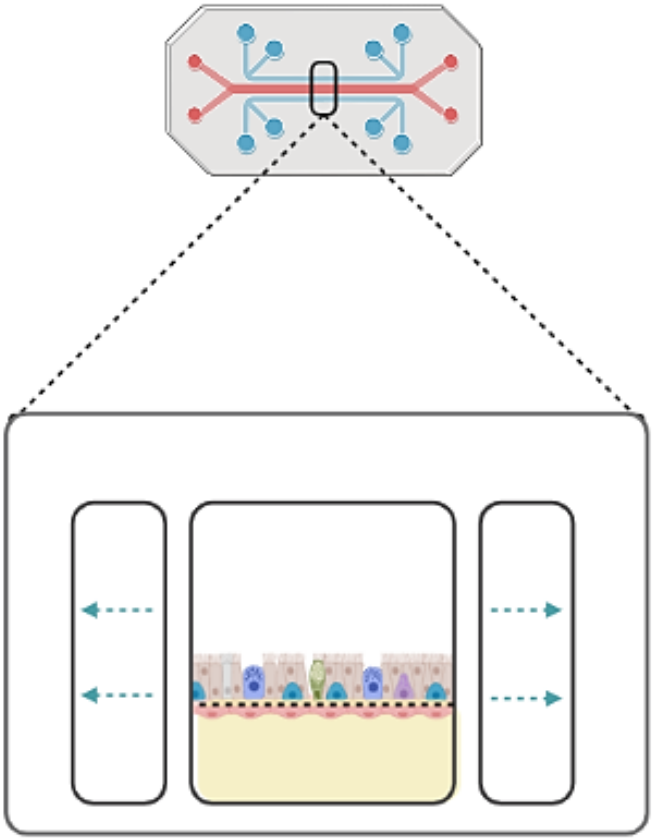


Figure 1.6 Lung-On-Chip (LOC) Model *Microfluidic channels are separated by a porous membrane (dotted line). The surrounding vacuum channels can induce flex (arrows), applying mechanical pressure and mimicking the movement of in vivo lung. Individual figure components rendered in Biorender.*

1.5.2.3 Lung Spheroid and Organoid Cultures

Lung spheroids and lung organoids are similar *in vitro* culture techniques that can be utilised for initial research on both animal and human lung. Spheroid and organoid methods also exist for a variety of other organs. Spheroids differ from organoids in their level of recapitulation and cell types present as the model develops; depending on the organ, fully developed organoids usually exhibit identifiable cell types also present *in vivo*, whereas spheroids may exhibit less organ-like structures and typical cell lineages (Cunniff, Druso, & van der Velden, 2021); (Sakalem, De Sibio, da Costa, & de Oliveira, 2021). Organoids are also usually seeded from cells directly and can even be seeded from embryonic or induced pluripotent cell lines. They are dependent on an extracellular matrix for physical support during development, and usually require specialised combinations of growth factors and specialist media. Spheroids can be generated from a variety of cell lines, but are more likely to be isolated directly from tissue, such as tumour explants. Organoids are capable of demonstrating more complex structures through self-assembly, with spheroids demonstrating cellular organisation in a 3D environment but with less apparent physiology (Sakalem, De Sibio, da Costa, & de Oliveira, 2021); (Lu, Cao, Zhao, Shen, & Xi, 2021).

Lung spheroids have been utilised both generally for cancer studies, and more specifically for drug efficacy against lung cancers (Douple, et al., 1895); (Bepler, et al., 1987); (Fjellbirkeland, Bjerkvig, & Laerum, 1998); (Shabalina, et al., 2021). Lung spheroids have also proven useful for investigation of drug delivery to treat pulmonary fibrosis (Cores, et al., 2020); (Dinh, et al., 2020).

Due to their higher level of differentiation, lung organoid research has focussed more on lung regeneration (Tan, Choi, Sicard, & Tschumperlin, 2017), and mimicry and investigation of respiratory infection response (Paolicelli, et al., 2019); (Salgueiro, et al., 2022). Due to the current climate, recent focus has been on SARS-COV-2 infection (Salahudeen, et al., 2020); (Tindle, et al., 2021) and efficacy of potential therapeutics (Hu, et al., 2020).

1.6 Aim and Objectives

The overall aim of this project is;

To demonstrate the genetic delivery capability of the GET non viral peptide based system within ex vivo models of the lung. Transience presents as a potential barrier to non-viral delivery, particularly the GET peptide based system, therefore demonstration of this systems efficiency within cell based models with higher order organisation than cell monolayers could be a step towards optimisation to combat potential vector transience.

The Objectives of this project are:

- To utilise murine Precision Cut Lung Slices as an ex vivo model in which to demonstrate the capabilities of the GET peptide non-viral delivery system
- To investigate an alternate perfusion materially that is removeable, to potentially improve the in vitro PCLS model and increase tissue slice exposure to the delivery system of choice (GET)
- To establish an in vitro Air Liquid Interface transwell model from human cells, for demonstration of non-viral delivery in a more translatable model

This PhD project aims to potentially demonstrate a comparison of GET non-viral delivery within an *ex vivo* and an *in vitro* model, and demonstrate the delivery capability of the novel GET peptide non-viral delivery system specifically by utilising both the FLR and FLH peptides. This is to highlight the non-viral systems delivery efficiency and capability, whilst also attempting to highlight the utility and benefit of using more non-invasive, cost effective models for future

potential genetic therapy testing. The lung was focussed on due to the potential for non-viral delivery to this organ, particularly in the context of genetic lung specific disorders such as Cystic Fibrosis.

If successful, demonstration of GET non-viral delivery to an in vitro lung model could potentially provide an alternative non-viral method in the future for gene therapy; it could be applied to correction of mutations such as the ΔF508 mutation found in 70% of cystic fibrosis patients, or in similar genetic diseases where the mutation is monogenic and easier to target.

Adding to the body of research on non-viral delivery methods is key to improving and moving forward non-viral delivery systems and further research can help provide useful information as to the types of genetic diseases they can be used to treat.

2. Chapter 2: Materials and Methods

2.1 Immortalised Human Bronchial Epithelial cells (iHBECs)

Cell work was carried out using immortalised human bronchial epithelial cells (iHBECs) originating in Dixon lab group LN storage. Cells were previously cultured and frozen stocks were made at passages P7, P10, and P15. Stocks were stored long term in liquid nitrogen. iHBEC cells were thawed for this work, and new frozen stocks made alongside general use and culture.

2.1.1 Thawing

iHBECs were initially thawed according to supplied protocol from Dr. Amanda Tatler. For a standard thaw, 1 vial of iHBECs were snap thawed in a water bath at 37ºC for around 2 minutes, or around ~50% thaw when both ice and liquid could be seen in the vial. In a sterile environment, the vial contents were added to a T75 flask containing pre warmed media and observed under a benchtop microscope to determine cell presence. Cells were left in an incubator at 37ºC for 24 – 48 hours to adhere, after which cell media was changed for fresh media. Cells were observed after the first 24 hours to confirm general health of culture post thaw.

2.1.2 Media preparation

2.1.2.1 KSFM

Keratinocyte Serum Free medium (KSFM) was purchased from Gibco (Thermofisher Scientific, Catalog number: 17005042) and was supplied with the required supplements, 1 × 25 mg Bovine Pituitary extract (BPE) and 1 × 2.5 µg Recombinant Endothelial growth factor (rEGF). Volumes of supplements were added according to original iHBEC protocol; 25 µg/ml BPE and 0.2 ng/ml rEGF was added per 500 ml base media. To maintain cell immortality, selective antibiotics used were G418 (geneticin) and Puromycin, and these were added according to original iHBEC protocol. G418 was purchased from Gibco (Thermofisher Scientific, 10131035) as a liquid solution at a concentration of 50 mg/ml, 20 ml total volume, and 25 µg/ml was added per 500 ml base media. Puromycin was purchased from Sigma (P8833-10MG) in powdered form (10 mg) and was diluted in distilled nuclease free water to create a working stock of 250 µg/ml. 250 ng/ml was added per 500 ml base media. For ease of use, aliquots of G418 and Puromycin were made, 250 µl and 500 µl respectively.

2.1.2.2 PneumaCult™

The PneumaCult™ media system was purchased from Stemcell. PneumaCult™ Ex Medium (Catalog # 05008) was used for initial expansion of cultures. PneumaCult™-ALI Medium (Catalog # 05001) was used to culture Air liquid interface cultures post air lift. Required supplements for both

media types were Hydrocortisone (Catalog # 07925) and Heparin (Catalog # 07980), purchased from Stemcell. All other required supplements were supplied by manufacturer with the base media. Manufacturer's supplied protocol was followed for all reagent preparation and use.

Ex Medium was prepared by adding 10 ml of PneumaCult™ - Ex 50x supplement and 0.5 ml Hydrocortisone stock to 490 ml basal medium. PneumaCult™-ALI Medium was prepared by adding 50 ml PneumaCult™-ALI 10x supplement to 450 ml basal medium. This was used to make aliquots of Maintenance medium. To make 10 ml Maintenance medium, 9.83 ml complete basal medium was combined with 100 µl PneumaCult™-ALI Maintenance supplement, 20 µl Heparin solution, and 50 µl Hydrocortisone stock solution.

G418 and Puromycin were added to Ex Medium at the same concentrations previously used for KSFM; no antibiotics were added to ALI Medium, as manufacturers protocol did not define antibiotic use with this media system.

2.1.3 iHBEC culture

iHBECs were cultured in standard T75 and T175 Nunc flasks, depending on required cell numbers. For initial experiments, Keratinocyte Serum free medium (KSFM, Gibco) was used for general cell culture. For later experiments, complete Ex-Medium (Stemcell) was used pre airlift and to expand cultures, with ALI-Medium (Stemcell) used post airlift. iHBECs were supplemented with fresh media every other day, 10 -12 ml per T75 flask and

33 – 35 ml per T175 Flask. Cell flasks were passaged at 80% confluence or higher, confirmed with visual observation on a standard benchtop microscope. Cells were washed once with sterile PBS before passage with 0.025% Trypsin-EDTA (Gibco) and incubated in trypsin for 10 minutes at 37ºC or until majority of cells had detached. iHBECs were seeded at 1.6 x 10^6 per T75 flask and 3 x 10^6 per T175 for optimum cell adherence and recovery. iHBECs were observed minimum every other day on a standard benchtop microscope to assess confluence, cell adherence, and any potential contamination.

2.1.4 Transwell culture at the air liquid interface (ALI)

Transwell cultures at the air liquid interface were carried out with reference to other published works and protocols demonstrating the technique (Jiang, Schaefer, & Chu, 2018) ; (Choe, Tomei, & Swartz, 2006); (Lenz, et al., 2014); (Ong, et al., 2016) (Schmid, et al., 2017); (Hu, et al., 2020).

Using these published works as guidance, initial transwell cultures were set up by carrying out a passage of a fully confluent iHBEC flask, followed by manual cell count using a benchtop microscope and using the resulting cell volume to seed transwell plates at around 90,000 – 100,000 cells per transwell insert. Media was added to both the basal and apical chambers pre-seeding, with cell solution added to the apical chamber. 100 µl media was kept in the basal chamber and 500 µl media was kept in the apical chamber for up to 48 hours. After 24 hours media was changed in the apical chamber, to allow cells to attach to the membrane. At 72 hours post seeding,

an air lift was performed, where all media was removed from the apical chamber to expose the apical surface to air (Figure 2.1). Basal media was changed for 500 µl fresh media, and in later experiments, this volume was reduced to 300 µl to prevent leaking into the apical chamber. Basal chamber media was changed every other day, and apical sterile PBS wash was performed at 2 weeks post air lift, and once a week after this timepoint. Transwell cultures were maintained up to day 28 (minimum) before fixing.

Sterile, tissue culture treated 12 well polycarbonate membrane transwell inserts, 0.4 um pore, 12mm, were purchased from Corning, Merck (CLS3401). Collagen coated 12 well inserts of the same pore size and membrane diameter were also purchased from Corning, Merck (CLS3493).

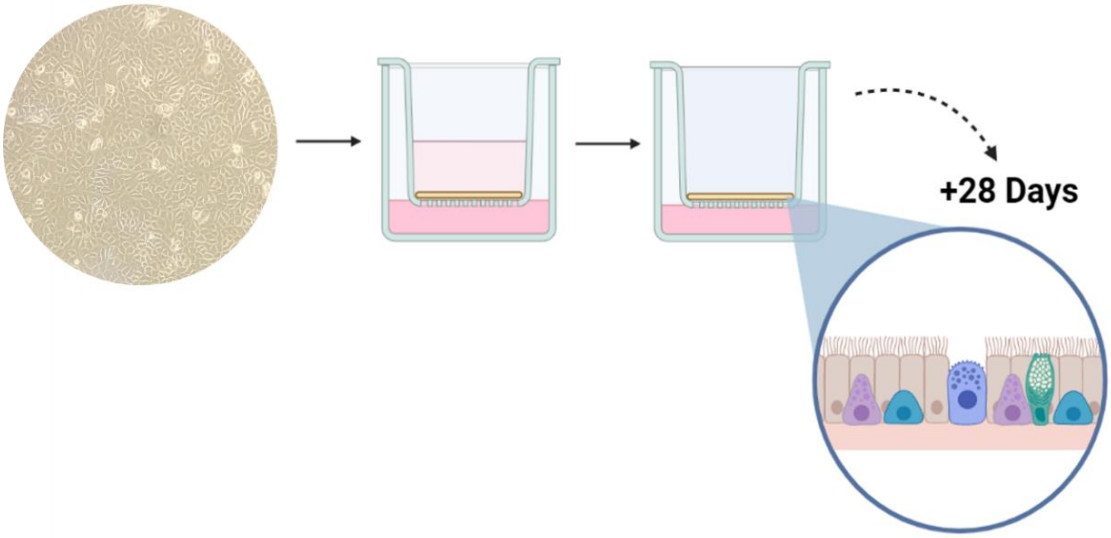


Figure 2.1 Transwell culture at the Air Liquid Interface (ALI) *immortalised human bronchial epithelial cells (iHBECs) were used to establish air liquid interface cultures. Cells were seeded onto transwells and allowed to reach confluence (>80%), after which cultures were air lifted. Cell layers were exposed to air at the apical surface continuously throughout culturing, with presentation of a mucociliary phenotype expected at around 4 weeks (28 days). Individual figure components rendered in Biorender.*

2.1.5 Transepithelial/Transendothelial electrical resistance (TEER)

TEER readings were taken of transwell cultures at 2 weeks post air lift (Day 14) and 4 weeks post air lift (Day 28). TEER readings were taken using an EVOM^2 TEER reader (WPI) fitted with STX2 chopstix and for later experiments, STX3 chopstix (Figure 2.2). EVOM^2 storage, maintenance and experimental readings were all carried out according to the manufacturer's Instruction manual for the EVOM2 epithelial Voltohmmeter (World Precision Instruments). AgCl pellets were calibrated in 1M KCL buffer overnight or for a minimum of 1 hour before use, and equilibrated in sterile, pre-warmed media at least 30 minutes before sample readings were taken. An unseeded sterile transwell was used to take blank readings to compare with seeded transwells. 500 µl media was added to apical chambers, and 1000 µl media was added to basal chambers, before chopstix arms were placed either side of the transwell insert. Chopstix pellets had to be completely submerged to give accurate readings. Readings were taken in triplicate from each sample, including the blank control transwell. Chopstix were disinfected with IMS post use and stored dry and dust free.

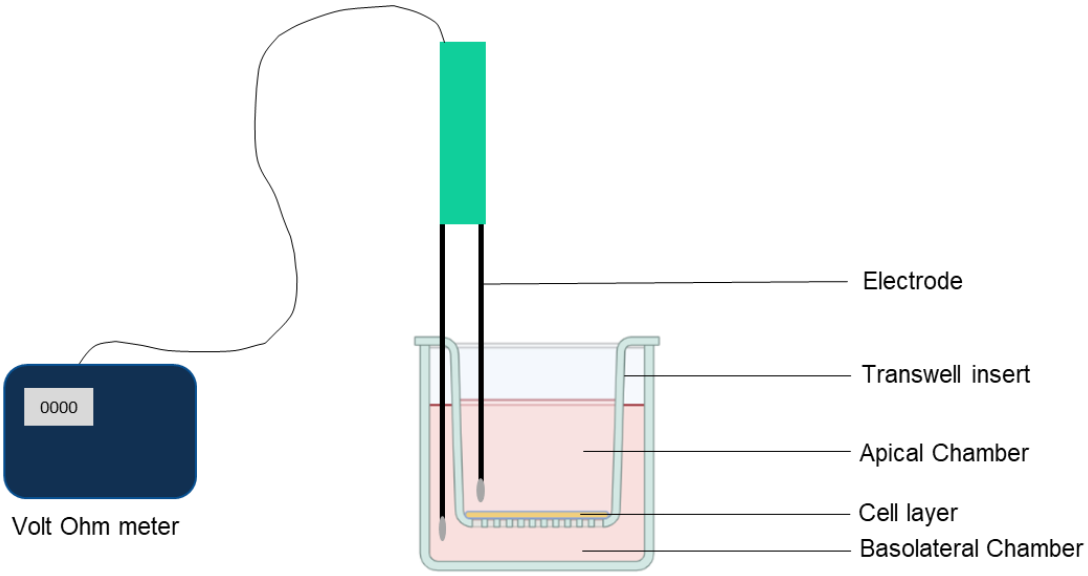


Figure 2.2 Transepithelial/Transendothelial electrical resistance (TEER) *Electrodes were placed either side of the transwell within the well, to measure the electrical resistance across the cell layer. Higher readings were indicative of increased tight junction formation, and potentially differentiation towards a complete mucociliary phenotype. Readings were taken at Day 14 (2 weeks) and Day 28 (4 weeks). Individual figure components rendered in Biorender.*

2.1.6 Immunofluorescence

A standard immunohistochemistry and immunofluorescence protocol produced by Abcam was followed for immunofluorescence staining. Samples were fixed at multiple timepoints, most commonly Day 14 and Day 28. Samples were washed with sterile PBS for up to 5 minutes, before fixing in PFA for 10 minutes at room temperature (25ºC). Enough fixative was used to submerge the cell surface, and fixative was added to both the apical and basal chambers. Post fixing, samples were washed twice with sterile PBS, and stored in PBS at 4ºC until immunofluorescent staining was carried out.

2.1.6.1 Antibodies

Antibodies were chosen to aid in identification of specific cell types that would be present in a differentiated epithelial lung layer. In initial experiments, antibodies used were alpha tubulin, to identify ciliated cells, P63, to identify basal cells, and FOXI1, to potentially identify ionocytes.

In later experiments, antibodies used were ZO-1, to identify presence of tight junction formation, P63, to identify basal cells, and MUC5AC, to identify mucus or any mucus producing cells (Table 1).

Alpha tubulin was purchased as an unconjugated primary (#62204) with a corresponding fluorescent Alexa Fluor 555 secondary (#A32727) both from Invitrogen. P63 was purchased as a fluorescent Alexa Fluor 488 conjugated primary from Abcam ([EPR5701], ab246727). FOXI1 was purchased as an unconjugated primary (Catalog #MA5-26379) with a corresponding

fluorescent Alexa Fluor 647 secondary (Catalog #A32728) both from Invitrogen. ZO-1 was purchased as a fluorescent Alexa Fluor 594 conjugated primary from Thermofisher (#339194). MUC5AC was purchased as a fluorescent Alexa Fluor 555 conjugated primary from Abcam ([EPR16904] (ab218714).

Antibody	Dilutions used
P63	1/100, 1/200
Alpha tubulin	1/100, 1/200
Alexa Fluor 555 secondary	1/200
FOXI1	1/100, 1/200
Alexa Fluor 647 secondary	1/200
ZO-1	1/200
MUC5AC	1/200

Table 1 *Dilutions of Antibodies used throughout Immunofluorescence (IF) experiments.*

2.1.6.2 Transwell preparation and staining

Fixed transwell samples were removed from storage PBS and using sterile forceps and a scalpel, the transwell membrane was carefully cut away from the transwell plastic. The membrane was cut into 4 quarters, and each quarter was deposited cell side facing upwards into a single well of a 24 well plate. Samples were covered in PBS to prevent membrane drying (Figure 2.3).

PBS was removed and a permeabilization step was carried out with PBS containing 0.25% triton X-100 for 10 minutes. Permeabilization solution was removed, and samples washed at least 3 times with sterile PBS. Samples were then blocked with PBST containing PBS, 1% BSA, and 0.1% Tween20, for 30 minutes. Samples were then incubated with antibody in 1% BSA in PBST, diluted according to manufacturers recommended dilutions (1/100, 1/200) for 1 hour at room temperature (25ºC). If secondary antibodies were required, samples were washed 3 times with PBS before incubation with appropriately diluted secondary antibody for 1 hour at room temperature (25ºC).

Once stained, membrane samples were carefully lifted from wells with sterile forceps and mounted in either plain fluoromount G (Thermo, 00-4958-02) or fluoromount with DAPI (Thermo, 00-4959-52) onto pre-labelled slides. Coverslips were mounted over samples and left to dry before storage at 4ºC.

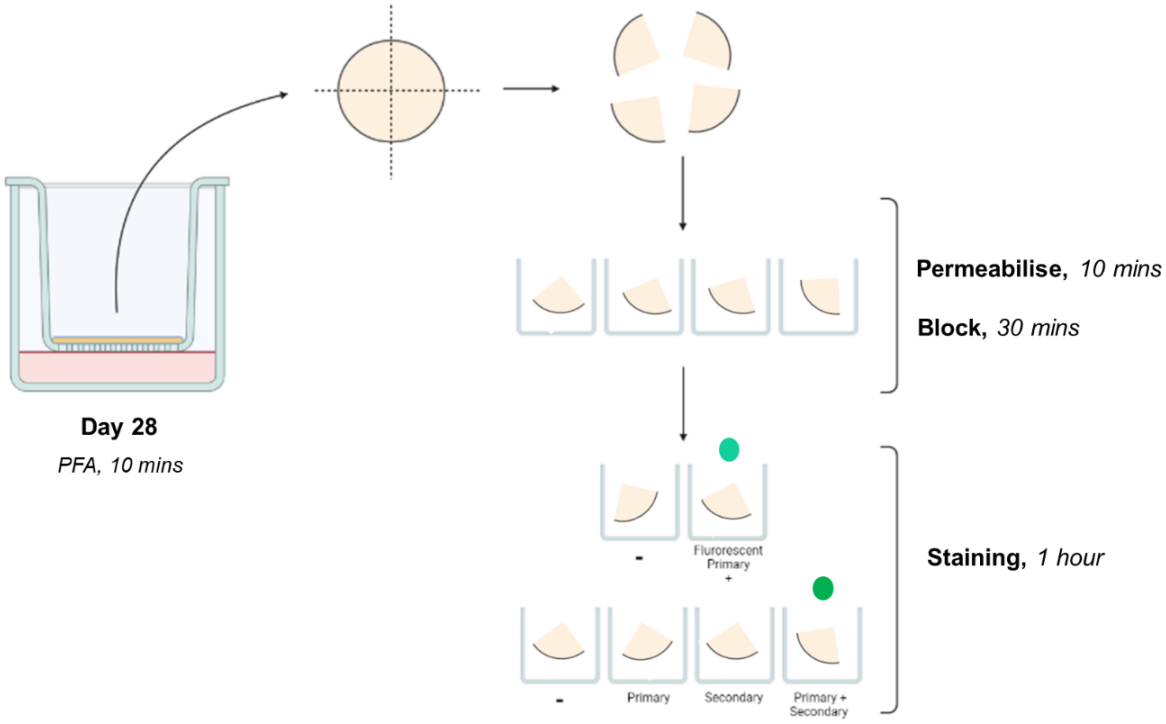


Figure 2.3 Transwell preparation and staining *Transwell samples were fixed at day 28 in PFA for 10 minutes, before careful separation of the membrane from the insert plastic. Membranes were sectioned into 4 quarters to increase experimental material. Samples were permeabilised, blocked, and then stained for specific cell markers. Fluorescent conjugated primary, or a primary and corresponding fluorescent secondary antibody were used. Individual figure components rendered in Biorender.*

2.1.6.3 Confocal microscopy

Sample slides were imaged on a Carl Zeiss Leica LSM710 confocal microscope, and samples were imaged at 40x magnification with water immersion, using the microscopes lasers and filters (Lasers: 405 nm Diode laser, Argon/2 (458, 488, 514 nm), HeNe1 (543/561 nm) and HeNe2 (633 nm), Fluorescence Filters: DAPI, Rhodomine (red) and FITC (green)). Imaging and image processing was carried out using Zeiss ZEN black software.

2.1.7 Plate preparation for bacterial culture and vector generation

Plates for bacterial growth were prepared by heating a bottle of solid pre-made agar in the microwave, in short bursts to prevent boiling over and spillage. Agar bottle was periodically removed and swirled to incorporate all solid agar. Completely liquid agar was kept in a 60°C incubator until needed or left to cool for 15 – 20 minutes before plate pouring. Labelled plates were laid out ready for use, and required antibiotic was added to cooled agar mixture. For Kanamycin plates, 200 µl of Kan50 (50 mg/ml) was added per 200 ml agar, and for Ampicillin plates, 200 µl Amp100 (100mg/ml) was added per 200 ml agar. Plates were poured and swirled carefully to cover bottom of the plate. Plate lids were left off as plates cooled to prevent condensate build up, for around 20 – 45 minutes, before plates were stacked upside down and stored at 4ºC until use.

2.1.8 Bacterial Transformation

Plasmid vectors were reconstituted in DNAse free water. Reconstituted vectors were added to thawed competent GT115 *e.coli* or DH5α *e.coli* at a ratio of 1:20. Combined bacteria and vector were kept on ice for 30 minutes, after which samples were heat shocked for 45 seconds at 42°C in a pre-heated water bath. Samples were removed and incubated on ice for 5 minutes, after which 200 µl SOC media was added to each sample at room temperature (25ºC). Samples were left in a shaking incubator at 32°C for 1 hour. 100 µl of each sample was used to lawn onto plates, one plate per sample. Plates were incubated in a static incubator overnight (12 – 16 hours).

After incubation overnight, individual colonies were picked from plates using a sterile 200 µl pipette tip per colony. Colony and tip were deposited into 5 ml liquid broth (LB) and left in a shaking incubator overnight (12 – 16 hours) with lids partially closed and taped.

2.1.9 Vector preparation

Bacterial cultures (5 ml) were visually observed for turbidity. Completely turbid samples were deposited into conical flasks containing 500 ml fresh broth and returned to shaking incubator overnight at 32ºC.

Large scale cultures were observed for opacity. Fully turbid samples were deposited into 500 ml spin bottles and weighed to ensure all samples would be balanced when deposited into the centrifuge. Sample bottles were loaded into a large scale floor standing centrifuge (Beckman Coulter) and spun at

6000g for 15 minutes, 4ºC. All liquid was then carefully poured from spin bottles to avoid disturbing the bacterial pellet. At this stage, bacterial pellets could be frozen and stored at -20 ºC if all liquid was removed. Bottles were stored lid down at -20 ºC to prevent any remaining traces of liquid from resuspending the pellet before freezing.

Bacterial pellets were prepared following the Qiagen Maxiprep protocol as outlined in the Qiagen plasmid purification handbook (version 02/2021, pages 23 – 29), using all reagents included in the Qiagen maxiprep kit.

2.1.9.1 Vector sequences

Plasmid vectors used included PMV-GLuc-2 (pCMV-GLuc 2) (Figure 2.4), a control plasmid for expressing Gaussia luciferase (NEB, Catalog # N8081), pGM206, and pGM206SMAR, which also expressed luciferase. These enhanced plasmids were designed to reduce transience of expression and enhance transfection. Both edited plasmids were smaller than the reporter plasmid to improve cellular uptake during transfection, and both included the GLux gene for luciferase expression. Both plasmids were designed to be CpG free, to aid in evasion of host immunity and further contribute to prolonged expression. A scaffold matrix attachment region (S/MAR) was inserted into pGM206SMAR after the Apa1 site, to aid in reducing transience of expression (Figure 2.5).

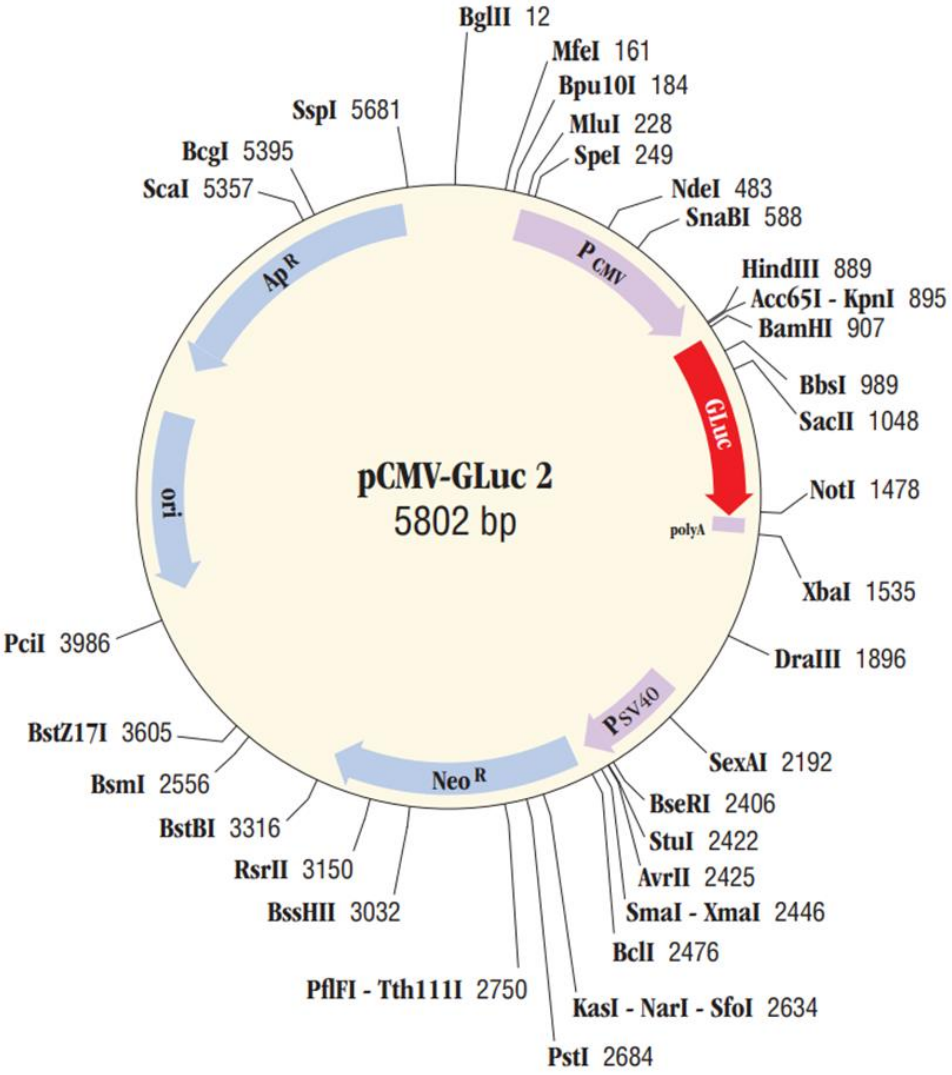


Figure 2.4 PMV-Gluc-2 Gaussia Luciferase plasmid map *pCMV-GLuc-2 is a mammalian expression plasmid that constitutively expresses secreted Gaussia luciferase, driven by a CMV promoter. pCMV-GLuc-2 plasmid was purchased originally from New England bioLabs (Catalog # N8081). Plasmid map created by New England Biolabs. (https://www.neb.com/products/n8081-pcmv-gluc-2-control-plasmid).*

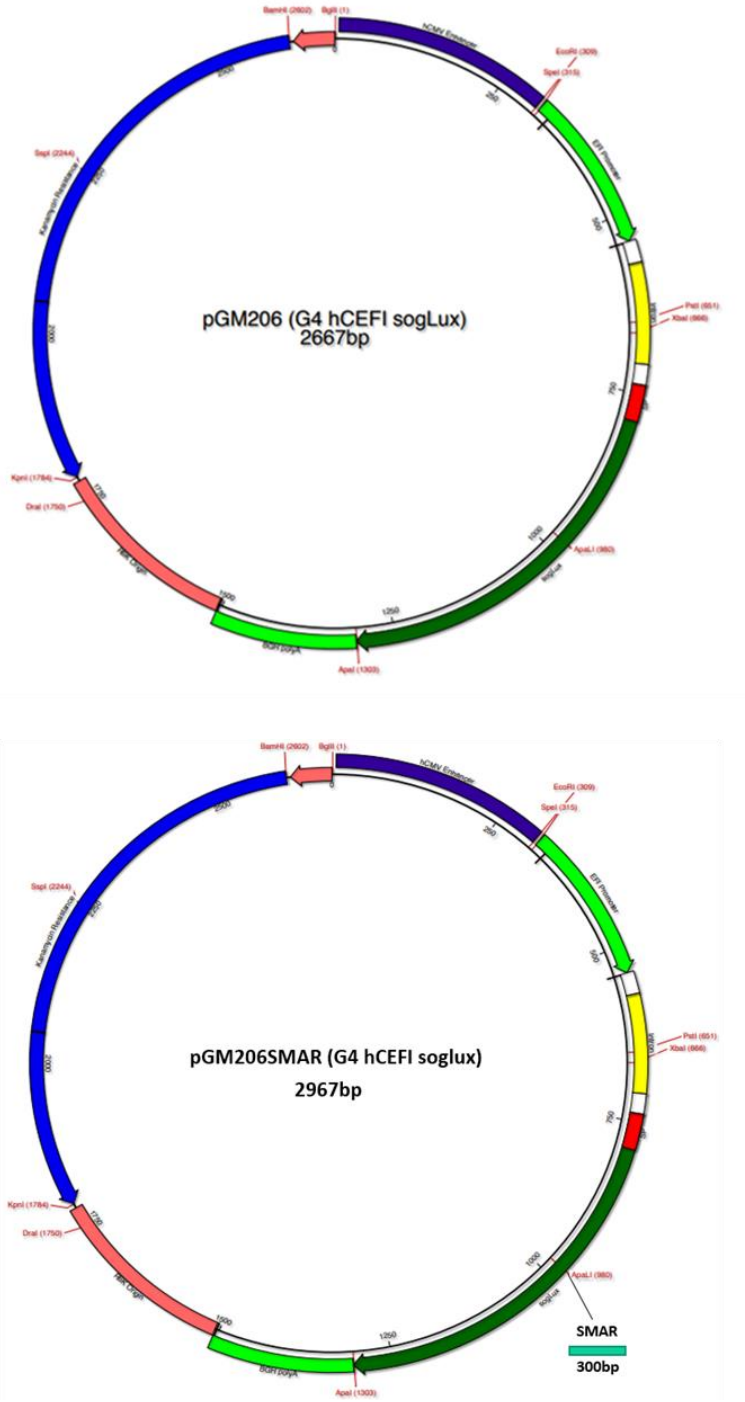


Figure 2.5 Enhanced luciferase plasmid maps *Enhanced plasmids that also expressed luciferase were used, named pGM206 and pGM206SMAR. Both plasmids were identical in sequence, apart from a single 300 bp Scaffold matrix attachment region (SMAR) inserted at the Apa1 site of pGM206SMAR. SMARs play some role in regulation of gene expression due to their structural role in chromatin organisation, so a SMAR site was added to pGM206 to make pGM206SMAR. This was to aid in prolonging previously transient expression.*

2.1.10 Transwell culture transfection

Transwell cultures were transfected at specific timepoints post Day 28 (4 weeks post air lift) dependent on individual assay. FLR, FLH, and both peptides in complex were used to deliver plasmid DNA. DNA vectors used for transfection (PMV-GLuc-2, pGM206 and pGM206SMAR) all contained the luciferase gene. For a single transfection, 2 µg of DNA was used per transwell as the standard unless stated otherwise. Transfections were carried out at a ratio of 0.85 µl FLR: 1 µg DNA. DNA volume was determined from DNA stock concentration (ng/µl) and combined with 25 µl Optimem for each sample. The volume of FLR used was determined according to the above ratio and combined with 25 µl Optimem per sample. Solutions of peptide and DNA were made up separately, then combined and left for 15 minutes to ensure nanoparticle formation. Media was changed on all samples whilst combined peptide and DNA solution was incubated at room temperature (25ºC), before 50 µl transfection solution was deposited per transwell into the basal chamber. Plates were gently shaken by hand to mix transfection into media, and left overnight in an incubator at 37ºC, 5% CO_2.

2.2 Precision cut lung slices (PCLS)

2.2.1 Animals

Lung sets were taken from 8-week-old BalbC male & female mice (Charles River, UK), with all animal procedures approved by the Animal Welfare

Ethical Review Board (AWERB) specifically to collect and use mouse tissue for non-ASPA purposes (approval number 000078).

2.2.2 Agarose preparation

Low melting point agarose (LMPa) was used in powdered form (Sigma, A9414-100G). Agarose was weighed and mixed with sterile PBS within a cell culture hood to make a 2% agarose liquid solution (2g LMPa: 200 ml liquid). The solution was then heated in a microwave for 2 – 3 minutes in 30 second intervals, to ensure agarose had fully dissolved. When no more agarose powder could be observed out of solution, melted agarose was returned to the hood and aliquoted into 1 ml eppendorfs whilst still warm. Tubes were left to cool at room temperature before storage at 4ºC until use.

2.2.3 PCLS Generation & storage

For PCLS generation, mice were humanely euthanized with sodium pentobarbital injection, followed by thigh femoral severing post death to confirm heart cessation. Chest cavity was dissected open to expose lungs, and cannulation of the trachea was performed to allow for insertion of a thin tube for agarose perfusion. The tube was carefully secured in place with thread.

Using a 1 ml syringe, 1.2 ml of agarose (2% LMPa) was perfused into the lungs, followed immediately by 0.3 ml air from a clean 1 ml syringe. Lungs

were then washed with cold PBS. After 2 – 3 washes, lungs were carefully extracted whole from the chest cavity, and stored in media (DMEM, Gibco). Lung lobes were separated, mounted and sliced using a Leica VT1200S vibrating microtome to produce 250 µm thick PCLS, with tissues kept on ice during slicing. PCLS were left to equilibrate in media overnight before any further processing. After this, PCLS were deposited in cryovials in 1 ml freezing solution (FBS, 10% DMSO), and vials were slow cooled at -80ºC in isopropanol or coolcell freezing containers (Sigma, CLS432001) before deposition in liquid nitrogen for long term storage (Figure. 2.6).

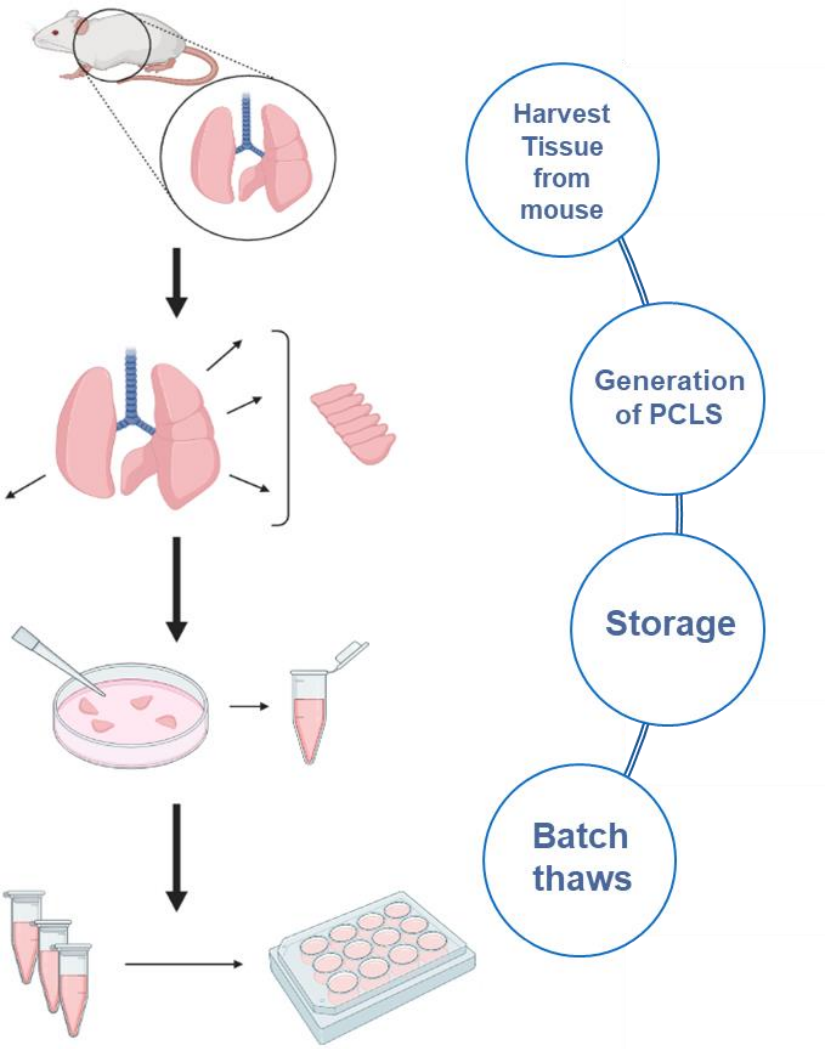


Figure 2.6 Precision Cut Lung Slice (PCLS) Method of Generation and storage *to generate PCLS, lung sets were agarose perfused before dissection, and removed after agarose had cooled and set to prevent leaking. Lobes were separated and sliced individually on a vibratome and kept cold on ice. Batches were stored long term in liquid nitrogen, 6 slices per vial, and thawed as needed for each planned experiment. Multiple batches were used per experiment. Individual figure components rendered in Biorender.*

2.2.4 General culture

Vials of PCLS contained n=6 samples, and were thawed and utilised for transfection, quantitative, and visual analysis as needed. Vials were removed from liquid nitrogen storage and rapidly thawed in a water bath at 37 ºC for 1 – 2 minutes maximum. Once 50% thawed, PCLS were deposited into 5 ml media (DMEM, Gibco) one vial per well, in a 6 well plate. Media in each well was changed 3 times, before individual plating of PCLS into a 24 well plate by carefully selecting an individual slice and gently lifting with a sterile pipette tip. After initial thaw (referred to as Day 0), PCLS were incubated in media with daily media changes on Day 1 and 2 to allow removal of DMSO & aid in recovery from thawing. An initial prestoblue viability assay was carried out on Day 3 post thaw.

2.2.5 PCLS Assay timeline

At point of thaw, PCLS were at Day 0; media was changed on the following two days, and a Prestoblue assay was carried out on the third day, referred to as Day 3 post thaw or Day 3 Pre transfection. Media was changed again on the fourth day, and samples were transfected on Day 5 (T5). Days were numbered after this point as Day post transfection, and luciferase assays were carried out on Day 1 (T5D1) Day 2 (T5D2), Day 3 (T5D3), Day 7 (T5D7), Day 10 (T5D10), and Day 14 (T5D14). Prestoblue assays were carried out post transfection, to compare to initial prestoblue assay carried

out on day 3 pre transfection, with viability assays taken on Day 3 (T5D3), Day 7 (T5D7), Day 10 (T5D10), and Day 14 (T5D14) (outlined in Figure 2.7).

2.2.6 PCLS Viability assay

Viability of PCLS was determined with a Prestoblue assay (PrestoBlue™ Cell Viability Reagent, Invitrogen). Media was removed and each PCLS was washed with 1 ml sterile PBS. The PBS wash was removed, and a 1:10 Prestoblue in HBSS solution (Hanks' Balanced Salt solution, Sigma) was added, 200 µl per PCLS. Prestoblue solution was removed at 90 minutes, or when initial colour change was seen from blue to pink within the control sample. 50 µl of Prestoblue solution was removed from each sample and deposited into a black 96 well plate (Corning® 96-well Black Flat Bottom), and plates were read on a TECAN infinite 200PRO multimode reader, at excitation/emission 560 nm/590 nm. Viability data was normalised by weight of sample, to give fluorescence per mg tissue.

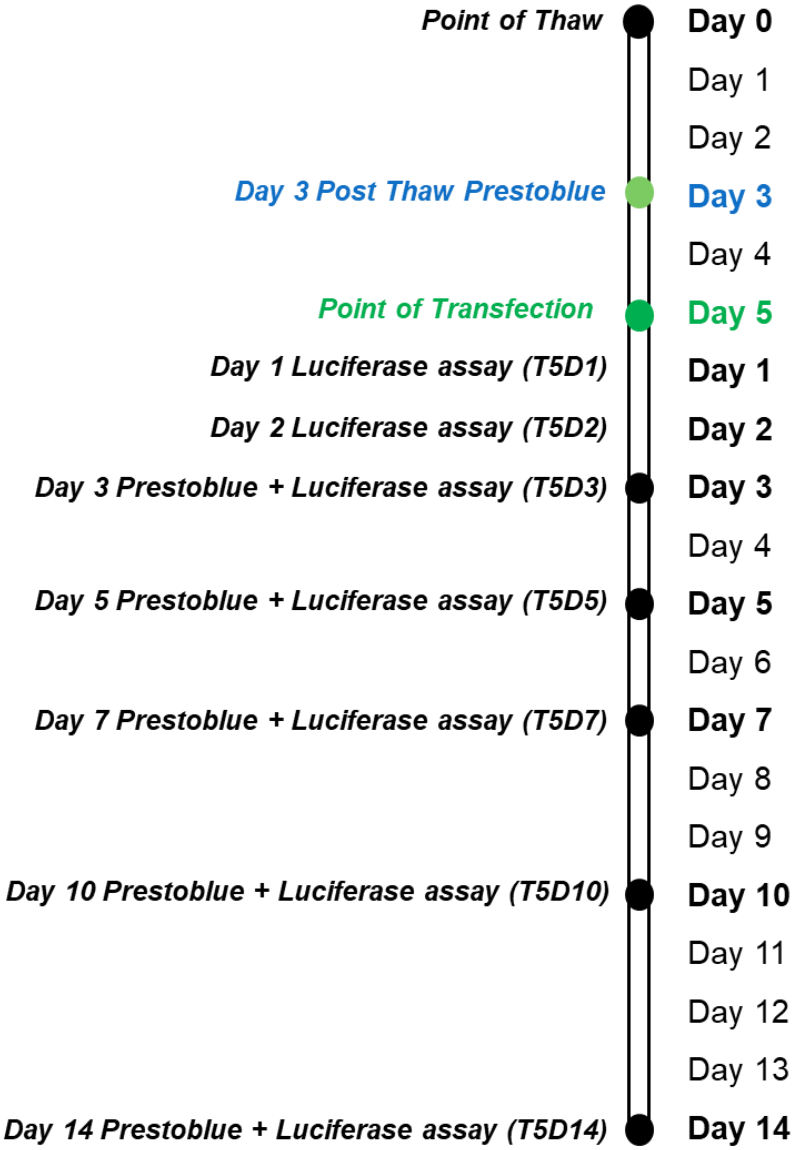


Figure 2.7 PCLS assay Timeline *Precision Cut Lung Slices (PCLS) were thawed on Day 0. A post thaw viability assay was carried out with prestoblue on Day 3 post thaw. All days after point of Transfection (Day 5) were numbered as day post transfection. Luciferase assays and Prestoblue assays were carried out on specific days to measure expression and viability post transfection.*

2.2.7 PCLS Transfections

PCLS were transfected 5 days post thaw. Transfections were carried out using the GET peptide FLR, FLH, and commercial transfection systems jetPEI® (Polyplus transfection), Lipofectamine2000, and Lipofectamine3000 (Invitrogen). DNA Vectors used for transfection were PMV-GLuc-2, pGM206 and pGM206SMAR. For a transfection, 2 µg of DNA was used per PCLS within a 24 well plate, 1 PCLS per well, as the standard. Transfections for PCLS were carried out at a ratio of 1.7 µl FLR: 1 µl FLH: 2 µg DNA and 1.7 µl FLR: 2 µl FLH: 2 µg DNA dependent on assay. DNA volume was determined from working DNA stock concentration (ng/µl) and combined with 25 µl Optimem for each PCLS. The volume of FLR and FLH used was determined according to the above ratio and combined with 25 µl Optimum per PCLS. Solutions of peptide and DNA were made up separately, then combined and left for 15 minutes pre transfection to ensure nanoparticle formation. Media was changed on all PCLS whilst combined peptide and DNA solution was incubated at 25ºC, before 50 µl transfection solution was deposited on each PCLS sample.

2.2.7.1 Luciferase expression assay for transfection efficiency

Transfection efficiency was measured using a Gaussia luciferase expression assay. After initial transfection with a luciferase vector, PCLS were left to incubate overnight, after which 10 µl of media was taken from each sample and deposited into a white 96 well plate (Corning® 96-well, White Flat

Bottom). Complete luciferase solution was made with luciferase buffer and substrate combined at 1:100 dilution (substrate: buffer). complete luciferase solution was added to samples wells at 50 µl per well, and the plate was immediately read on the Tecan infinite M200 plate reader (Luminescence mode, Integration time 500 ms).

2.2.7.2 Centrifugation of transfections

Standard transfections were carried out as described previously, with specific conditions spun in a benchtop centrifuge immediately post transfection; 300g, 5 minutes, 25ºC. Plates were spun and post spin media change was carried out as required before return to incubation, 37ºC, 5% CO^2.

2.2.8 LiveDead assay

A LIVE/DEAD ® Viability/Cytotoxicity Kit was used for LiveDead staining (Molecular probes, 03224) and staining was carried out in accordance with manufacturer's instructions. Minor amendments were made to optimise assay for staining PCLS. PCLS were washed with sterile PBS to remove any media. Dead stain was added to PBS at a 500-fold dilution, and gently vortexed. Live stain was added to PBS and Dead stain solution at a 2000-fold dilution, and final solution was vortexed gently to mix. As standard, 200 µl of Livedead stain solution was used for each PCLS. PBS was removed from samples and LiveDead stain solution was added in a cell culture hood

with the light turned off. The plate was then covered and incubated at room temperature for 20 minutes, before stain was removed and samples were washed twice with sterile PBS. Samples were imaged in 200 µl PBS on a fluorescent microscope with an incubator box.

2.2.9 Wax embedding of samples

PCLS samples were fixed in Formalin for 1 hour room temperature, or 4ºC overnight. Samples were deposited into snap shut meshes and stored inside plastic cassettes within petri dishes. Petri dishes were filled with PBS to prevent samples from drying out. Samples were taken to QMC Histology department for wax embedding.

2.2.10 Microtome of wax embedded samples

Wax embedded samples were kept on ice before each sample block was sliced on a microtome to 5 µm thickness, with each individual slice mounted on a separate labelled slide. Once mounted and labelled, all slides were deposited in a dryer oven for 3 hours, at 57ºC. Slides were stored at 25ºC in slide boxes until immunohistochemistry was carried out.

2.2.11 Immunohistochemistry

Paraffin wax embedded tissue samples were submitted to the histology department, QMC hospital, Nottingham. Select samples were submitted for

microtoming, and other samples for both microtoming and haematoxylin and eosin (H&E) staining.

2.2.12 Statistical Methods

All statistics were carried out using GraphPad prism software (Version 7). Where relevant, data was analysed using an ordinary one-way ANOVA statistical test. Standard deviation bars were applied to bar and line graphs, and statistical significance was displayed as asterisks (*, **, ***) where * denotes $p< 0.05$, ** denotes $p< 0.01$, and *** denotes $p< 0.001$ significance. All error bars represented standard deviation (SD).

2.2.13 Gelatin PCLS

2.2.13.1 Gelatin preparation

Gelatin was weighed to create 10% and 12 % gelatin solutions in sterile dH2O. Powdered Gelatin (from bovine skin, Sigma, G9391) was added to cold dH_2O, and the combined solution was heated in a water bath at 40ºC to ensure gelatin melted into solution. Once fully homogenate, gelatin solution was aliquoted into 1 ml eppendorfs in a cell culture hood. Any remaining gelatin solution was stored in plastic 100 ml volume beakers. Gelatin was left to solidify at room temperature before storage at 4ºC long term.

2.2.13.2 Gelatin perfusion

Gelatin perfusion of murine lung sets was carried out similarly to the previously described agarose perfusion (2.2.3 PCLS Generation and Storage). Gelatin aliquots were heated in a dry heating block to 37ºC until liquid before dissection, then cooled to around 20 – 25ºC before perfusion into the lung set via a thin tracheal tube. 1.2 ml gelatin was used, followed by 0.3 ml air. Lungs sets were washed with cold PBS to allow gelatin to set before excision and storage in cold media.

2.2.13.3 Storage

All Gelatin PCLS generation and storage was carried out as previously described for agarose PCLS. (1.2.3 PCLS Generation and Storage). With Gelatin PCLS, care was taken to keep samples on ice when at room temperature, to maintain a low temperature for samples and maintain gelatin in a set state.

2.2.13.4 Thawing and General culture

Gelatin PCLS were thawed in a similar manner to agarose PCLS; vials of frozen Gelatin PCLS were thawed as rapidly as possible, and all reagents and plasticware used was kept on ice as much as possible to keep temperatures of samples low.

2.2.13.5 LiveDead assay

Livedead Assay was carried out as previously described for agarose PCLS. Livedead was carried out on fresh (not previously frozen or thawed) Gelatin PCLS, at 12 hours post incubation.

3. Chapter 3: Utilising Precision Cut Lung Slices (PCLS) as an in vitro model in which to demonstrate non -viral delivery

3.1 Introduction

An important part of a successful gene delivery product is translatability; delivery needs to be demonstrated in cells and potential models to confirm successful delivery and eliminate possible complications by demonstrating safety and efficacy. An *ex vivo* tissue model contributes in part to that, by providing a more elevated system than a single cell monolayer in which to test delivery. An *ex vivo* tissue model such as precision cut lung slices (PCLS) generated from various animal lung tissue, or even human tissue explants, could be key in effective demonstration of various methods of viral and non- viral delivery.

Mouse PCLS were generated, frozen and utilised to demonstrate transfection efficiency of the GET peptide system. A variety of delivery parameters were investigated, such as DNA dosage, serialised delivery, comparison with commercialised non-viral delivery agents, delivery of enhanced gaussia luciferase vectors, effect of physical force of transfection uptake, and potential effects of serum free conditions on transfection and overall viability.

3.2 Demonstration of transfection in PCLS

Precision cut lung slices (PCLS) were transfected to determine levels of expression post-transfection using the GET peptide system. A reporter plasmid for luciferase (PMV-GLuc 2) was delivered to PCLS samples, with untransfected PCLS as an experimental control. FLR peptide was used to deliver the reporter plasmid, with FLR:FLH complexed peptides used at both full dose (2 µg per PCLS) and half dose (1 µg per PCLS), denoted as FLR:FLH 1 and FLR:FLH 0.5 respectively. This was to determine potential optimum amount of peptide to use for PCLS delivery. Lipofectamine3000 was also used as comparison to a commercial delivery system.

All transfected samples showed significant difference in expression from the untransfected control. Expression appeared to be highest for the majority of transfected conditions between the first and third day post transfection, with steady decline in expression towards the final day of assay (Day 14). Lipofectamine3000 showed higher levels of expression between day 3 and day 14 comparative to other transfection conditions, however by final day of assay no expression was significantly higher than the untransfected control. Only condition FLR:FLH 0.5 showed any significant difference comparative to untransfected samples at day 14 (Fig. 3.1).

FLR:FLH complex at full dose (FLR:FLH 1) demonstrated minimally higher expression than FLR:FLH complex at half dose (FLR:FLH 0.5) and FLR over time. However, this expression was minimal and did not appear to be statistically significant (Fig 3.1).

Overall, PCLS proved to be easily transfectable under a variety of conditions. Both the GET peptide system and a comparable commercial agent produced high early expression in samples, with similar patterns of declining expression observed across all samples, regardless of the transfection agent used. All initial expression observed was significant comparative to untransfected controls, with lipofectamine sustaining higher expression 1 week post transfection than other conditions. Despite this, all transfection conditions showed similar levels of expression at final day of assay.

Despite some minimal expression increase between FLR conditions, no actual significant difference was observed between FLR peptide used alone, FLR:FLH 0.5, or FLR:FLH 1, demonstrating that amount of peptide used may not be effective in drastically increasing expression within PCLS. It is important to note uneven n numbers for conditions during experimentation; with increased or more even n numbers per condition, more significant differences may have been seen in terms of expression.

3.3 PCLS viability compared pre and post transfection

Alongside measuring expression, viability of PCLS samples was also monitored pre and post expression with prestoblue assay. 3 days before transfection, all samples showed very similar viability, with no significant difference observed. At both 1 week and 2 weeks post transfection, samples showed minimal difference in initial pre transfection viability, with increased viability towards day 14. No significant difference could be seen between untransfected and transfected samples either pre or post transfection at any time point, indicating that transfection had not affected viability of PCLS. Samples continued to be viable at both initial point of transfection and during expression, up to final day of assay (Fig 3.2).

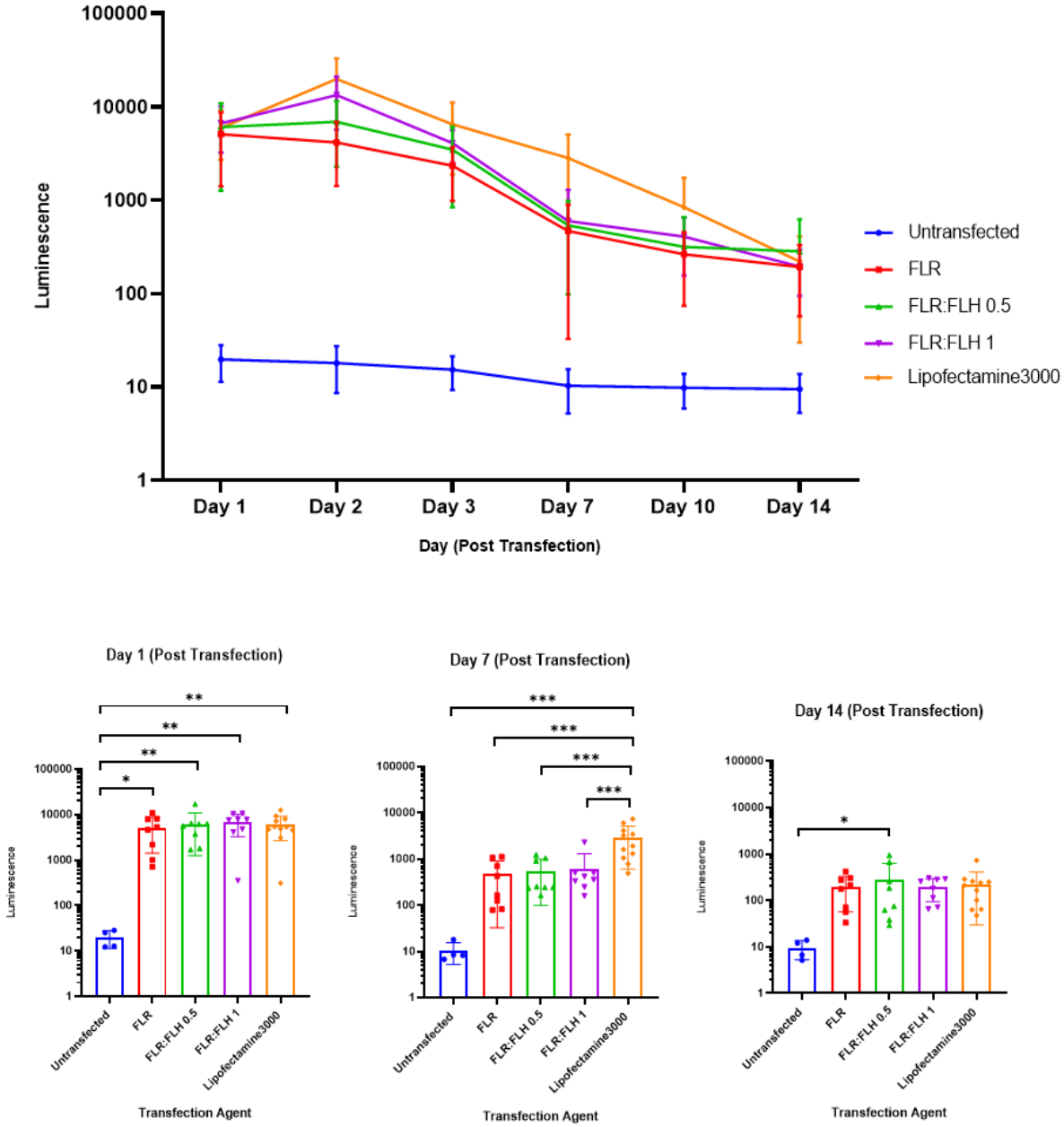


Figure 3.1 Demonstration of Transfection and subsequent expression in PCLS *Initial expression of all transfected samples was significantly higher than an Untransfected samples, demonstrating the transfectability of the PCLS model with both GET and a comparable non-viral delivery agent. Expression declined over time, regardless of delivery system used, with lowest expression seen on Day 14 in all conditions. untransfected control (n=4), FLR (n=8), FLR:FLH 0.5 (n=8), FLR:FLH 1 (n=8), Lipofectamine3000 (n=11). Error bars represent the standard error (s.d.)*

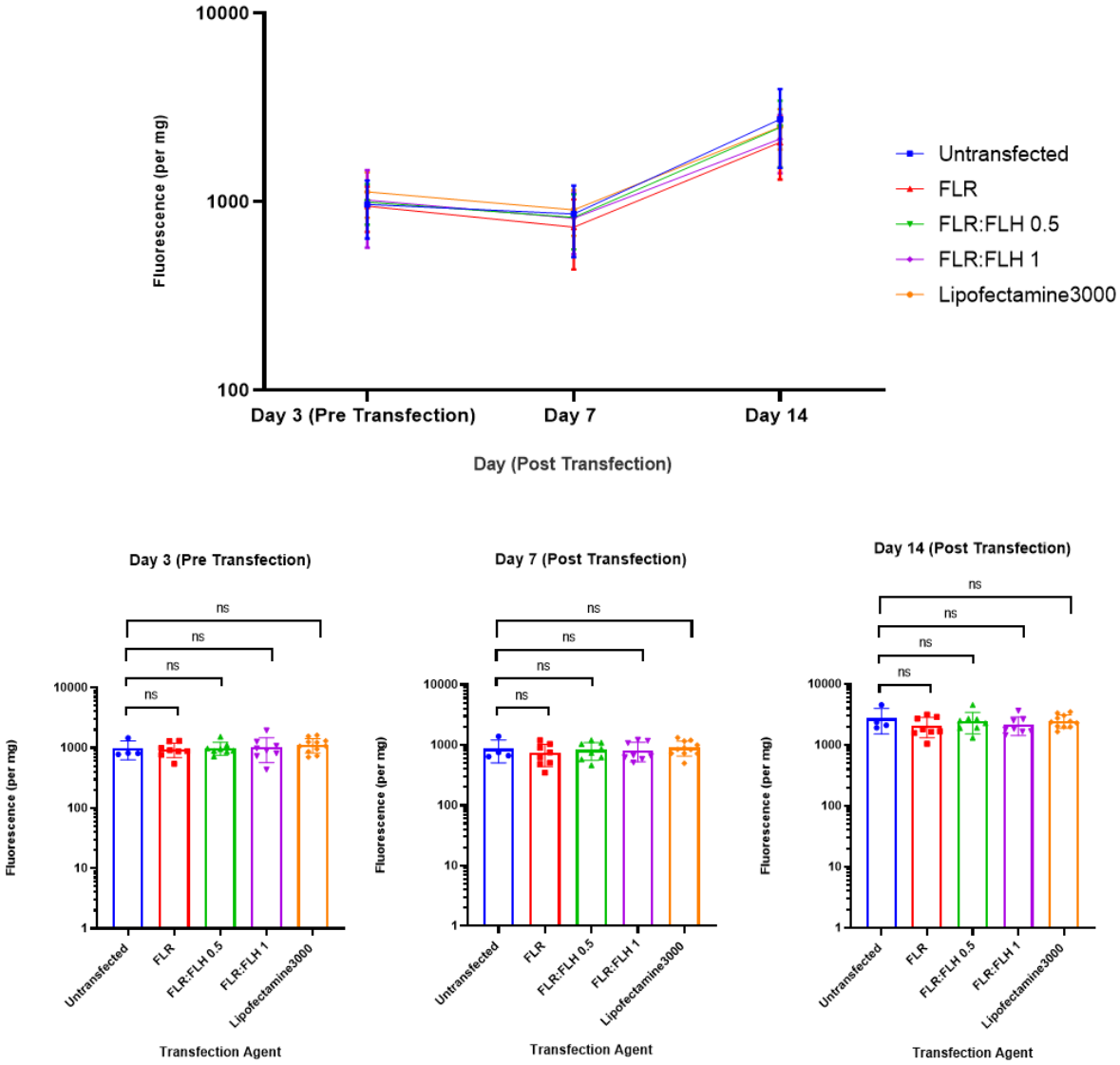


Figure 3.2 Demonstration of Viability in PCLS, up to 2 weeks post transfection *Transfected PCLS showed no significant difference in viability over time comparative to untransfected samples, indicating that transfection agents or cargo had no direct detrimental effect on sample viability, over 14 days to end of assay. untransfected control (n=4), FLR (n=8), FLR:FLH 0.5 (n=8), FLR:FLH 1 (n=8), Lipofectamine3000 (n=11). Error bars represent the standard error (s.d.)*

3.4 Visual qualitative analysis of PCLS viability post transfection

Viability of PCLS during transfection was also observed with qualitative analysis using a LiveDead assay. Samples were stained and imaged at Day 0, the day before transfection, Day 1 and Day 5 post transfection. Standard PMV Gluc-2 reporter plasmid was delivered with FLR:FLH complex and JetPEI, a comparable commercial agent, alongside an untransfected control.

At day 0, live cells (green) were easily observed in all samples. Some background fluorescence and individual dead cells (red) could also be observed. Live cells were most easily imaged around smaller airways or bronchioles (Figure 3.3). on the first day post transfection (Day 1) minimal difference could be observed in fluorescence from the previous Day 0. Individual dead cells could be seen, but overall, no significant red fluorescence was observed in any samples. Day 5 post transfection also showed similar levels of intensity in fluorescence for both live and dead, with some individual dead cells appearing more distinct in both untransfected control and PEI conditions.

Immunohistochemistry (IHC) was also carried out post- transfection, to observe potential effect of the transfection system on tissue structure and viability. A DNA only control was processed alongside FLR only and FLR:FLH samples, both delivering the standard luciferase plasmid PMV-Gluc-2. Nuclei in samples can be identified by Haematoxylin stain (blue-purple) and ECM and cytoplasmic regions can be identified by Eosin stain (pink). Both stains were identifiable in all samples, including untransfected

DNA only control (Figure 3.4). Across all samples, specific lung structures were easily identifiable, with most common structures being alveoli. The lung structure of the tissue slice remained open within all samples, and no visible differences could be observed between the control and transfected samples. Initial H&E stain of samples shown here helped to visually confirm the lack of difference in structure in untransfected and transfected samples, demonstrating the safety and lack of toxicity of the GET peptide system.

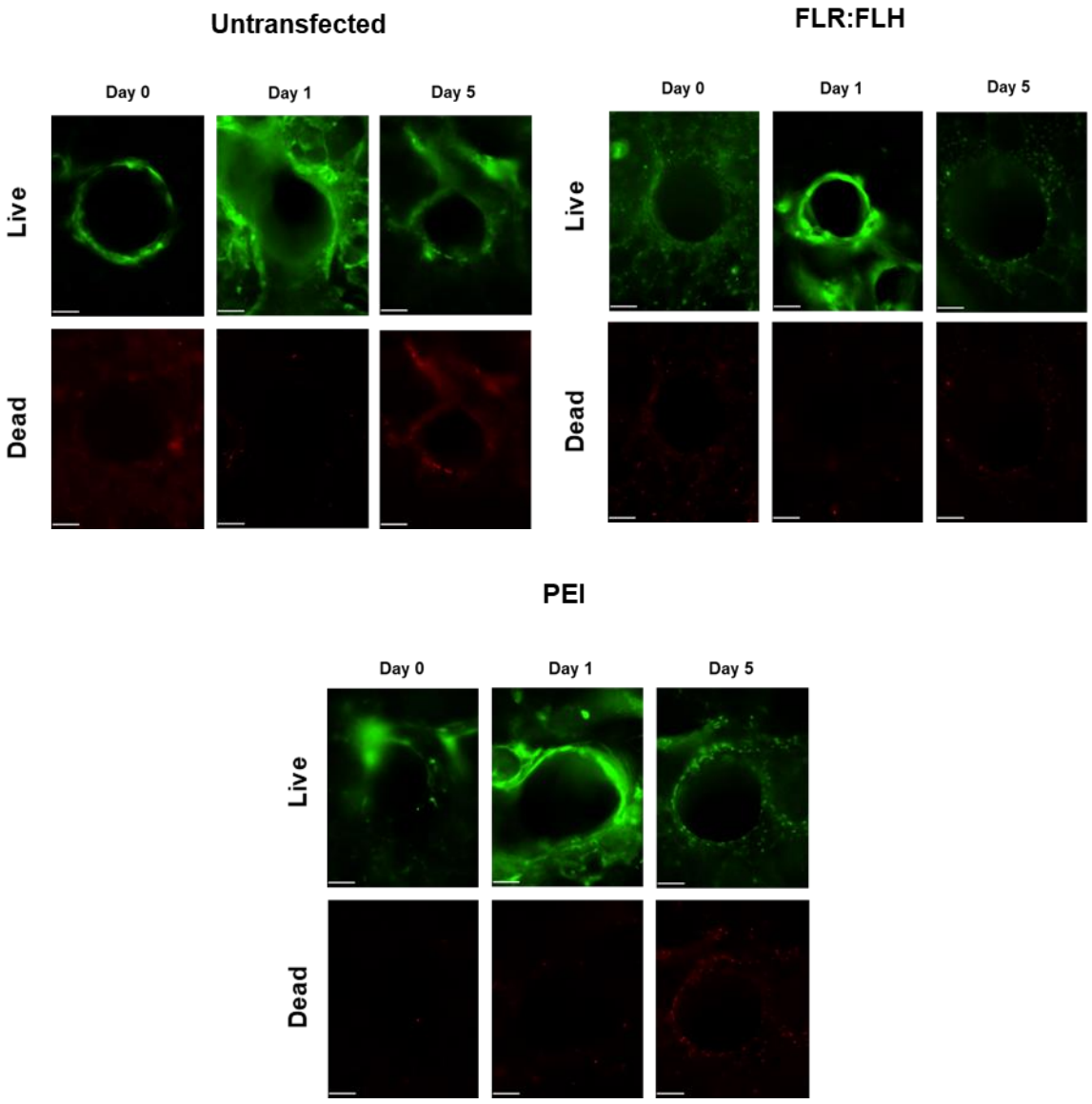


Figure 3.3 Livedead of PCLS before and after transfection *Minimal difference was seen in fluorescent intensity between untransfected PCLS or transfected samples, regardless of whether the GET peptide system or a commercial comparative system (PEI) was used. Samples were still viable at Day 5 regardless of condition, with minimal to no increase in dead cells across 5 Days. This indicated transfections were causing minimal to no toxicity issues in transfected PCLS. 20x objective, Scale bar 200 µm.*

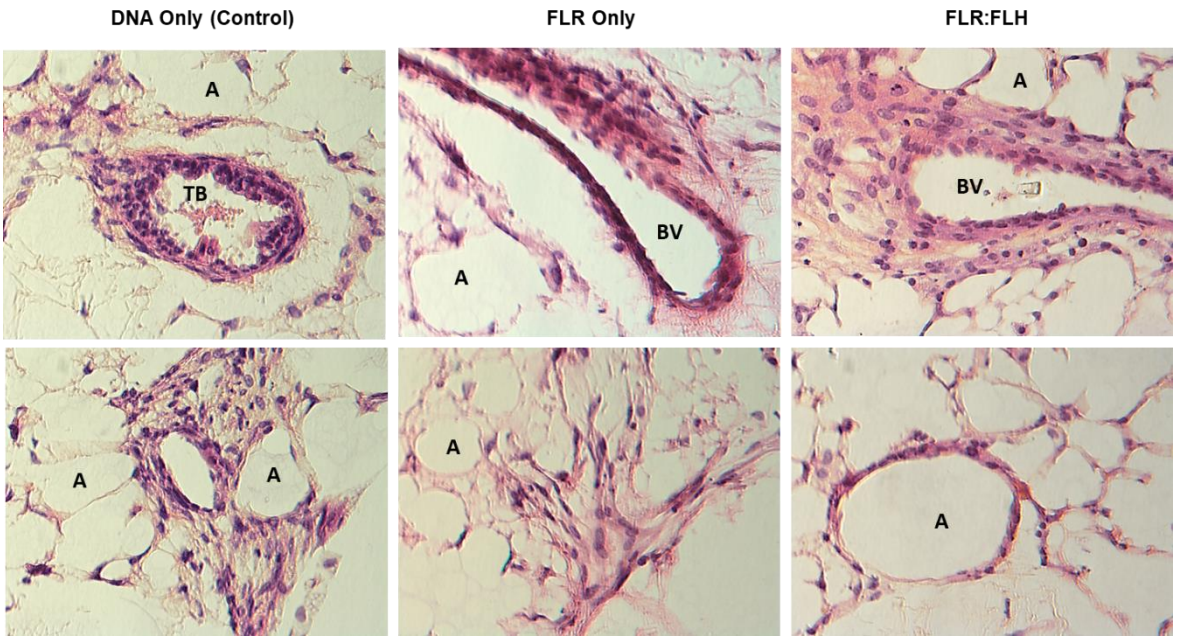


Figure 3.4 Haematoxylin and Eosin (H&E) staining of Untransfected and Transfected PCLS *A DNA only control was stained alongside samples where FLR peptide and FLR peptide complexed with FLH had been used to deliver plasmid DNA. Across all samples, common lung structures could be clearly identified, including Terminal Bronchioles (TB), Blood Vessels (BV), and Alveoli (A). 40x Objective, 3 µm sample thickness.*

3.5 Utilisation of enhanced plasmid

Alongside the reporter luciferase plasmid, enhanced forms of luciferase plasmids were utilised for optimisation of delivery to PCLS. These plasmids, termed pGM206 and pGM206SMAR, were designed to reduce transience seen with the standard reporter plasmid (PMV-GLuc-2). The overall aim was to improve longevity of expression. To optimise delivery within PCLS, standard reporter luciferase and enhanced luciferase plasmids were used to investigate optimal concentrations of DNA and the potential of serial delivery, to establish the effect this would have on the viability and expression profiles within the target tissue.

3.5.1 Variation of Plasmid Concentration

Standard Luciferase reporter plasmid (PMV-Gluc-2) was delivered to PCLS alongside two enhanced luciferase plasmids, pGM206 and pGM206SMAR. All plasmids were delivered at 1 µg and 2 µg, to investigate the effect of dosage on expression and viability profiles of PCLS tissue. All plasmids were delivered with FLR:FLH peptides in complex, as initial delivery (Figure 3.1) demonstrated some increased expression in PCLS comparative to FLR used alone.

All transfected samples demonstrated increased expression profiles comparative to an untransfected control, with standard reporter plasmid PMV-GLuc-2 demonstrating the highest initial expression. However, over

time, enhanced vector pGM206SMAR demonstrated highest expression when compared to other transfected samples, with most the noticeable difference in expression evident at day 3 post transfection. A sharper decline in expression was observed in the standard luciferase reporter plasmid, whereas a slower decline in expression over time was observed in both enhanced luciferase plasmids (Figure 3.5).

Despite some minimal differences in expression, no significant difference was observed between 1 µg and 2 µg in any plasmid used. Variation in plasmid concentration appeared to have minimal to no effect on expression profiles, regardless of whether standard or enhanced plasmids were used for transfection.

Viability profiles of all samples were also compared alongside expression profile data. Viability of untransfected samples appeared initially lower than transfected samples, but all samples followed a similar pattern over time of gradual reduction in viability towards day 14 (figure 3.6). Of significant note is the initial higher viability pre transfection of pGM206SMAR samples comparative to all other conditions, as there was no significant difference in viability between any other conditions independently. Post transfection, similar significant difference in viability was observed between pGM206SMAR samples and the untransfected control, along with specific 1 µg and 2 µg conditions.

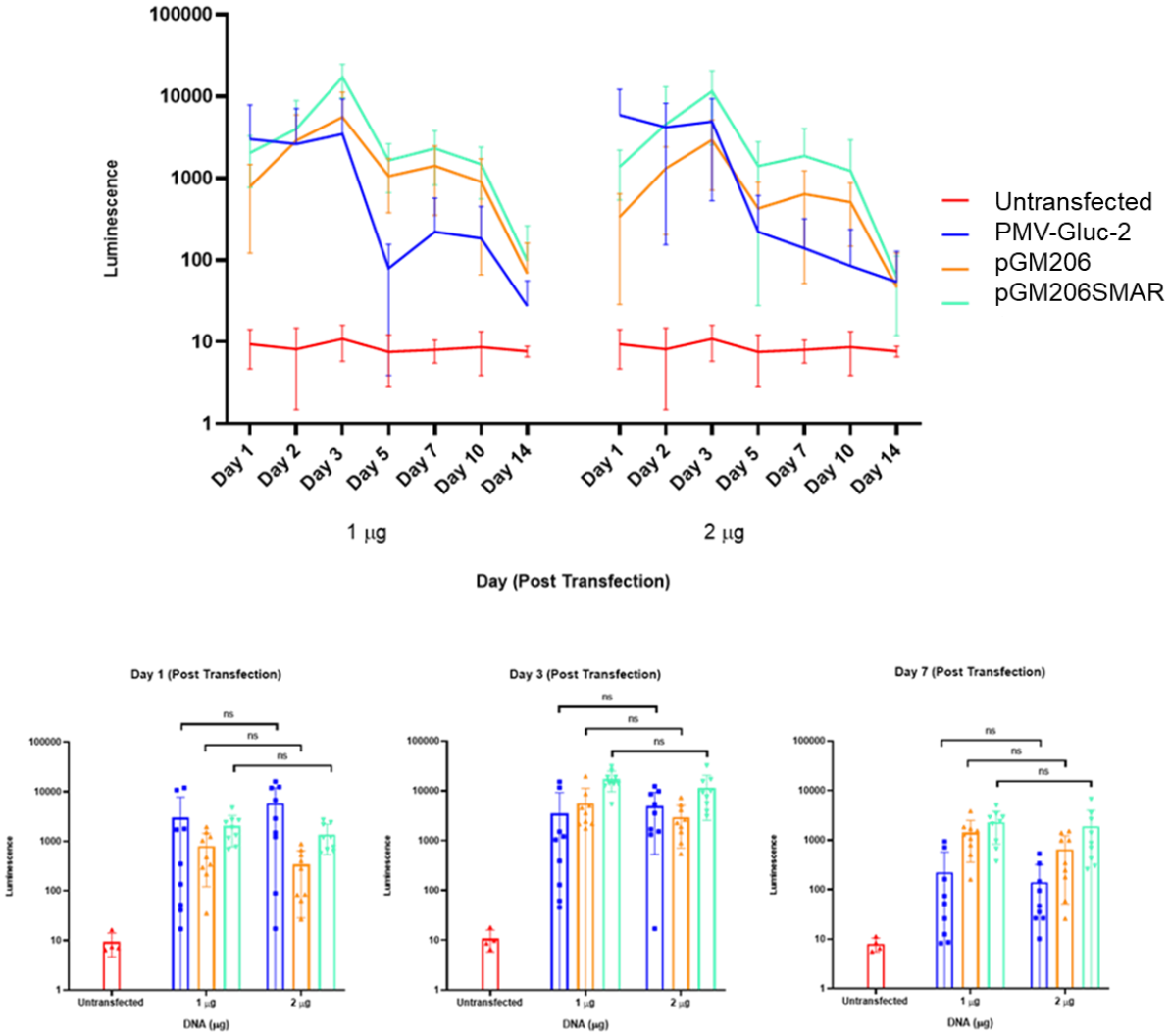


Figure 3.5 Comparison of DNA plasmid concentration variation on Expression in PCLS *Expression profiles of concentration variation demonstrated no significant differences between 1 µg and 2 µg doses, regardless of plasmid used. However, pGM206SMAR demonstrated an increased expression profile over time, comparative to all other plasmids used and an untransfected control. The largest difference in expression between transfected plasmids could be observed at Day 3 post transfection. untransfected control (n=4), all other experimental conditions (n=9). Error bars represent the standard error (s.d.)*

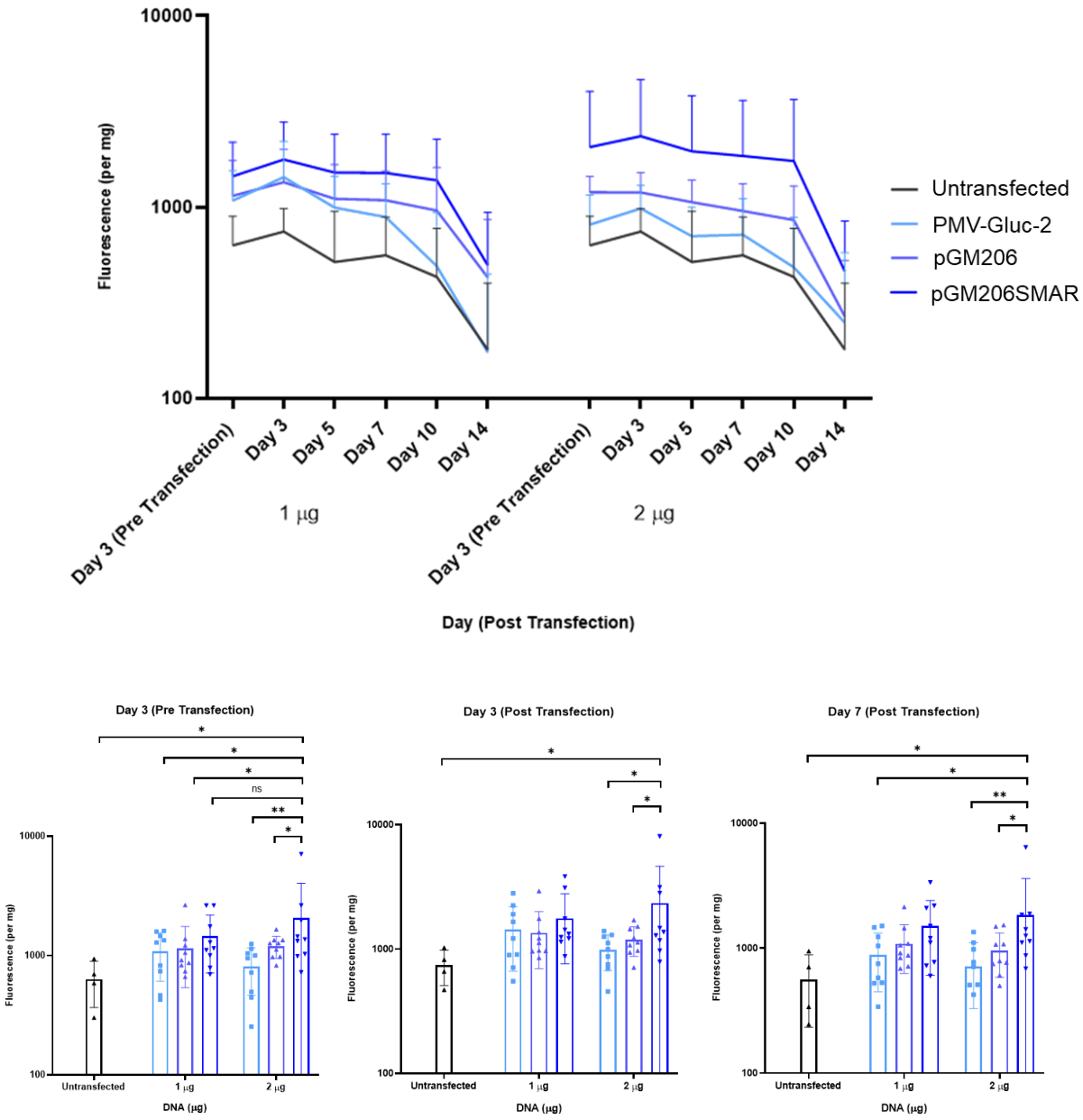


Figure 3.6 Viability of PCLS samples at differing plasmid concentrations over time *All conditions demonstrated a similar pattern of decline over time, with pGM206SMAR demonstrating highest viability. This was apparent in this experimental condition even pre transfection, highlighting the constant variability seen throughout PCLS experimentation. untransfected control (n=4), all other experimental conditions (n=9). Error bars represent the standard error (s.d.)*

3.5.2 Serial Delivery

Alongside concentration variation, serial delivery parameters were also investigated, to aid in optimisation of PCLS transfection and improvement of overall expression from tissue. Concentration variation (Figures 3.5, 3.6) was also employed alongside Serial delivery to determine if a combination of specific dosage delivered at specific intervals serially would have any effect on expression or viability profiles of PCLS.

Standard Reporter luciferase plasmid (PMV-Gluc-2) was delivered alongside both enhanced luciferase vectors, pGM206 and pGM206SMAR. 1 µg and 2 µg concentrations of plasmid were employed, and delivery was varied to every 2 days (E2D) and every 3 days (E3D).

When serial delivery was every 2 days (E2D), initial expression at Day 1 post transfection showed standard luciferase plasmid was significant comparative to other conditions (Figure 3.7). At day 3 post transfection, enhanced plasmid pGM206SMAR demonstrated higher expression at both concentrations than all other conditions, however this was not statistically significant. At a week post transfection (Day 7), minimal difference in expression could be observed between conditions.

When serial delivery was every 3 days (E3D), a clearer pattern could be observed across Day 1, Day 3, and Day 7 (Figure 3.7). Enhanced plasmid pGM206SMAR demonstrated highest initial expression that proved significantly different from other conditions, which continued in both Day 3 and Day 7 expression profiles.in E3D conditions, pGM206 demonstrated the

lowest expression profile over time, whilst standard luciferase plasmid demonstrated a similar expression profile to E2D serial delivery.

Alongside expression profile data, viability profiles could also be observed for samples to see if serialised delivery was affecting sample viability. Serial delivery every 2 days (E2D) showed a similar pattern in decline of all conditions, with standard luciferase reporter plasmid (2 µg) and enhanced plasmid pGM206 (2 µg) demonstrating the most decline in viability over time comparative to initial pre transfection viability (Figure 3.8).

Serial Delivery every 3 days (E3D) showed less variation between conditions, with most conditions declining at a similar rate, relative to their initial pre transfection viability. Enhanced plasmid pGM206 (1µg) demonstrated an unusual increase between day 10 and day 14. In both every 2 day and every 3 day serial delivery viability profiles, untransfected controls became unreadable between day 7 and day 10, but all other conditions still demonstrated viability up until day 14 (Figure 3.8).

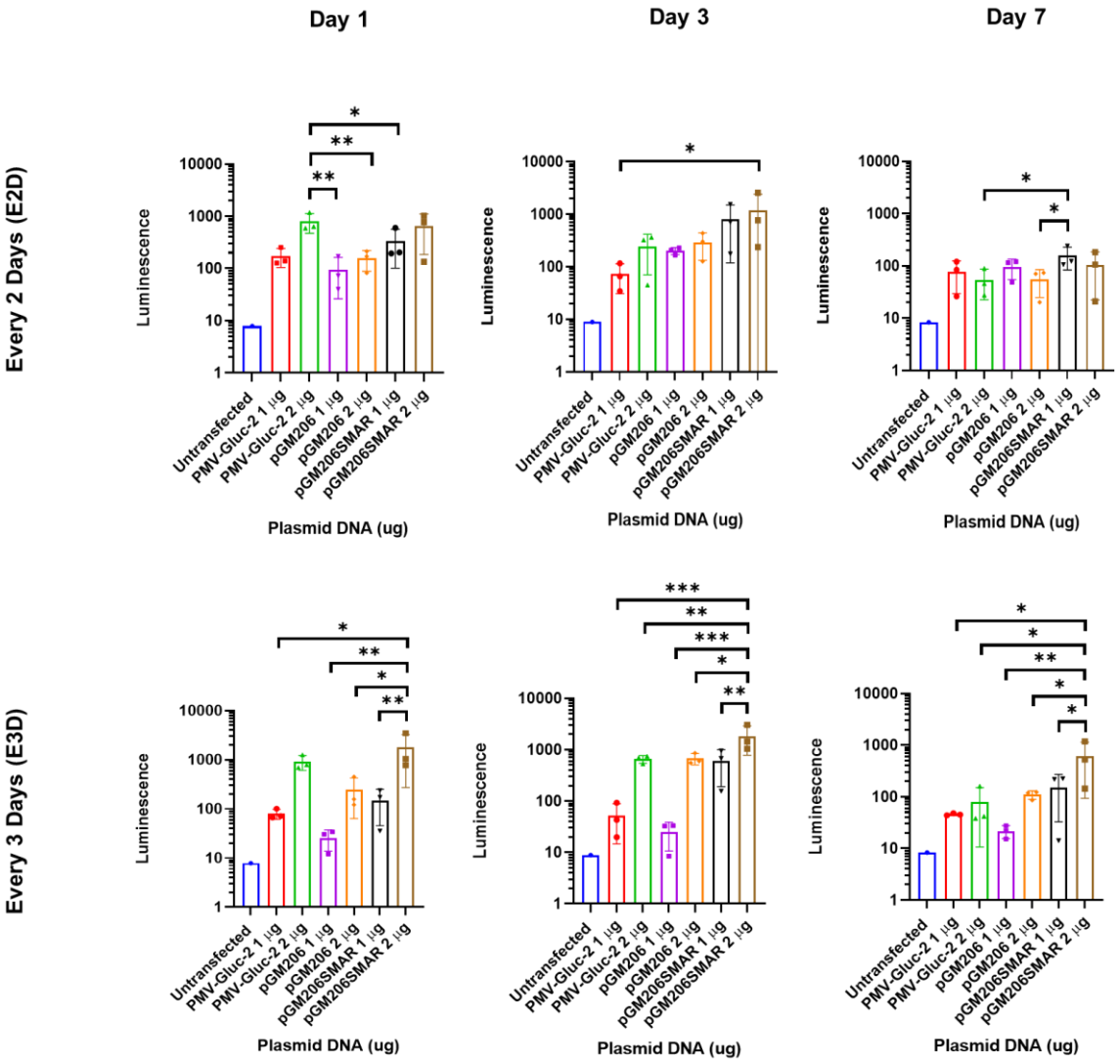


Figure 3.7 Expression profiles of PCLS Undergoing Serial Delivery every 2 days and every 3 days *Serial delivery took place every 2 Days (E2D), and every 3 Days (E3D). Little difference between plasmid concentration conditions was observed in E2D delivery, however some significant difference was observed in E3D delivery. Use of pGM206SMAR plasmid, particularly at 2 µg dose, appeared to show increased expression comparative to other plasmid conditions and concentrations. untransfected control (n=1), all experimental conditions (n=3). Error bars represent the standard error (s.d.)*

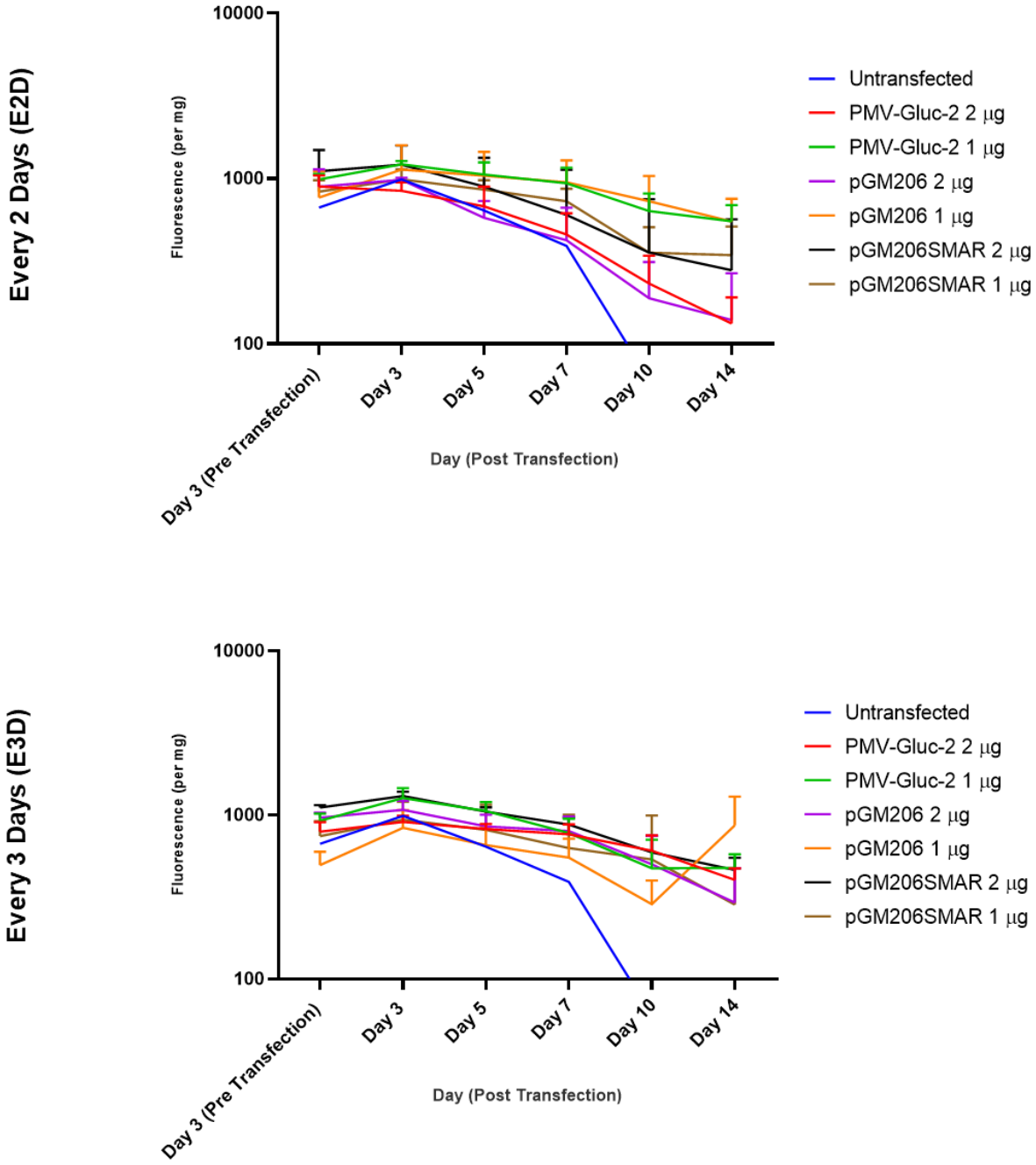


Figure 3.8 Viability of PCLS samples undergoing serial delivery *Decline was observed in all samples over time, particularly in the untransfected control group. Minimal difference was observed between serial delivery conditions or between individual experimental conditions, potentially indicating that point of delivery or plasmid used did not detrimentally affect sample viability of time. Untransfected Control (n=1), all other experimental conditions (n=3). Error bars represent the standard error (s.d.)*

3.6 Use of serum in PCLS culture

PCLS research is varied on the use of serum during culture; many studies opt for serum free conditions during PCLS experimentation, regardless of the type of study (Bryson, et al., 2020); (Li, et al., 2020); (Neuhaus, et al., 2018). However, no individual study has elucidated any potential issues or benefits to serum incorporation whilst culturing PCLS either short of long term. Not utilising serum during the culture process could be to reduce variability during experimentation; however, specific serum components may be key to maintaining the health and viability of a variety of cell types present within the explant tissue.

Thus, Serum presence was investigated as part of this work to determine if the absence or presence of serum may have any direct effect on PCLS viability, and to determine any detrimental effect on expression profiles of PCLS samples.

3.6.1 Effects of absence of serum from culture

Multiple delivery conditions were used to deliver standard luciferase reporter plasmid (PMV-Gluc-2) to PCLS tissue under both serum free (SFM) and serum (growth medium) conditions alongside and untransfected control. In both expression profiles and viability profiles, clear differences could be observed between samples cultured with and without serum.

Expression data for Growth media samples (growth medium) showed initial high expression, followed by gradual decline towards Day 14, similar to

expression profiles observed in previous transfection experiments (Figure 3.1). Regardless of delivery condition, all samples showed a similar expression profile over time. Using FLR peptide only for delivery appeared to produce the lowest expression of all transfected samples, but FLR:FLH in complex demonstrated similar delivery over time to Lipofectamine2000 and Lipofectamine3000, and demonstrated higher expression overall than PEI (Figure 3.9)

In contrast, expression data for serum free samples (SFM) showed a much lower initial expression, with minimal increase over time towards Day 14. The majority of delivery conditions demonstrated expression levels similar to or lower than the untransfected control. Only Lipofectamine2000 showed some expression around Day 2 to Day 3, showing levels around 100-fold higher than all other conditions. However, by Day 5, lipofectamine2000 expression declined to level with all other conditions (Figure 3.9).

Viability data also showed visible differences when comparing Serum (growth medium) samples to serum free (SFM).

For samples in growth media (growth medium) all delivery conditions demonstrated a similar pattern in viability, and all were in line with or slightly above the untransfected control (Figure 3.10). Viability of all samples remained stable over 14 days, regardless of delivery condition used.

Samples in serum free conditions (SFM) had a distinctly different viability profile over time. Despite initial pre transfection viabilities being similar to growth media samples, a quick decline was observed in all delivery conditions cultured serum free (Figure 3.10). The untransfected control

displayed no viability after Day 5, and the FLR:FLH delivery condition displayed no viability just before Day 10. All other delivery conditions demonstrated viability up until Day 14, but distinctly lower than the viability at Day 14 of serum cultured samples.

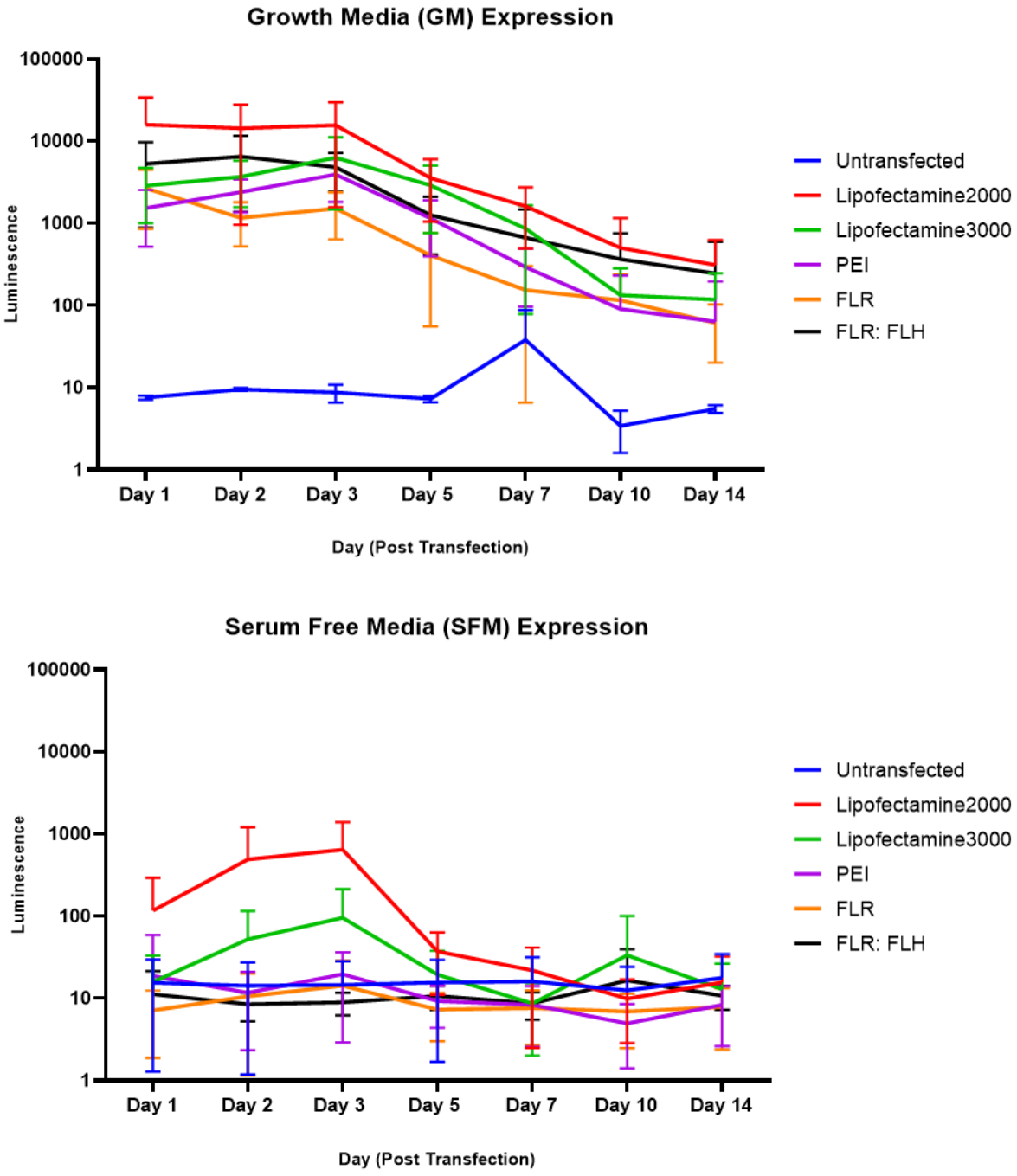


Figure 3.9 Comparison of expression profiles of PCLS in Growth Media and Serum Free Media (SFM) *Comparing Serum and Serum free effect on PCLS demonstrated clear differences in expression, even when differing transfection agents were used for delivery. Initial expression of all transfected samples was higher in growth media than serum free media, regardless of transfection agent. For both GM and SFM experiments, Untransfected control (n=2), FLR:FLH (n=8), all other experimental conditions (n=11). Error bars represent the standard error (s.d.)*

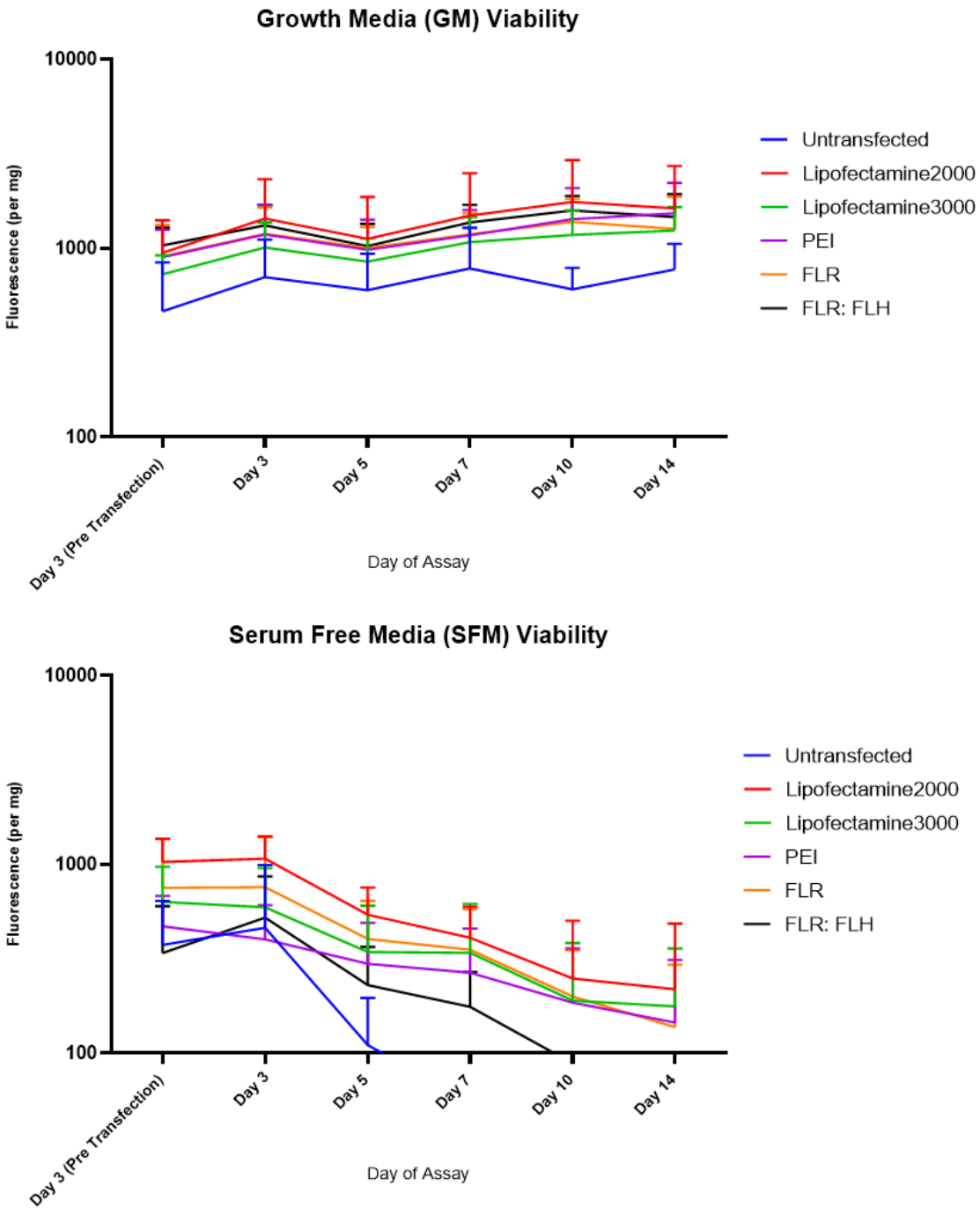


Figure 3.10 Comparison of Viability of PCLS in Growth Media (growth medium) and Serum Free Media (SFM) *A clear difference was observed in viability profiles of PCLS cultured in Growth Media (growth medium) and Serum Free Media (SFM). Despite minimal differences in viability Pre-Transfection, Growth media samples displayed similar viability profile over time to initial PCLS delivery experiments. SFM samples showed quicker decline in viability over time comparative to growth medium samples within the same experiment. For both GM and SFM experiments, Untransfected control (n=2), FLR:FLH (n=8), all other experimental conditions (n=11). Error bars represent the standard error (s.d.)*

3.6.2 Effects of selective presence of serum

After investigation of serum and serum free samples, the effect of selective presence of serum was investigated. Presence of serum was varied before and after point of transfection. Experimental conditions were growth media used both before and after transfection (growth medium>growth medium), growth media used pre transfection, with serum free media used post transfection (growth medium>SFM), serum free media used pre transfection, with growth media used post transfection (SFM>growth medium) and serum free media used both before and after transfection (SFM>SFM).

All experimental conditions were tested with an untransfected control, FLR peptide delivery only, and FLR:FLH combined peptide delivery. Enhanced luciferase plasmid pGM206SMAR was used for all transfections.

Expression profiles of all conditions over 14 days demonstrated clear differences between untransfected and transfected samples (Figure 3.11 A). some difference could also be seen between peptide conditions, as samples where FLR:FLH was used demonstrated some higher initial expression than samples where FLR was used alone. growth medium>growth medium samples where FLR:FLH was used to deliver plasmid demonstrated the highest initial expression.

Viability profiles of all conditions over 14 days also showed decline within all samples over time; SFM>SFM samples within untransfected and FLH conditions became unviable around Day 5, with other serum free conditions also becoming unviable before day 14 (Figure 3.11 B).

Closer examination of expression profiles at specific timepoints also demonstrated some significance between serum conditions; difference was most apparent on Day 1 and Day 3, where overall growth medium>growth medium and growth medium>SFM had the highest expression. When FLR peptide only was used, growth medium>SFM appeared to demonstrate highest expression, however when FLR:FLH was used for delivery, growth medium>growth medium demonstrated highest expression. Particularly in FLR:FLH delivery, it appeared that the more serum used, the higher the expression seen (Figure 3.12).

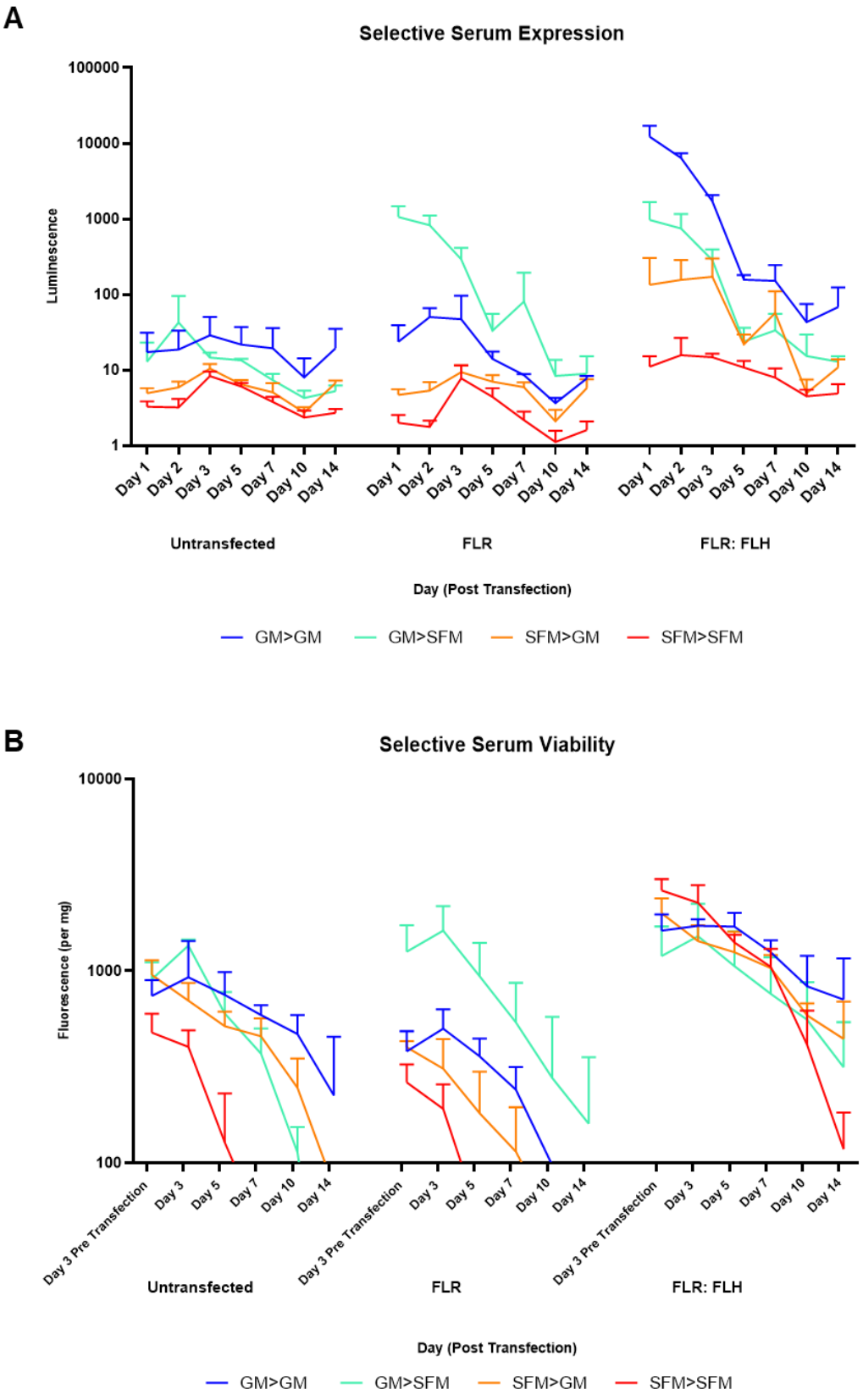


Figure 3.11 Expression and Viability Profiles of Selective Serum use in PCLS Culture *(A) Expression profile up to Day 14 for all samples. Samples where growth media was used appeared to demonstrate higher viability than serum free samples, particularly when using FLR:FLH for delivery. (B) Viability profile up to day 14 for all samples. Delivery condition appear to have more impact on viability over time than presence or absence of serum within media, as all FLR:FLH samples had more sustained viability over two weeks than any other delivery condition. All experimental conditions (n=3). Error bars represent the standard error (s.d.)*

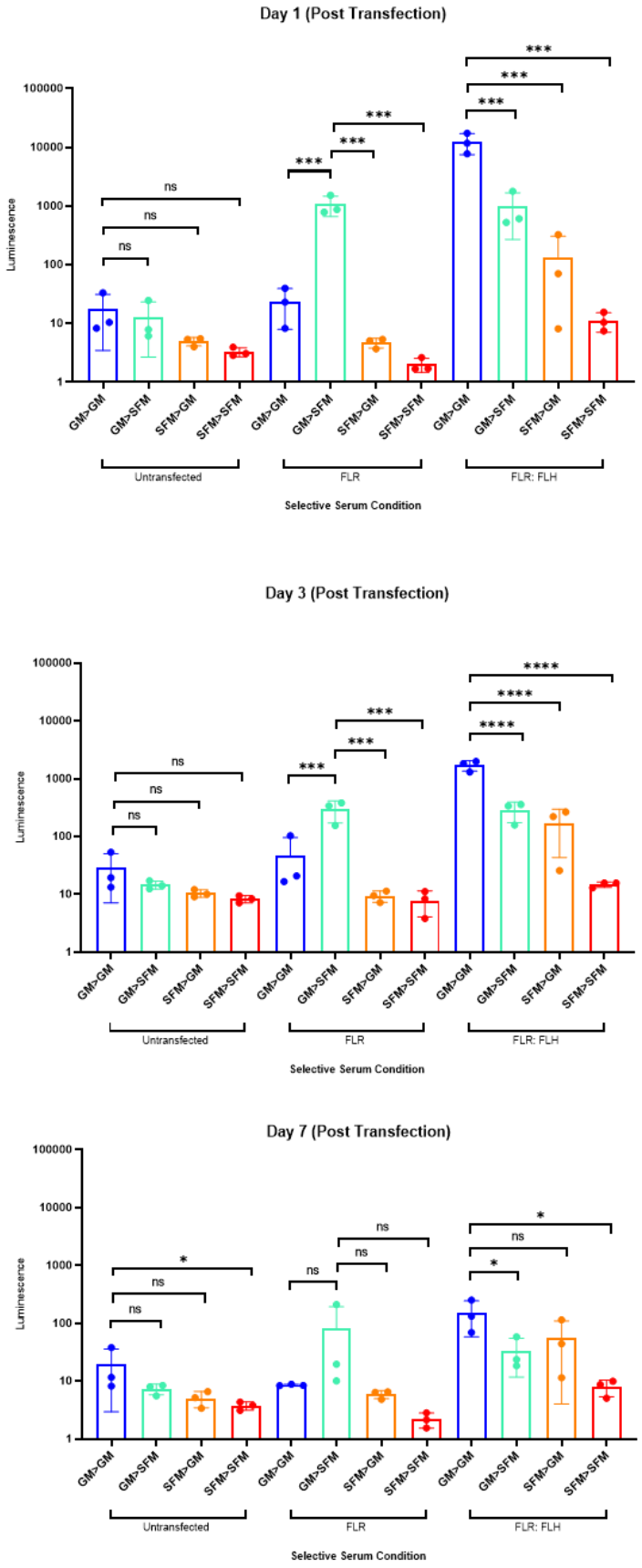


Figure 3.12 Expression Profiles of Selective Serum use in PCLS Culture *Minimal difference could be seen within untransfected controls, regardless of absence or presence of serum. Significant difference could be observed most often between samples in growth medium>SFM and growth medium>growth medium conditions and all other serum conditions. (n=3) per experimental condition. Error bars represent the standard error (s.d.)*

3.7 Physical force to aid transfection permeation

The effect of centrifugal force on transfection was also investigated, to determine if applying physical force immediately post transfection could aid in transfection permeation. Standard transfection conditions were compared with a standard transfection centrifuged, a standard transfection centrifuged with a complete media change, and 10 times standard transfection with a complete media change (RCF 10x). Standard reporter luciferase plasmid (PMV-GLuc-2) was used for all transfections.

Expression data showed minimal difference between conditions over time; however, all conditions showed uniformly high initial expression at day one. Initial expression from centrifugation post transfection with no media change (Figure 3.13 A, RCF) showed the highest expression seen in any PCLS transfection experiment. Expression overall appeared to be high regardless of transfection condition.

Viability profiles over time also appeared similar to previous transfection experiments (Figure 3.13 B). Minimal difference was seen over time, regardless of transfection condition, with all conditions showing minimal difference in viability from the point before transfection (Day 3 pre transfection) to Day 14.

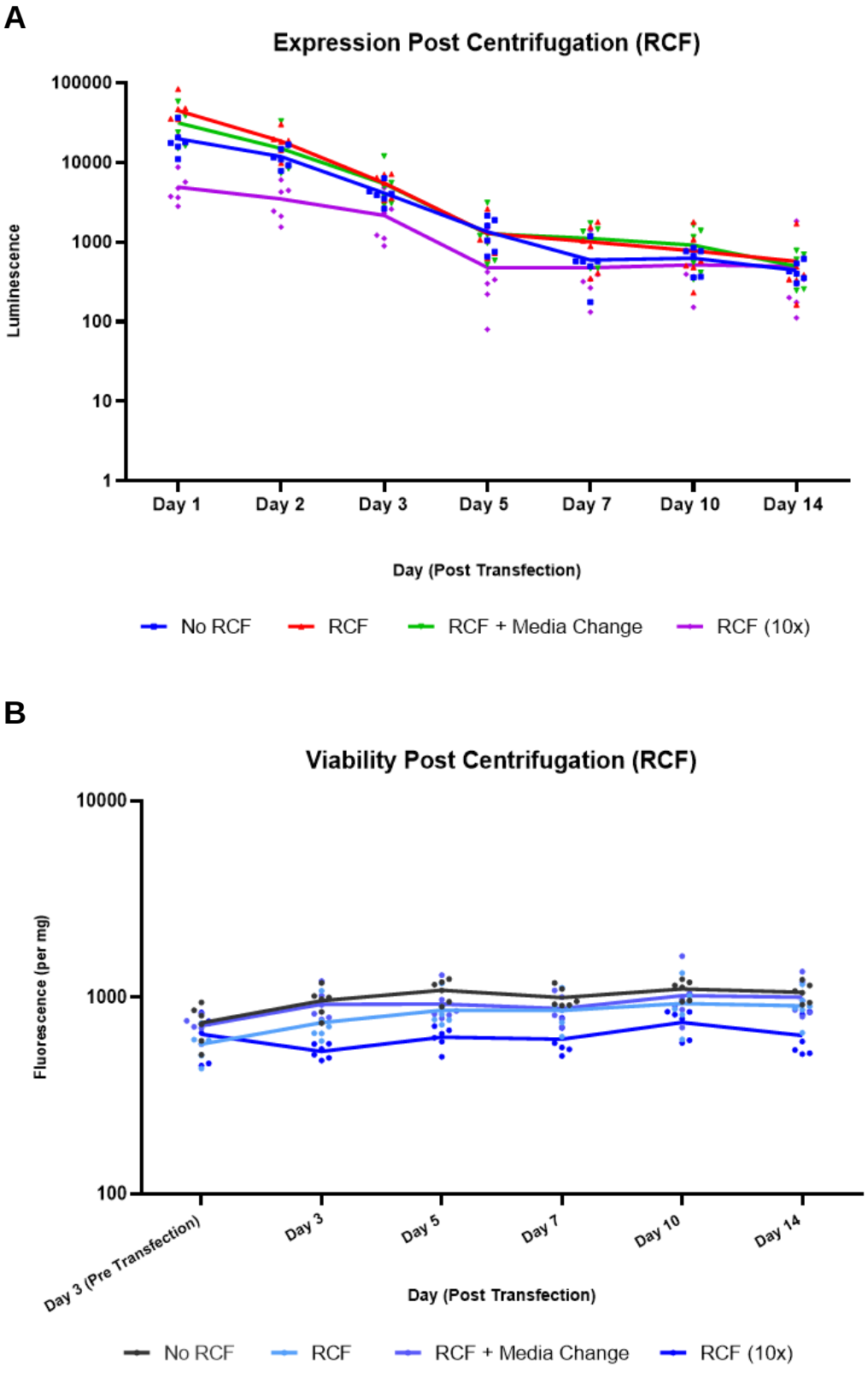


Figure 3.13 Expression and Viability of PCLS with and without Centrifugation (RCF) *Minimal difference was observed between both expression and viability profiles of all conditions. Viability profiles were in line with previous non RCF experiments, with expression profiles appearing significantly higher overall than any other non-RCF experiment. (n=6) per experimental condition. Error bars represent the standard error (s.d.)*

3.8 Discussion

Within this chapter, Precision cut lung slices were utilised to demonstrate GET peptide non-viral delivery to an *in vitro* model. Initial work aided in determining viability of PCLS as an *in vitro* model post transfection with GET and determined its Transfection efficiency with reporter and enhanced plasmids for Gaussia luciferase, measured by luminescence.

Visual confirmation of viability of PCLS was also carried out with Livedead staining and H&E stains of dead fixed tissue post transfection.

Multiple following experiments involved changing variables to further optimise and refine both PCLS as an *in vitro* delivery model, and to test the limitations of the GET non-viral peptide delivery system. DNA plasmid concentration, potential effect of absence of serum from cultures, selective presence of serum in cultures, effect of centrifugation on transfection efficiency, and potential for use of alternate perfusion materials for PCLS generation were all investigated.

3.8.1 Transfection efficiency within the model

Reporter plasmid (PMV-Gluc-2) and enhanced plasmids (pGM206, pGM206SMAR) incorporating a Gaussia luciferase gene were used for transfections, as luminescence could be easily read post transfection to give quantification to potential expression. Important to note is the fact that luminescence output gave no information on transfection localisation (for example, where within the precision cut lung slice transfections may be

happening) or transfection dispersity amongst the cell population of the slice (for example, if peptide delivery was intense for a single or a few cells whilst other cells may not have been transfected at all). Elucidation of transfection localisation could be achieved if a fluorescent plasmid was used, such as GFP, or the luciferase reporter plasmid could be fluorescently labelled.

Expression was always higher for transfected conditions comparative to untransfected controls, both in initial experiments (Figure 3.1) and in some later experiments with variations to conditions (Figure 3.5, Figure 3.7, Figure 3.9). In selective serum experiments however, there was less of a difference between the expression of experimental conditions comparative to untransfected controls, dependent on the conditions used (Figure 3.11, Figure 3.12).

A key difference is between the GET non-viral peptide and commercial controls such as lipofectamine. In initial experiments (Figure 3.1) a clear difference in expression can be observed between Lipofectamine3000 and all variable conditions that include the FLR peptide, particularly around a week following transfection (day 7). An argument can be made for lipofectamines potential toxicity at the *in vitro* stage, as toxicity has been observed in multiple cell types (Wang, Larcher, Ma, & Veedu, 2018), however in experimentation here, lipofectamine performs similarly or better overall to the GET peptide system in terms of expression, (Figure 3.1, Figure 3.9) whilst having no discernible effect on viability of PCLS tissue over time (Figure 3.2, Figure 3.10). This could potentially be due to the use of whole tissue slices, comparative to cell monolayers used in other experimentation.

Overall, Initial transfection data shown here demonstrates that good, significant expression profiles can be achieved in PCLS tissue, both when using the GET non-viral delivery peptide and other equivalent commercial non-viral based delivery systems; a case can be made both for the GET peptides potential as a transfection agent, and for PCLS as a reliable transfection study model.

3.8.2 Viability of tissues

In initial experimentation, viability appeared to improve over time, with highest viability seen at day 14, regardless of transfection condition (Figure 3.2).

Following experiments showed varying viability profiles, most likely dependent on the specific variables used within each experiment. Aside from initial experimentation, overall viability throughout experiments usually declined over 2 weeks towards the final day of the assay, regardless of transfection condition; similar viability decline patterns were observed in transfected samples and untransfected controls alike.

Visual viability was also investigated alongside quantitative viability using prestoblue; Livedead of live slices post transfection and histological H&E staining was used to discern if transfection had any effect on tissue structure and by extension, overall tissue viability.

Livedead staining was carried out both pre and post transfection, and comparison of untransfected controls, FLR:FLH peptide delivery, and PEI delivery of the same standard luciferase plasmid was carried out. Although

less intense fluorescence for live cells (green) was observed across all samples at day 5 post transfection, there was no visible increase in dead cells (red) at this timepoint either. All delivery conditions also displayed very similar fluorescence intensities for both live and dead cells at Day 5 post transfection (Figure 3.3).

Based on visual staining results, transfected samples did not appear to be less viable post transfection, with no localised effect on tissue structures observed.

This initial research demonstrates that regardless of the delivery system used, precision cut lung slices can be a useful tool for expression studies and prove to be an easy model for transfection and expression studies due to minimal loss of viability even post transfection.

Immunohistochemistry (IHC) was also carried out on samples; H&E staining was used on post transfection samples which included standard plasmid delivered by FLR peptide only, FLR: FLH complexed, and a control (DNA only). This was to further look at the GET non-viral system potential toxicity and determine its potential localised effect on tissue post transfection.

Independent lung structures could be easily observed in all samples, with natural lumens of blood vessels and air spaces within alveolar in particular clearly visible. Nuclei appeared dark purple, with alveolar web like structures and lung parenchyma appearing light pink. Of note is that regardless of transfected or untransfected samples, all samples displayed very similar structure, with no visible discernible differences in presence and shape of

structures such as alveolar spaces, presence of blood vessels, and bronchioles (Figure 3.4).

H&E is composed of Haematoxylin and eosin; Haematoxylin (purple) can identify nuclear material like heterochromatin and the nucleus, with eosin (pink) identifying cytoplasm and ECM components. Clear definition between the nuclear and cytoplasmic components can make visualisation of tissue structure easier, and issues such as inflammation or necrosis can be more easily identified.

An argument could be made for the GET peptides low toxicity when used to deliver within PCLS mouse lung tissue, due to the lack of visible difference between transfected samples and GET free controls; however, this is only initial quantitative data, and could be strengthened more with comparative images particularly from commercial controls previously used such as lipofectamine or PEI.

3.8.3 Effect of variation in plasmid concentration

Plasmid concentration was varied for some experiments, to both determine if plasmid dose could be optimised with no compromise in transfection efficiency, and if reducing the plasmid concentration demonstrated any improvement in sample viability.

All previously described vectors, standard luciferase reporter (PMV-Gluc-2) and enhanced luciferase vectors (pGM206, pGM206SMAR) were delivered with FLR:FLH complexed GET peptide, at both 1 µg and 2 µg doses.

Transfected conditions were compared to an untransfected control. Both expression and viability profiles were monitored over time.

Overall, enhanced vectors appeared to demonstrate higher sustained expression for longer than standard reporter luciferase, regardless of concentration of plasmid used. Statistically, no significant differences were observed between 1 µg and 2 µg samples where the same plasmid was used (Figure 3.5). Important to note was the high variation within specific transfected groups; in standard reporter luciferase particularly, individual samples ranged from as low as the untransfected control, with other samples in the same group demonstrating around 100-fold increase at the same timepoint. This deviation within transfected conditions was minimal and less observed in enhanced vector conditions.

Viability profiles were also in line with similar experiments. Each condition reduced in viability over time relative to its pre transfection initial viability, with no condition displaying more decline than any other. This was apparent for both untransfected samples and transfected samples. Both concentrations (1 µg and 2 µg) showed very similar viability profiles over 14 days, with no discernible difference observed between the two (Figure 3.6).

Overall, the effect of plasmid variation on both expression and viability appeared to be minimal. No discernible differences were observed in expression profiles between 1 µg and 2 µg doses, and the use of reporter or enhanced vector appeared to have more effect on level of expression than amount of plasmid used. Viability also appeared to be unaffected directly by plasmid concentration variation, with viability profiles mirroring each other

and previous experiments, regardless of condition. Significantly, 2 µg pGM206SMAR samples appeared to have the highest initial viability pre transfection, and thus presented with higher viability overall at later experimental timepoints (Figure 3.6). if these particular samples were overall more viable than those in all other conditions, this potentially could have been a contributing factor to the increased expression observed in this experiment for this enhanced vector; further experimentation would be required to confirm this theory.

3.8.4 Effect of serial delivery

Initial experiments with serial delivery involved some dose variation to aid in delivery optimisation and confirm if smaller doses delivered at an increased frequency may have improved expression. This also allowed observation of viability of samples over time to confirm there was no reduced viability as a result of increased use of both plasmids and the GET peptide system.

Expression in these initial experiments appeared to be lower on average than previously observed in other PCLS experiments, whilst viability appeared to have a similar decline over time towards day 14 and similar initial pre transfection viability. Important to note is that N numbers of samples for each group were lower than in some other experiments, so this is considered very initial experimentation only.

Viability also did not appear to be directly affected by serial delivery, or dosage change within serial delivery conditions. Initial pre transfection viability appeared to show less variation than in other experiments, however

more variance was observed by day 14 across all conditions: some specific conditions seemed to have declined in viability over time more than others particularly in every 2 day delivery. All conditions in every 2 day delivery (E3D) appeared to show less decline in viability over time. This could be related directly to the delivery condition, as less transfection would have been delivered to E3D samples overall: however, as stated previously, n numbers were lower for this experimentation, which makes it difficult to draw direct conclusions on the exact cause both expression outputs and sample viability.

Untransfected control appeared to become unviable between day 7 and day 10 for both every 2 day (E2D) and every 3 day (E3D) delivery (Figure 3.8). As generated PCLS give very variable results from experiment to experiment, this could be an indicator of potential lower viability batches of PCLS used that could have had a direct effect on the outcome of this experiment.

Overall, initial results seem to indicate no discernible difference in expression between the two serial delivery conditions, or between dosages of plasmid used. It appears as with some previous experiments, choice of enhanced plasmid over standard reporter plasmid could have some direct outcome on level of expression. There were potentially some viability differences in more frequent delivery (every 2 days) as opposed to less frequent (every 3 days). With minimal n numbers of PCLS in each condition, it is difficult overall to definitively state outcomes; however, plasmid choice may be more significant to expression outcome and transfection efficiency than modifying dosage or delivery timepoints directly.

3.8.5 Significance of Serum in PCLS culture

As all ongoing work utilised serum within media for PCLS culture, which appeared juxtapose to other PCLS culture methods observed in the literature, significance of serum and its potential impact on expression, and viability, was investigated. Initial serum vs. serum free experimentation used both FLR peptide only alongside FLR:FLH in complex, and comparative commercial agents including Lipofectamine 2000, Lipofectamine3000, and PEI. All delivery agents were used to deliver standard reporter luciferase plasmid (PMV-Gluc-2) with the only difference being serum included or omitted from the media used for culture.

Effect on expression was apparent when comparing expression profiles of all growth media samples to serum free samples. Growth media (growth medium) samples appeared to show a very similar pattern to previous experiments, with high initial expression observed in all conditions with gradual decline over time towards day 14. by comparison, all serum free media (SFM) samples were uniformly lower in expression, with values observed up to 100-fold lower for initial expression than in growth media conditions. Many conditions were in line with the untransfected control, with minimal change or increase at any timepoint (Figure 3.9).

Lipofectamine2000 appeared to have better expression in serum free conditions, and initial expression seen was around 10-fold lower than the lowest expression observed in growth media samples. Lipofectamine2000 also seemed to perform the best in Growth media conditions, with initial

expression being around 10-fold higher than other conditions such as PEI and FLR.

Viability profiles all showed some clear difference between growth media and serum free samples. Growth media (growth medium) samples demonstrated a pattern in line with previous experiments, similar to expression profiles for this experiment, with some small increase even observed over time towards day 14. Untransfected control was also in line with all other conditions, and thus a good indicator and confirmation of lack of toxicity post transfection.

Serum free samples (SFM) showed a marked difference in viability over time. Despite very similar initial viabilities averaging between 500 – 1000, quick decline was observed across all samples, regardless of condition. Untransfected control appeared to become non-viable around day 5, with FLR:FLH also becoming non-viable around Day 10 (Figure 3.10). Other conditions appeared to retain some viability even at day 14, but these were significantly lower than those observed in all growth media samples.

Lipofectamine2000 samples gave the highest results, particularly in serum free conditions. In growth media conditions, both FLR:FLH and lipofectamine2000 appeared level in terms of viability.

Overall, removal of serum did appear to be having some direct impact on both expression and viability; viability in particular was impacted, and this loss of viability could be the reason expression was also seen to reduce. Samples with better viability, particularly initial pre transfection, appeared to have higher expression, regardless of the non-delivery system used.

3.8.5.1 Effect of Selective use of serum

Some selective serum experimentation was also carried out, as removal of serum from culture appeared to have some effect on both expression and viability; as observations showed that the initial pre transfection viability may have some effect on longer term viability and expression, serum was selectively utilised both pre and post transfection. Conditions used were growth media both pre and post transfection (growth medium>growth medium), growth media pre transfection and serum free post transfection (growth medium>SFM), serum free media pre transfection and growth media post transfection (SFM>growth medium), and no growth media used at any time (SFM>SFM). This was initially investigated with the GET peptide system only against an untransfected control, in an aim to observe any expression profile differences between standard and enhanced peptide complex.

When selectively using serum in media, the more growth media used, (growth medium) the higher the expression seen overall; this was most apparent when FLR:FLH peptide was used for plasmid delivery (Figure 3.12). Expression was also a lot higher initially when FLR:FLH complexed peptide was used for delivery. (Figure 3.11). This expression profile was somewhat expected, as the FLH domain is added to the FLR peptide improve transfection.

From initial selective serum experiments, it appears that including serum in growth media, combined with use of FLR:FLH complexed peptide, seems to demonstrate the best expression comparative to untransfected controls, FLR peptide used alone, or conditions lacking a serum component. This also

aligns with earlier experiments, which all contained serum. FLR:FLH peptide is however only similar to commercial delivery systems such as PEI and Lipofectamine, and doesn't not appear able to outcompete these systems completely. The GET non-viral system does have the advantage of minimal to no toxic effects both *in vitro* and in initial *in vivo* work (Abu-Awwad, Thiagarajan, & Dixon, 2017); (Osman, et al., 2018).

Viability profiles also showed some variation between conditions used. In untransfected samples and FLR samples in particular, serum free media used throughout (SFM>SFM) showed a lower initial viability; this could be directly due to only ever being thawed and cultured in serum free media. However, in FLR:FLH samples, SFM>SFM appeared to have the highest initial viability. SFM>SFM did however demonstrated the most decline relative to initial viability. From initial results, FLR:FLH did appear to have the most sustained viability over time, but it was unclear if this was linked directly to choice of delivery agent for transfection. As all samples in this group started with overall higher initial viabilities, viability may be attributed to this instead. Despite higher initial viabilities from all serum conditions, expression within even FLR:FLH samples was still only minimally better than in FLR samples. This could potentially mean presence of serum is a requirement for successful transfection and more sustained expression over time.

It is important to note that despite data normalisation to slice weight (mg), a large amount of variation is seen when using PCLS tissue. Variation in initial starting viabilities could be due to each batch of PCLS generated, or individual animals they were generated from.

Some argument could be made for serum utility in the success of transfections and expression from samples; however, it is unclear if selective serum has a direct impact on expression of viability of samples over time. With no significant difference observed in untransfected samples regardless of selective use of serum, but some observed between samples where growth media was used comparative to those where less was used (Figure 3.12), it could be suggested that the more growth media included at both initial thaw stage and whilst culturing and transfecting, the more likely sustained expression and longer time viability.

3.8.6 Effect of Physical force on transfection and expression

Due to PCLS taking their support structure from perfused and set agarose, rather than the pressure gradient present in the lung *in vivo*, there was the possibility agarose material may be acting like a hydrogel. Whilst useful in holding the slices ‘open’ and allowing support of airway structures, the agarose could also be potentially reducing transfection capacity by preventing transfections from reaching some specific subsets of cells.

To determine if agarose could be having a detrimental effect on direct transfection, low centrifugal force was utilised to aid in transfection penetration of tissue. Transfections were carried out with no centrifugal force (No RCF), centrifugal force without any media change pre incubation (RCF) centrifugal force with media change pre incubation (RCF + media change) and centrifugal force with 10x the volume of a standard transfection with

media change pre incubation (RCF 10x). FLR:FLH peptide complex was used to deliver standard luciferase reporter plasmid (PMV-Gluc-2).

Expression profiles appeared vastly increased comparative to previous experimentation with no centrifugal force used (Figure 3.13 A). although a similar pattern appeared if initial higher expression immediately post transfection with gradual decline over time, initial numbers were around 100 fold higher than observed in any previous experiments. The only condition which demonstrated initial expression lower than around 10,000 was RCF (10x), in which 10x the standard volume of transfection had been used to try and observe toxicity limits and potentially improve expression seen in tissue. From initial results, it appeared increasing transfection volume did not improve transfection efficiency or expression comparative to standard volumes that were also centrifuged.

Of all conditions, standard transfection where no media changes were carried out before incubation overnight (RCF) had the highest initial expression and appeared to have minimally higher sustained expression until Day 14. This could be attributed to transfection material being present in media overnight, whereas this would not have been the case for other conditions.

Viability was also very similar for all conditions, a similar pattern over time appeared comparative to previous experiments. Lowest of all conditions was 10x transfection volume (RCF 10x), but this was minimal. Minimal decline was observed in all conditions over time, suggesting increased transfection penetration had no detrimental effect on viability in any condition (Figure 3.13

B). Overall, it seemed expression could be improved with the introduction of low centrifugal force, suggesting that agarose in PCLS may in fact be having some reducing effect on transfection success across the whole piece of tissue. This presents the potential to investigate alternate perfusion materials which may be present less of a physical barrier to transfection penetration.

4. Chapter 4: Investigating Gelatin as an alternate perfusion material to improve the in vitro PCLS Model

4.1 Introduction

In PCLS research, the standard perfusion material of the lungs for PCLS generation is agarose, or specifically low melting point agarose (LMPa). When used as a perfusion material, the solution concentration of the agarose can vary from around 1% - 2% (Henjakovic, et al., 2008); (Neuhaus, et al., 2017); (Rosner, et al., 2014) but this can be dependent on the species of the tissue being used for slice generation. Variation in the methods can also be due to the protocol being used by each independent research group. There currently is no universal standardised method for PCLS generation, as there are observed variations in many method areas including, but not limited to, agarose concentration, and deliberate inclusion or exclusion of specific lung lobes.

Despite its utility in holding slice structure effectively, agarose is a non-removable material, effectively meaning PCLS tissue is encased in a type of hydrogel and is not a piece of independent *ex vivo* tissue in culture. This creates the potential, particularly within delivery studies, for agarose to prevent delivery to the multiple cell types present within a precision cut lung slice. Individual studies have highlighted the lack of removability of agarose in samples post slice generation (Neuhaus, et al., 2018), but other studies conversely highlight within their methods that the agarose can be washed out with media over time (Ressmeyer, et al., 2006); (Temann, et al., 2017); (Song, Davidovich, Lawrence, & Margulies, 2016) or that it can be melted

away at 37ºC post incubation of samples (Hirn, et al., 2014). Individual studies also postulate that long term culture (up to 4 weeks) can lead to dissolution of agarose from the tissue, observable by loss of slice structure (Rosales Gerpe, et al., 2018).

Only recently has some research featured the use of a different perfusion material. A previous study utilised gelatin as the sole perfusion material; however, lungs were cored to 15 mm and then sliced at around 0.5 – 2mm (Birzle, Martin , Yoshihara, Uhlig, & Wall, 2018). Most PCLS studies usually only generate slices around 200 – 300 µm, with the highest around 500 µm (Bryson, et al., 2020).

A more recent study also utilised gelatin as the perfusion material, at a concentration of 20% in solution, and also fully embedding in gelatin of the lung lobes pre-slicing to create slices for short term infection studies. However, no mention is made of how long slices are cultured, or what PCLS viability or slice structure appears to be past 1 day (Kolbe, et al., 2020).

From previous studies, it is still unclear if gelatin would make a reliable alternate removable perfusion material for PCLS generation. Due to its lack of toxicity and simple temperature dependent removal, it would be a useful and reliable alternative to agarose if it provided the same structural benefits to PCLS post-slicing. Hence, some initial experimentation was carried out in this project to aid in determination of gelatins feasibility and reliability as a replacement perfusion material for use in PCLS generation and long-term culture, and to establish if gelatin PCLS would be more effective than the current agarose PCLS for use in delivery dependent study.

4.1.1 Gelatin PCLS behaviour in culture

Initially, gelatin PCLS were frozen down in batches, with a small number of slices kept for immediate optimization and investigation into gelatin PCLS behaviour.

Samples were numbered to aid in before and after comparisons, and each sample was imaged both before and after incubation. Pre incubation, images were taken within 1 hour of slice processing, and following images were taken 24 hours post incubation at 37ºC (Figure 4.1).

Distinct visual differences could be observed in the same samples before and after incubation; observable structure pre incubation was similar to all previous agarose PCLS samples, with a web like structure of alveoli clearly visible. After 24 hours of incubation at 37ºC, samples had lost most of their structure; by eye, slices appeared to have ‘balled up’ and would no longer lay flat within wells. Microscope images showed a distinctly different structure even at the same magnification as the previous day. Whilst some small gaps could be seen, the clear distinct shape of the alveoli seen pre-incubation was no longer present (Figure 4.1).

At 24 hours, cells had also started to aggregate within the bottom of the well underneath the remains of the PCLS tissue (Figure 4.2). Many observable cells formed distinct Rouleaux stacks, a typical formation seen of red blood cells. This may have been due to the primary nature of the tissue. All samples were continued in culture, with images taken at Day 3 and Day 6. The cell

population became adherent and confluent, and by day 6, multiple distinct cell morphologies were observable.

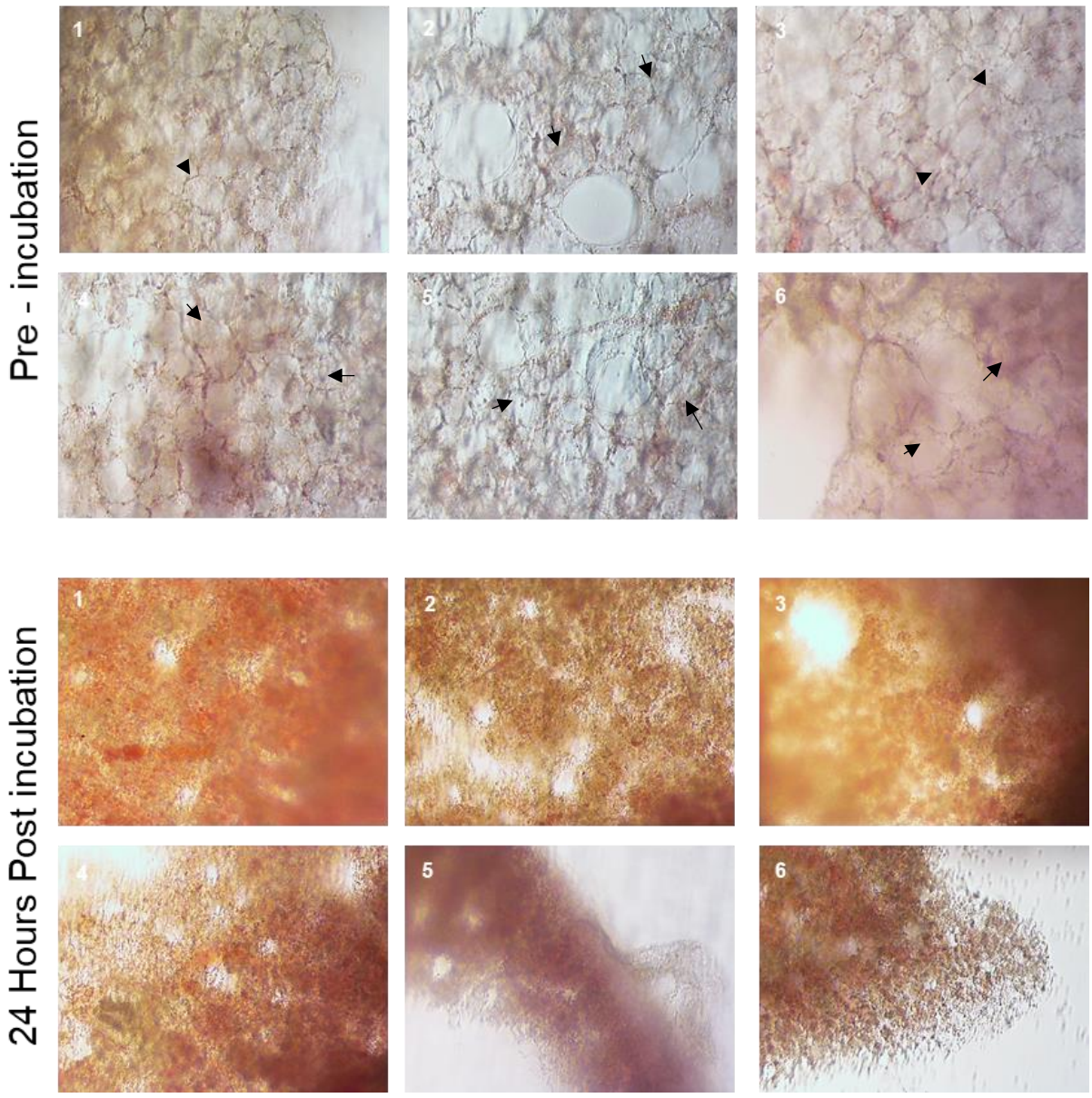


Figure 4.1 Gelatin PCLS pre and post incubation at 37ºC *Samples of Gelatin PCLS (1 – 6), imaged pre and post incubation at 37ºC. Pre incubation, alveoli can be easily seen (arrows), as perfused Gelatin is still present in the sample and holds the PCLS structure as it was initially sliced. Samples were also imaged the following day (24 hours Post incubation). Previously identifiable structures appeared reduced in size, and in places absent. Previous slice translucency had also significantly reduced. Colour change from pale pink to darker pink/ red was also observed in the main body of tissue slices. 20x objective used.*

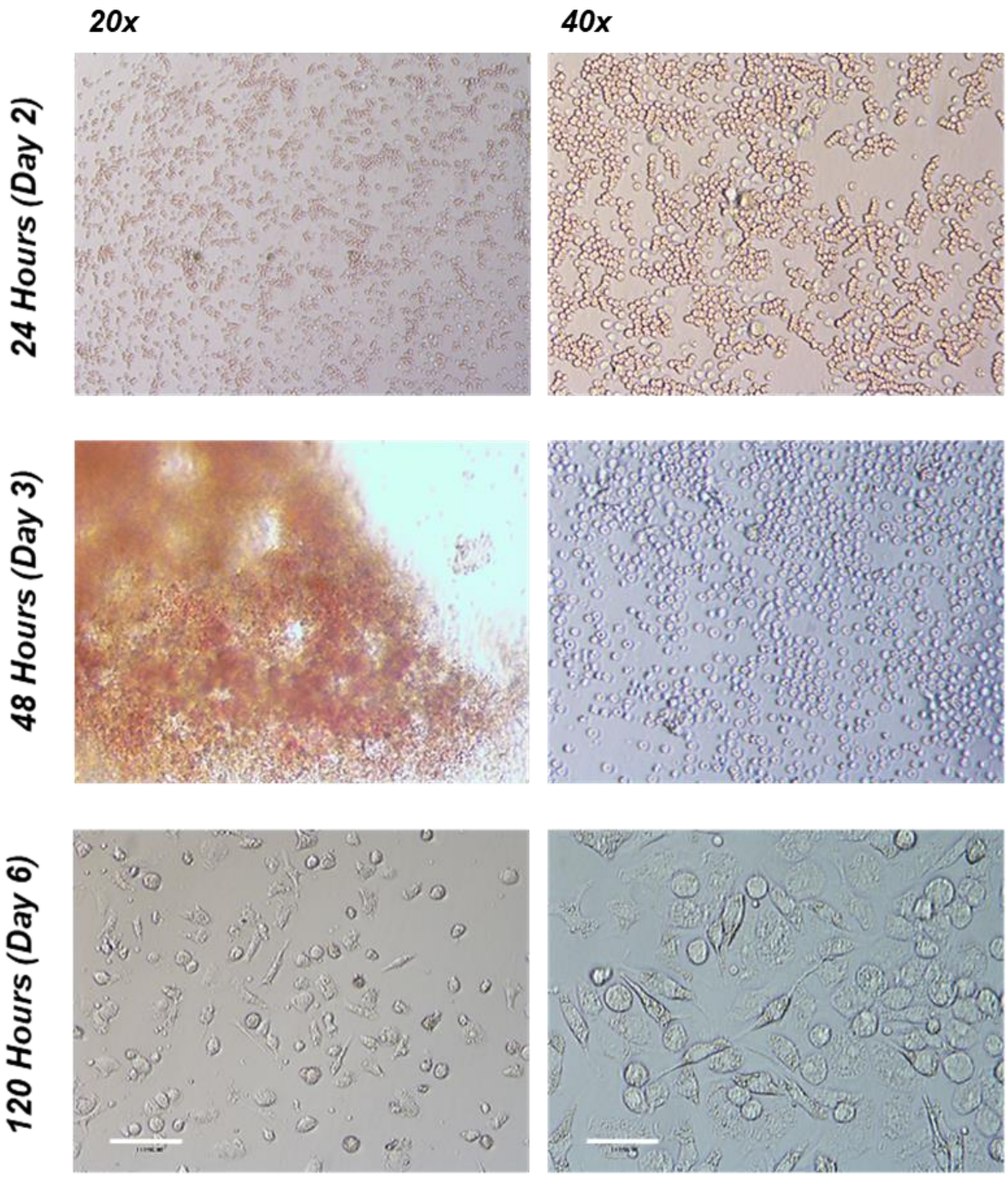


Figure 4.2 Visible cell disaggregation post incubation of Gelatin PCLS *At 24 hours (Day 2), individual cells were visible in the bottom of wells underneath remnants of PCLS tissue, alongside red blood cells in distinct Rouleauxs. At 48 hours (Day 3), remnants of tissue were still left, and disaggregated cells in wells had separated fully from each other. At day 6, populations of adherent cells appeared to be forming, with more than one distinct morphology observed. Scale bar: 156 µm, 20x and 40x objectives used.*

4.1.2 Livedead assay for visual qualitative analysis

Livedead of Gelatin slices was also carried out 24 hours post incubation (Figure 4.3). Significant live cells (green fluorescence) could be observed across all samples, specifically at 5x magnification. Further magnification aided in identification of dead areas of the slice (red fluorescence). More common and even distribution of dead cells could be observed at both 10x and 20x magnification, but live cells appeared more widespread that dead cells, with dead cells appearing more commonly towards the edges of the sample. It was unclear if bleed through of fluorescence between filters was occurring.

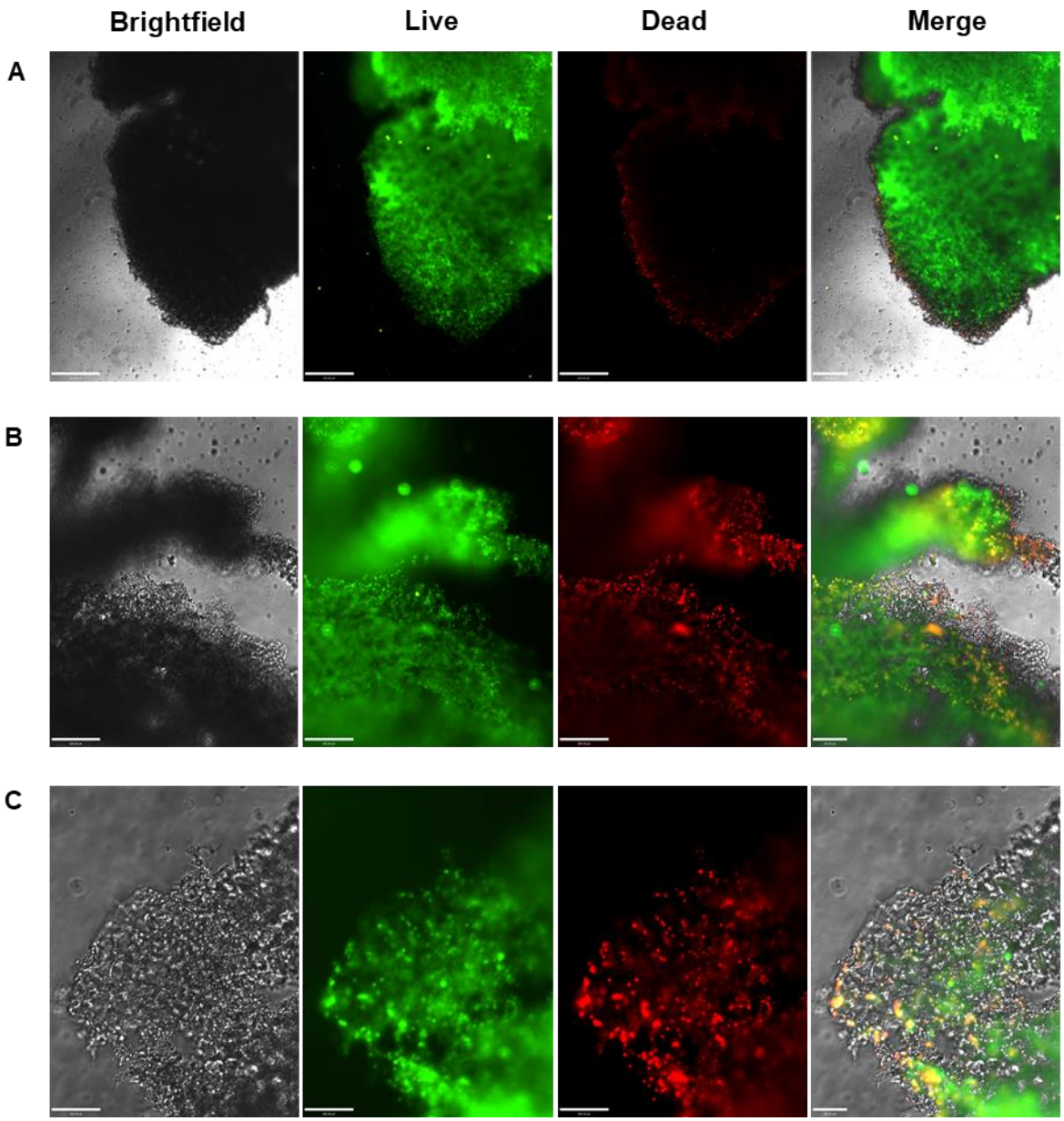


Figure 4.3 Livedead staining of Gelatin PCLS samples, 24 hours Post incubation. *(A) Sample at 5x magnification, stained with LiveDead. At lower magnification, PCLS outline can be seen, with significant Green (live) within the body of the slice, and red (Dead) observed along slice edges. (B) Sample at 10x magnification, stained with LiveDead. Further magnification highlights significant Green (Live) but also some red (Dead) cells present, with red fluorescence less intense than green. (C) Sample at 20x magnification, stained with LiveDead. Both Green (live) and Red (dead) fluorescence appears evenly distributed, with green (Live) appearing more than red (dead) fluorescence. LiveDead staining and imaging demonstrates slice viability post gelatin melting. Scale Bar for unmerged images: 200 µm, for Merged images: 140 µm.*

4.1.3 Visual confirmation of slice reduction pre and post incubation

To aid in confirmation of gelatin leaving PCLS and to demonstrate visually this loss of slice structure, gelatin PCLS were deposited into transwells, and agarose was used as ‘glue’ around the slice to hold it in place and give indication of its original placement (Figure 4.4). Each sample was photographed before incubation, and at 1 hour post incubation. Alongside photographs of samples, a drawing tool was used to aid in visualisation of the difference in slice size pre and post incubation.

Original tissue size is more obvious post incubation, as the agarose ‘glue’ leaves a clear outline comparative to the final slice size after the gelatin has melted. All slices lost significant surface area and reduced in size but did not ball up as previous samples had when within wells; this may be due to the transwell membrane providing some support, or the agarose ‘glue’ around the edges of the slice aiding in holding open the slice until eventual detachment and reduction post gelatin melting.

4.1.4 Viability and expression from initial transfection experiments

Samples within transwells were also used for initial transfection, to test potential expression levels from non-agarose slices, and also to confirm viability of any gelatin perfused tissues post gelatin melting (Figure 4.5).

When observing viability profiles, agarose PCLS free in media comparative to samples ‘glued’ to the well showed no significant difference in viability, with agarose covered PCLS demonstrating lower viability. Samples in

transwells also demonstrated lower viability, with Gelatin PCLS samples showing no viability at all. most likely, this was a combination of gelatin melting post incubation, and slice disaggregation. Overall, standard agarose PCLS free in culture showed the highest viability, with Gelatin PCLS showing no viability post transfection.

When observing expression, ‘glued’ agarose demonstrated expression no different to free floating agarose PCLS. Agarose PCLS in agarose heavy conditions (in transwell or agarose on agarose) demonstrated minimal expression, suggesting that excess agarose could be inhibitory to transfection and subsequent expression. Gelatin PCLS samples demonstrated minimal to no expression, regardless of condition.

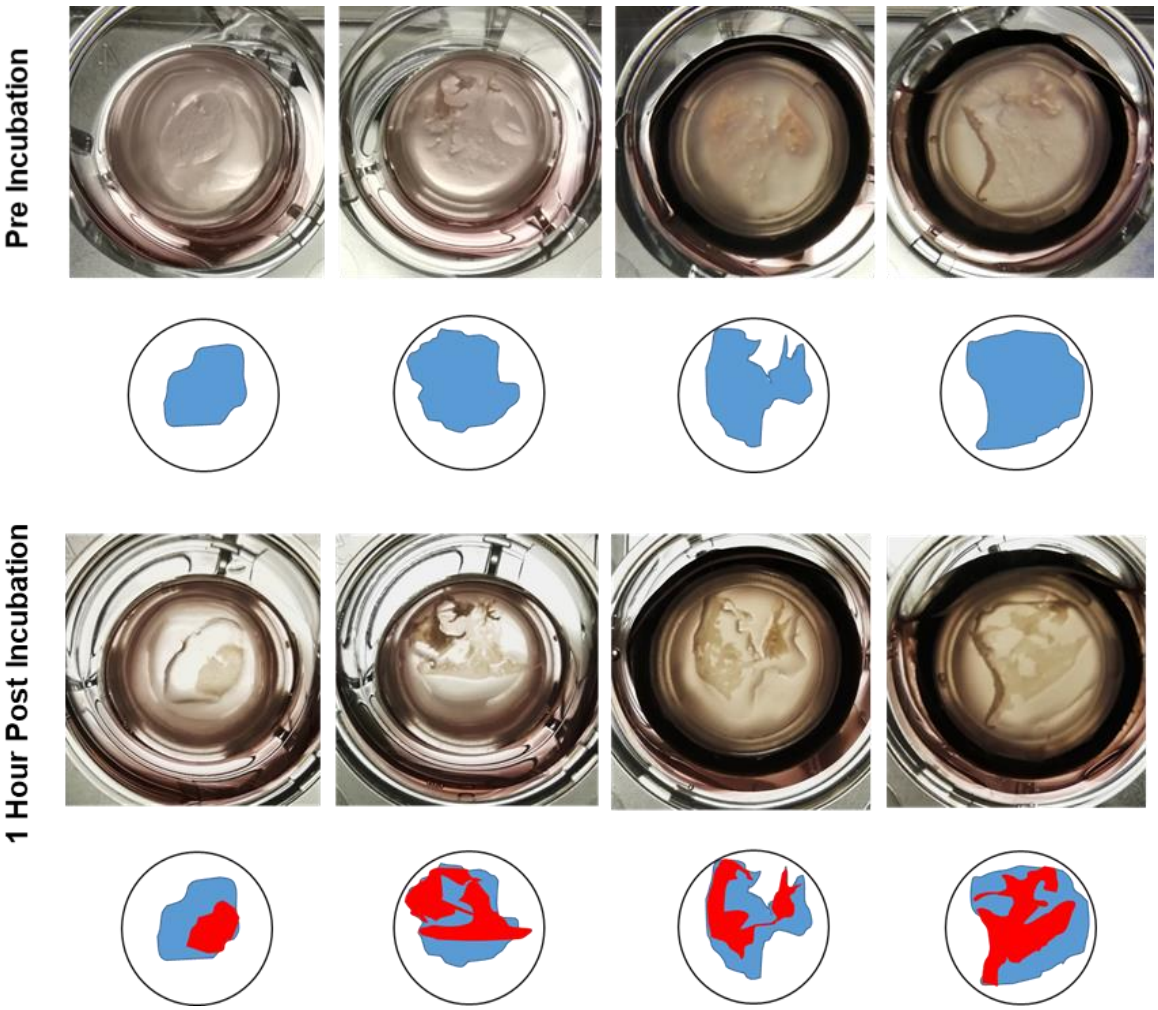


Figure 4.4 Appearance of Gelatin PCLS within transwells, pre and post incubation *Images of transwells within plates before and after initial incubation highlighted issues with using Gelatin as the perfusion agent. Photography and visual analysis allowed for identification of the initial slice area (blue). Post incubation, slice reduction in all samples can be seen clearly, as the agarose used around the Gelatin PCLS shows clearly the edge of the PCLS at its original pre incubation size (red).*

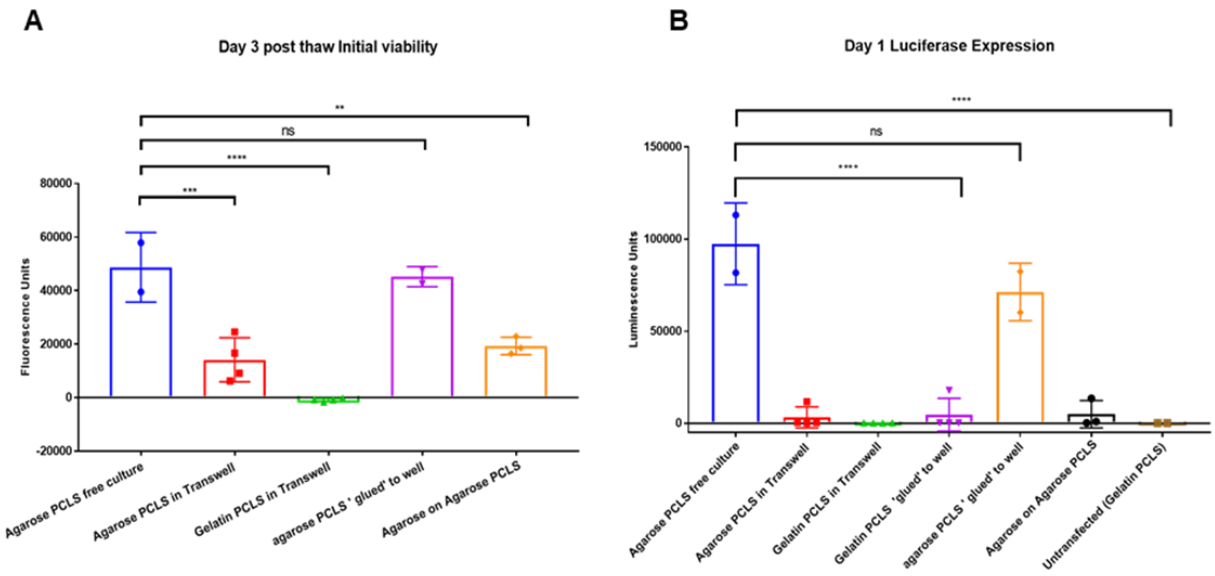


Figure 4.5 Viability and expression profiles of Initial Gelatin PCLS comparative to agarose PCLS and varying agarose 'glue' conditions. *(A) viability of all conditions 3 days post thaw. Agarose PCLS samples show good initial viability comparative to previous agarose PCLS only experiments. n numbers of experimental groups, from Left to Right; (n=2), (n=4), (n=4), (n=2), (n=3). (B) Day 1 expression (post transection) of all conditions. Free agarose PCLS demonstrated highest expression, as expected comparative to previous agarose only PCLS experiments. n numbers of experimental groups, from Left to Right; (n=2), (n=4), (n=4), (n=4), (n=2), (n=3), (n=2). All error bars represent the standard error (s.d.)*

4.2 Discussion

Within this chapter, Gelatin was considered and investigated as an alternate perfusion material for generation of PCLS; due to its lack of toxicity, easy manipulation, and temperature sensitivity which would allow for it to maintain structure during PCLS generation but would be easy to remove at point of culture and transfection, it appeared to be a promising potential alternative. the same method was used to generate Gelatin PCLS as for previous agarose PCLS, with minor amendments to account gelatins temperature sensitivity. Gelatin PCLS were used fresh never frozen, and remaining samples were frozen and stored immediately for later use, as previously described. Experiments were carried out to test gelatins feasibility as a potential material replacement for agarose, which included observation of integrity of slices pre and post incubation, general slice viability, and transfection potential and initial expression from gelatin PCLS.

4.2.1 Effect on temperature changes on Gelatin PCLS integrity

Initially, Gelatin PCLS were processed on ice as much as possible, to prevent Gelatin from melting out of tissues pre-emptively as gelatins melting point begins at around 31º C. Once processed, samples were imaged to observe lung structure, and confirm similar structural support was present comparative to that observed in agarose PCLS. Samples appeared uniform and consistent, and alveolar air spaces and web like structure could be easily observed. Larger common lung structures including blood vessels and bronchioles were also visible, and coarse focus allowed for visualisation

‘through’ the sample to confirm intact structures all the way through the slice. Due to the very open lung structure, light could easily pass through slices, with very pale pink coloration and translucency observed.

By comparison, images of the same slices 24 hours post incubation (Figure 4.1) look significantly different. Whilst previous structures and airways could still be observed, these appeared significantly smaller than in pre incubation. slices appeared dark pink to red in colouration, with all previously translucency lost. Previous alveolar structures had also disappeared. Throughout all samples, previous easily seen tissue structure appeared to be absent; it was clear significant structural changes had happened since pre incubation, and this was most likely due to Gelatin completely melting from the samples into the media. it was unexpected how quickly this material could melt completely from samples, and how quickly all previous structure of the slices was lost completely.

To determine the extent slice structural loss and potential degradation, samples were continued in culture, imaged and monitored over the course of a week. Wells underneath slices were also imaged, to confirm extent of any degradation of tissue.

Images of the base of the wells underneath floating slices in particular highlighted direct cell loss post incubation (Figure 4.2). at 24 hours, many individual cells could be observed, and red blood cells appeared to be present due to the formation of many stacks of rouleauxs. At 48 hours, despite some physical portion of slices observable to the naked eye, viewing the sample and the well beneath showed loss of structure and increased cell

numbers present below the sample. At around day 6 of culture, morphological changes could be observed in the now adherent cell population.

continued culture of slices post incubation aided in confirming complete loss of structure, and also confirmed slice disaggregation; with cells actively leaving the slice and attaching to the well in such vast numbers, this confirmed that even remaining remnants of visible slice would most likely lack the physical structure required for further experimentation and could possibly no longer be considered PCLS.

4.2.2 Viability of Gelatin PCLS post structure loss

Livdedead was also carried out on samples at 24 hours post incubation, in an attempt to confirm if slice viability was lost completely as structure was lost. Staining and imaging of remaining slice portions showed that despite structural loss, much intense green fluorescence was seen, indicating live areas of the tissue (Figure 4.3). some red fluorescence highlighting dead areas was observed, particularly at edges of samples. Despite gelatin proving to be a too easily removable material resulting immediate structure loss, its removal did not appear to have an impact on sample viability; of structure could be maintained, samples would still be viable for further experimentation.

4.2.3 Initial investigation of transfective ability comparative to agarose PCLS and agarose-based conditions

In an attempt to develop a way to utilise gelatin PCLS without significant structure loss, samples were deposited in transwells, which would allow for support and manipulation above the liquid whilst still supplying nutrients from the media below. Agarose was utilised to ‘glue’ the gelatin PCLS to the transwell membrane pre incubation, also filling the space between the slice and the transwell outer. If the slice was secured, there was the potential for the structure to be maintained even after Gelatin melting and removal. Agarose was used as the ‘glue’ as it would not be affected by the temperature change on incubation.

Samples were prepared on ice, with images taken directly before incubation. slice outline was easy to visualise and distinguish from the surrounding agarose. Due to previous rapid structural loss, Samples were incubated for 1 hour before removal and immediate observation and imaging.

Slice reduction was immediately apparent, even after only an hour of incubation. Following each outline of samples pre and post incubation and superimposing one over the other highlighted the extent of the reduction in both slice size and loss of structure (Figure 4.4). Samples did appear flatter and less ‘balled up’ than previous free floating samples, which could most likely be attributed to the support of the transwell membrane.

Transfection and prestoblue was also carried out on transwell samples, to obtain quantitative data on viability and transfection potential if the transwell

and agarose ‘glue’ proved successful. These were compared to various agarose samples in ‘glued’ and free floating conditions.

Initial expression and viability data for this experiment confirmed previous results, and gelatin PCLS proved untransfectable even when attempts were made to support structure loss post gelatin removal. Agarose PCLS performed similarly to previous experiments, with no viability of transfection issues observed; interesting to note was when agarose PCLS were ’glued’ in place with agarose, the extra agarose in this situation did not seem to affect transfection, but when used to cover the slice, no transfection was possible. This could support the theory that agarose, at least in increased amounts, can prevent transfection penetration and reduce transfection success. From these experiments, gelatin was confirmed as an unviable alternative to agarose as a perfusate material; however, agarose PCLS were somewhat proven to be the most viable and transfectable samples, and excessive agarose presence was observed to have some detrimental effect on transfection success. In future, modifications such as lowered agarose concentrations in the perfusion solution could be utilised and investigated.

5. Chapter 5: Establishing an in vitro Air Liquid Interface model (ALI) for demonstration of non-viral delivery

5.1 Introduction

Previous research has established Air liquid Interface culture (ALI) as a useful method for investigating drug delivery (Schmid, et al., 2017), (Lenz, et al., 2014) and aerosolised toxicity studies (Herzog, et al., 2014), (Upadhyay & Palmberg, 2018), (Raemy, et al., 2012). There is also focus on investigation of aerosolization of potentially therapeutic molecules (Hu, et al., 2020). It has also proved to be a useful method in delivery studies (Ong, et al., 2016); (Lenz, et al., 2014) and for investigation into a variety of lung relevant disease states (Munis, Hyde, & Gill, 2020), (Eenjes, et al., 2021) (Slepushkin, Staber, Wang, McCray, & Davidson, 2001), (Prulière-Escabasse, et al., 2005) by allowing replication of the lining of the human lung in a controlled environment, without the expensive and potentially wasteful process of a small or large scale animal study. Despite lacking the full anatomical structure observed *in vivo*, multiple lung cell types are present within air liquid interface fully differentiated cell layers, allowing the mucociliary phenotype of epithelial lung to be achieved on a smaller scale (Jiang, Schaefer, & Chu, 2018).

Here, utilising previously published research utilising ALI, development of air liquid Interface mucociliary layers was attempted, using immortalised human bronchial epithelial cells (iHBEC). The final aim was to utilise any developed ALI layers as a model to test transfection with the GET peptide non-viral

delivery system. A significant amount of optimisation was required, and confirmation of successful differentiation was quantified with Transepithelial/Transendothelial electrical resistance (TEER) of potentially developed layers, alongside investigation with a variety of antibody markers using immunofluorescent technique and sample imaging using fluorescent and confocal microscopy.

5.2 Initial transfection of iHBECs

To establish if the iHBEC cell line would be useful for non-viral delivery studies post differentiation at the air liquid interface, monolayers were developed and transfected to confirm GET peptide delivery ability to this cell type. Untransfected controls were compared against luciferase reporter plasmid (PMV-GLuc-2) and enhanced luciferase plasmid (pGM206SMAR). All plasmids were delivered with FLR peptide only, and FLR:FLH peptides in complex.

Reporter plasmid (PMV-GLuc-2) exhibited initial high expression 3-fold higher than the untransfected controls, when delivered with FLR peptide only. Minimal difference could be observed between FLR:FLH delivery and FLR only delivery. 1 week post transfection (Day 7) showed some decrease in expression. However, even at Day 21 post transfection, samples were still expressing levels above the untransfected controls (Figure 5.1).

Enhanced plasmid (pGM206SMAR) demonstrated a high expression profile over all timepoints, with less decline in expression than reporter plasmid. Initial expression was high, similar to reporter plasmid, with subsequent days

expression showing very minimal decrease in expression. At Day 7, enhanced plasmids samples showed minimal difference to Day 1 expression, regardless of whether delivery was with FLR only or FLR:FLH in complex. A similar amount of expression was also seen at Day 21 post transfection.

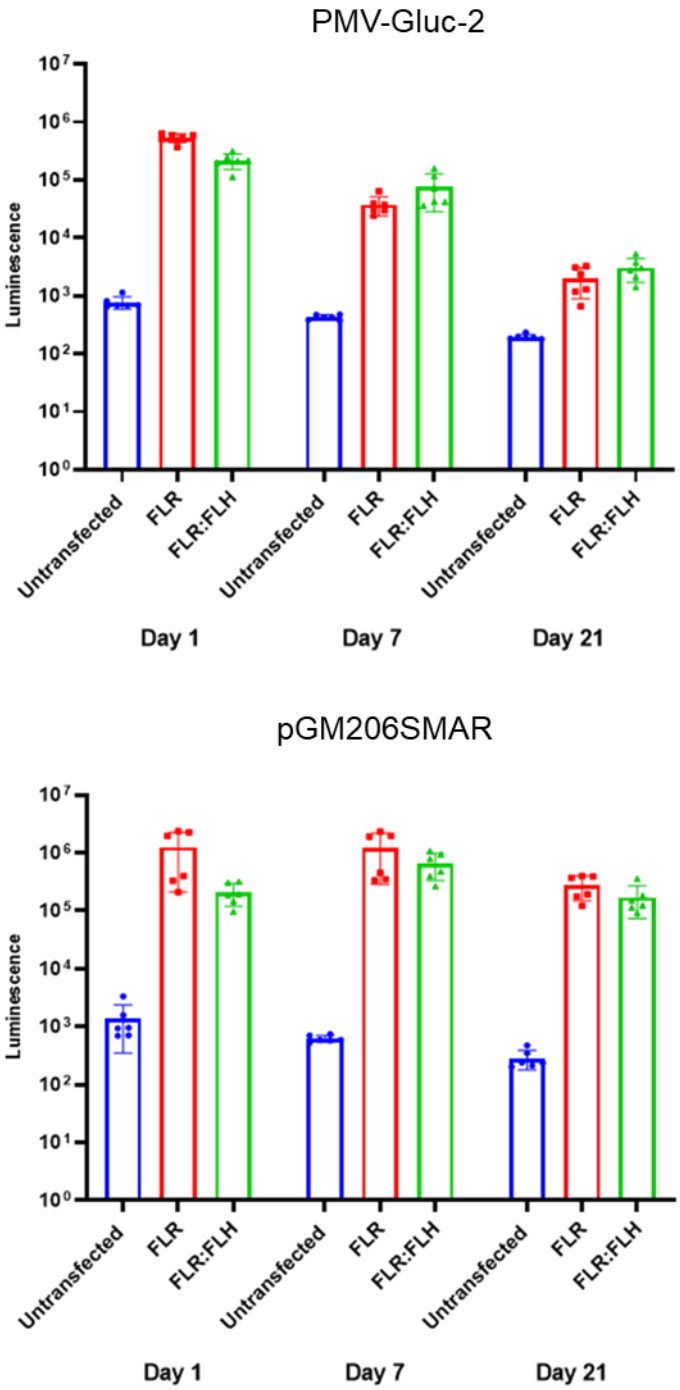


Figure 5.1 Initial proof of transfection in iHBEC monolayers *Cell monolayers were transfected to determine if the cell type would be transfectable post differentiation at the air liquid interface (ALI) and to test GET peptide delivery ability with the iHBEC cell line. All experimental groups (n=6). All error bars represent the standard error (s.d.).*

5.3 Initial transwell cultures

Initial transwell samples were seeded using confluent iHBEC cells, and once established on transwell membranes, were air lifted no later than 72 hours post seeding. The apical surface was then continuously exposed to air, with KSFM media deposited in the well under the membrane. This was regularly changed every other day to maintain cultures. Samples were then imaged every week to visually determine any morphological changes, and initial transepithelial/transendothelial electrical resistance readings (TEER) were carried out at 2 weeks and 4 weeks (Day 14 and Day 28). Post culturing, samples were fixed and antibody markers P63, αTubulin, and FOXI1 were used to carry out Immunofluorescence (IF) to establish if specific cell types were present, to aid in confirmation of an established mucociliary epithelial lung layer. P63 was used to identify basal lung cells, αTubulin was used to help identify any cilia or ciliated cells, and FOXI1 was used with later samples to identify any ionocytes. Processed layers were imaged fluorescently to determine presence and location of any differentiated cells in the layer.

Imaging of initial transwell samples over time highlighted formation of cell clusters forming on top of the original monolayer seeded on the transwell. These structures were visible from around 1 week post seeding (Day 7) and continued to be visible and develop even to 4 weeks post seeding (Day 28). Some clusters appeared linked and branched towards each other (Figure 5.2, indicated with arrows). This may have been indication of some initial development of a differentiated layer. To aid in confirmation of any layer development, samples were fixed and used for Immunofluorescence.

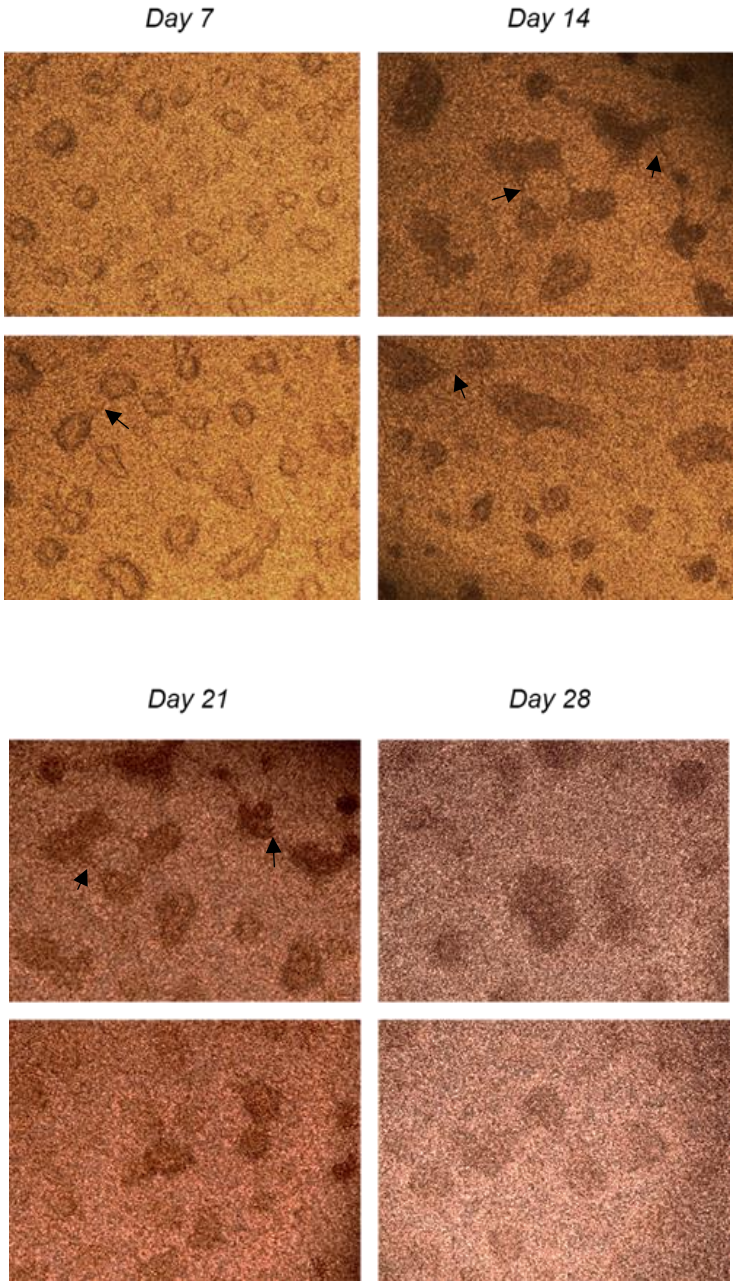


Figure 5.2 Initial imaging of developing transwell samples *Initial iHBEC samples at the Air Liquid interface developed cell clusters, which appeared to be forming above the initial layer of confluent cells. These clusters were apparent from 1 week at the air liquid interface, and still visible at 4 weeks ALI (Day 28). 10x objective used.*

5.3.1 Transepithelial/Transendothelial electrical resistance (TEER) of initial layers

Transepithelial/Transendothelial electrical resistance (TEER) is a method used to read the electrical resistance across a cell layer; it is used most often in lung and gut transwell experimentation to determine formation of tight junctions, and thus successful barrier formation and layer differentiation (Srinivasan, et al., 2015); (Altube, Caimi, Huck-Iriart, Morilla, & Romero, 2021). Other techniques, such as immunofluorescence, are used in conjunction with TEER readings to aid in confirmation of layer development.

TEER readings were taken from initial transwell samples. following this, TEER readings from subsequent transwell experiments were taken at Day 14 and Day 28 (Figure 5.3).

For Initial TEER readings (Figure 5.3, A) 1 reading was taken from 1 well of each plate in culture. Plate 5 was not included due to minimal samples on this plate and potential risk of infection. Despite minimal data from initial readings, some clear difference in resistance (Ohms) could be observed between samples, dependent on day. Day 14 sample appeared to be lower than the unseeded blank transwell, however established cultures at post 4 weeks air lift (Day 40, Day 47) demonstrated increased resistance comparative to the earlier timepoint and the blank transwell. It was established that multiple readings would be needed from multiple wells in future TEER reading experiments.

TEER readings of subsequent transwell experiments (Figure 5.3, B) were taken at 2- and 4-weeks post air lift (Day 14 and Day 28), with 3 readings

taken from each plate read. All samples read demonstrated higher resistance than the blank unseeded control, with small increase observed in resistance over time from Day 14 to Day 28. Overall, resistance readings were lower than expected, as established layers utilising this cell type and similar cell types ranged from around 300 – 800 ohms within the literature (Rayner, Makena, Prasad, & Cormet-Boyaka, 2019); (Kuek, et al., 2018); (Sakagami, 2006).

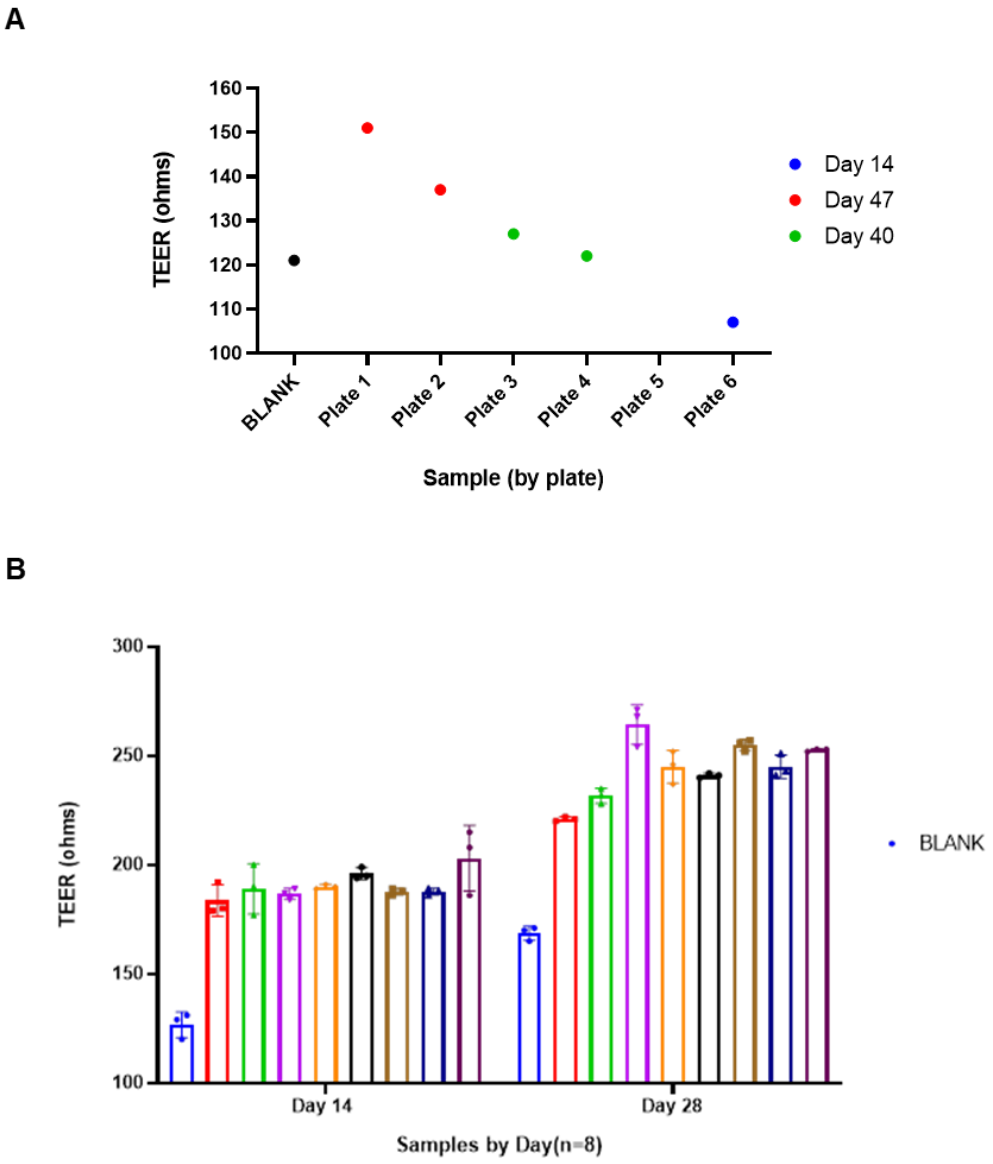


Figure 5.3 Initial TEER readings of early transwell samples *(A) Initial optimisation of TEER readings of on first Air liquid interface samples (ALI) were taken from each plate in currently in culture; each set of plates were at a different timepoint, and from this some difference in electrical resistance of the layer could be seen between samples at 2 weeks (Day 14) and samples beyond 4 weeks (Day 40, 47). (B) Following set of transwell samples at Air liquid interface. 3 readings were taken from each well, with 8 wells used from each plate. Regardless of timepoint, all readings for samples were higher than the unseeded transwell control (Blank). Some overall increase in electrical resistance of the layer could be observed between Day 14 and Day 28 for all samples. All experimental groups (n=3); all error bars represent the standard error (s.d.).*

5.3.2 Immunofluorescence with initial markers

Immunofluorescence of previously cultured samples was carried out with multiple antibody markers to aid in identifying any differentiated cell types that may have been present in any developed cell layers. Markers used were P63 (lung basal cells), αTubulin (ciliated cells), FOXI1 (ionocytes).

5.3.2.1 P63 for basal cell identification

Initial P63 immunofluorescence was optimised slightly to determine ideal antibody concentration. Antibody was used at 1/100 and 1/200 concentrations. DAPI stain was also used to identify cell nuclei.

Within samples, previously observed cell clusters (Figure 5.2) could be observed. DAPI staining also appeared more frequent and intense within these cell clusters (Figure 5.4). in specific cell clusters, some intense green fluorescence could be seen in 1/200, potentially indicating a positive result. Overall, minimal intense green fluorescence could be observed.

5.3.2.2 αTubulin for ciliated cell identification

Initial αTubulin immunofluorescence demonstrated positive staining within most of the cytoplasm of visible cells (Figure 5.5). DAPI staining helped to confirm cell location by identifying cell nuclei. Further magnification to 40x made cell outlines easier to visualise. αTubulin appeared to be present

throughout the cell cytoplasm in all samples, suggesting a lack of marker specificity.

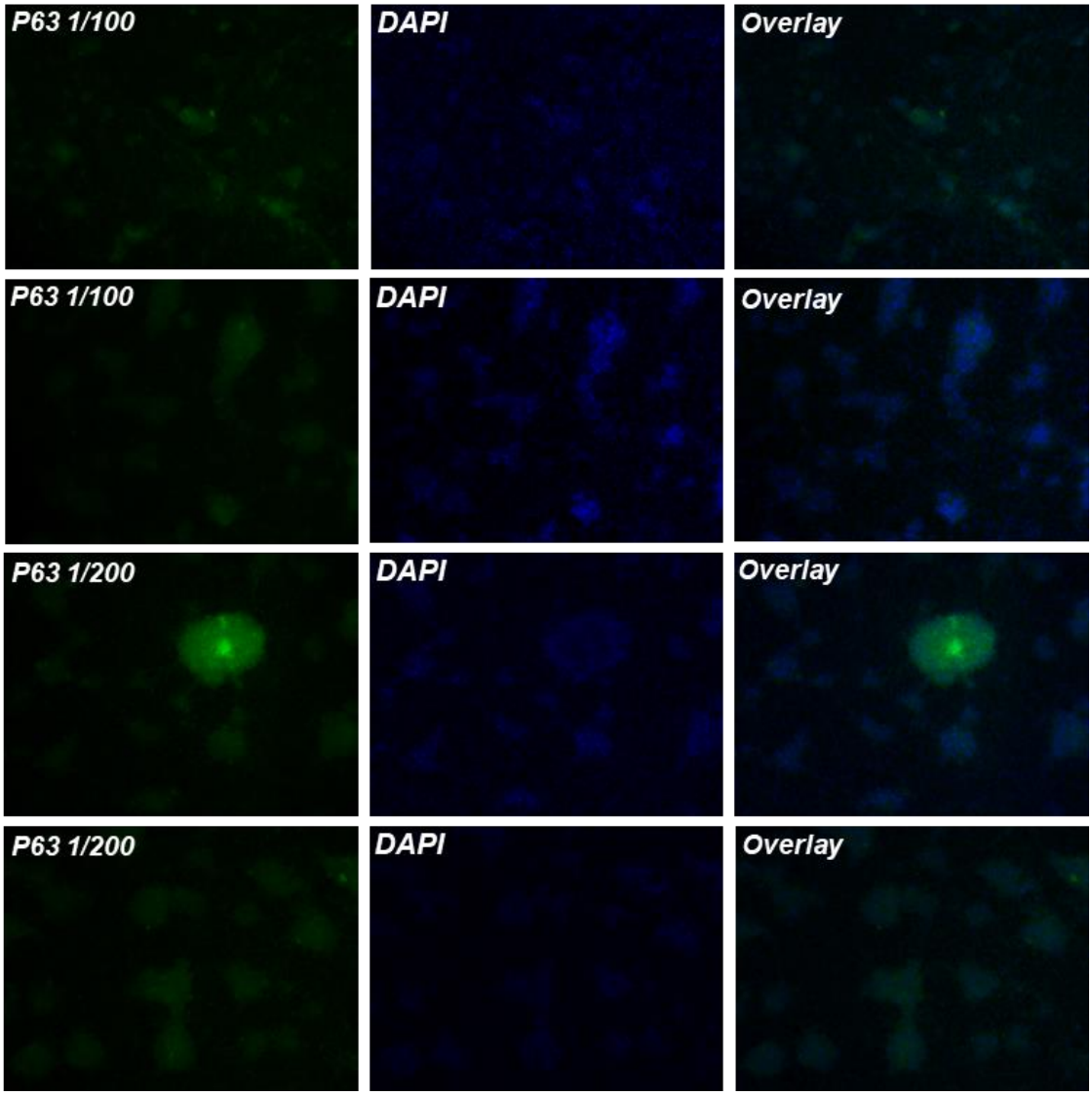


Figure 5.4 Initial Immunofluorescence using P63 Marker *P63 marker was used for initial attempts at identification of lung basal cells in transwell samples. 20x magnification. it was unclear if fluorescence observed was representative of the presence of P63 within the samples.*

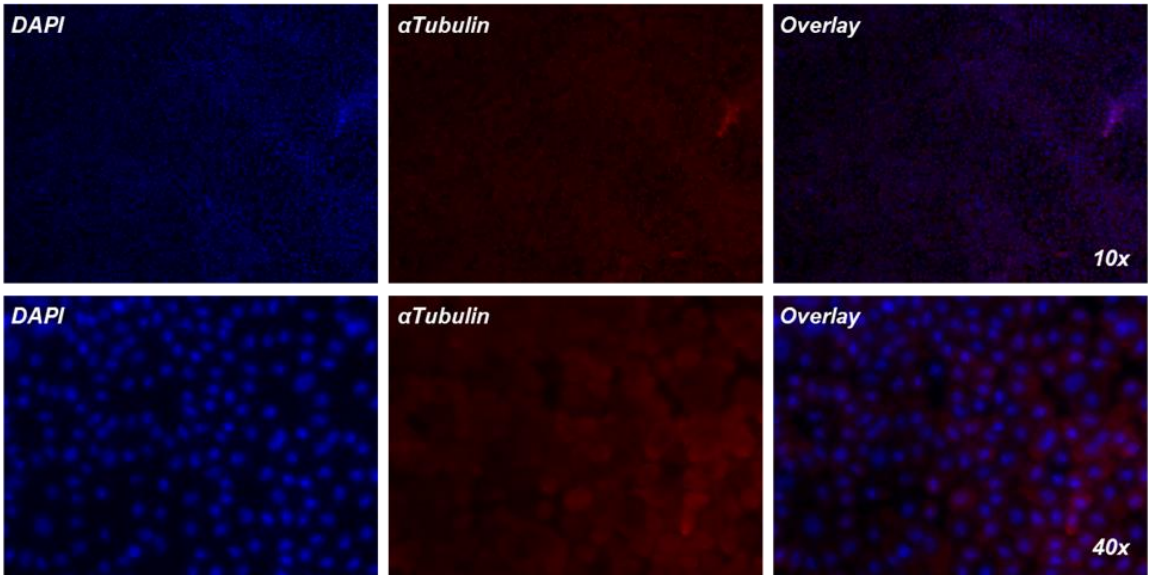


Figure 5.5 Initial Immunofluorescence using αTubulin Marker *αTubulin was used for initial attempts at identification of cilia/ ciliated cells in transwell samples. αTubulin appeared uniformly everywhere throughout all cell cytoplasm, so it was unclear if this was background fluorescence, or representative of positive staining.*

5.3.2.3 Comparative timepoints to determine presence of specific cell types

Samples were fixed at specific timepoints; Day 0 (initial day post Air lift) Day 7 (post Air lift) and Day 14 (2 weeks post air lift). all 3 previously mentioned markers were used; however, no fluorescence could be observed within samples apart from DAPI staining in both P63 and FOXI1 immunofluorescence.

Immunofluorescence over specific timepoints (Figure 5.6) demonstrated that αTubulin could be seen as early as the first day post air lift and was present in the majority of the cell cytoplasm. This was also observed previously in initial αTubulin immunofluorescence (Figure 5.5). Over time, some development of the cell layer was seen, as cells reduced in confluence, and changed slightly in morphology; by Day 14, some cells were only identifiable by their nuclei, as no αTubulin was present in their cell cytoplasm. Despite some layer development, the issue remained that most likely this marker lacked the required specificity.

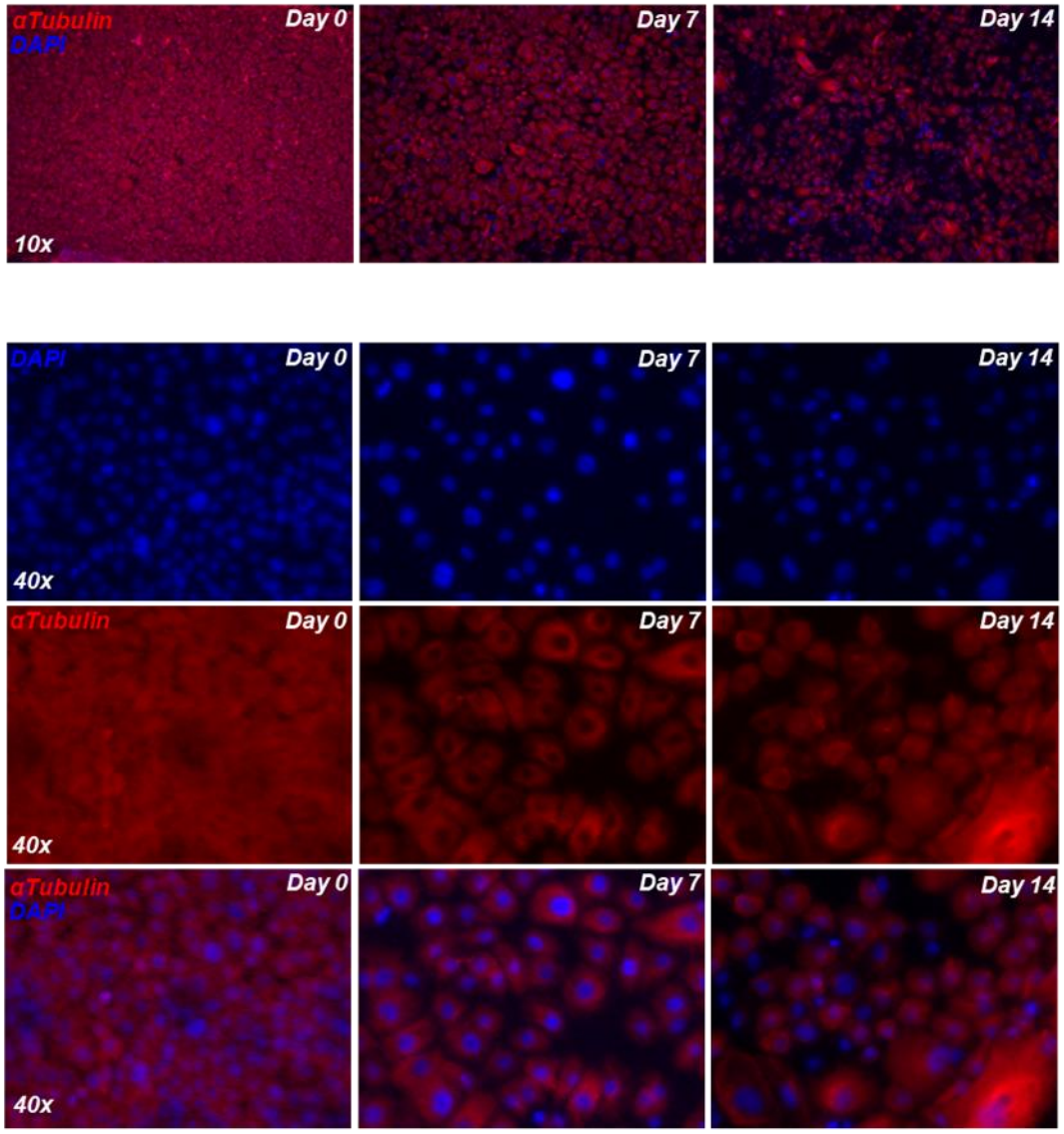


Figure 5.6 Comparative immunofluorescence over time using αTubulin *Marker samples were fixed, stained, and imaged at specific timepoints up to 2 weeks (Day 14). using samples over a period of 2 weeks helped to further discern if αTubulin staining was genuine, and not merely background fluorescence.*

5.3.2.4 Immunofluorescence confirmation with Confocal Microscopy

Confocal microscopy was utilised to image previous samples, to improve quality of images and further aid in confirmation of any localised fluorescence within samples (Figure 5.7).

In P63 samples (Figure 5.7, A), the shape and outline of cell clusters previously observed was clear; more intense fluorescent areas appeared within the cluster, but overall, no difference in fluorescence intensity was apparent in samples (P63) comparative to controls (No AB).

In alpha tubulin samples (Figure 5.7, B) DAPI stained nuclei were seen in all conditions, with controls (No AB, Secondary only). Stained sample (αTubulin) had both distinct DAPI stained nuclei and localised fluorescence in the cytoplasm highlighting presence of alpha tubulin.

In FOXI1 samples (Figure 5.7, C) both controls and stained samples appeared similar in fluorescence intensity and location; DAPI stained nuclei were observable on all conditions, with minimal red fluorescence appearing in the cytoplasm of all samples.

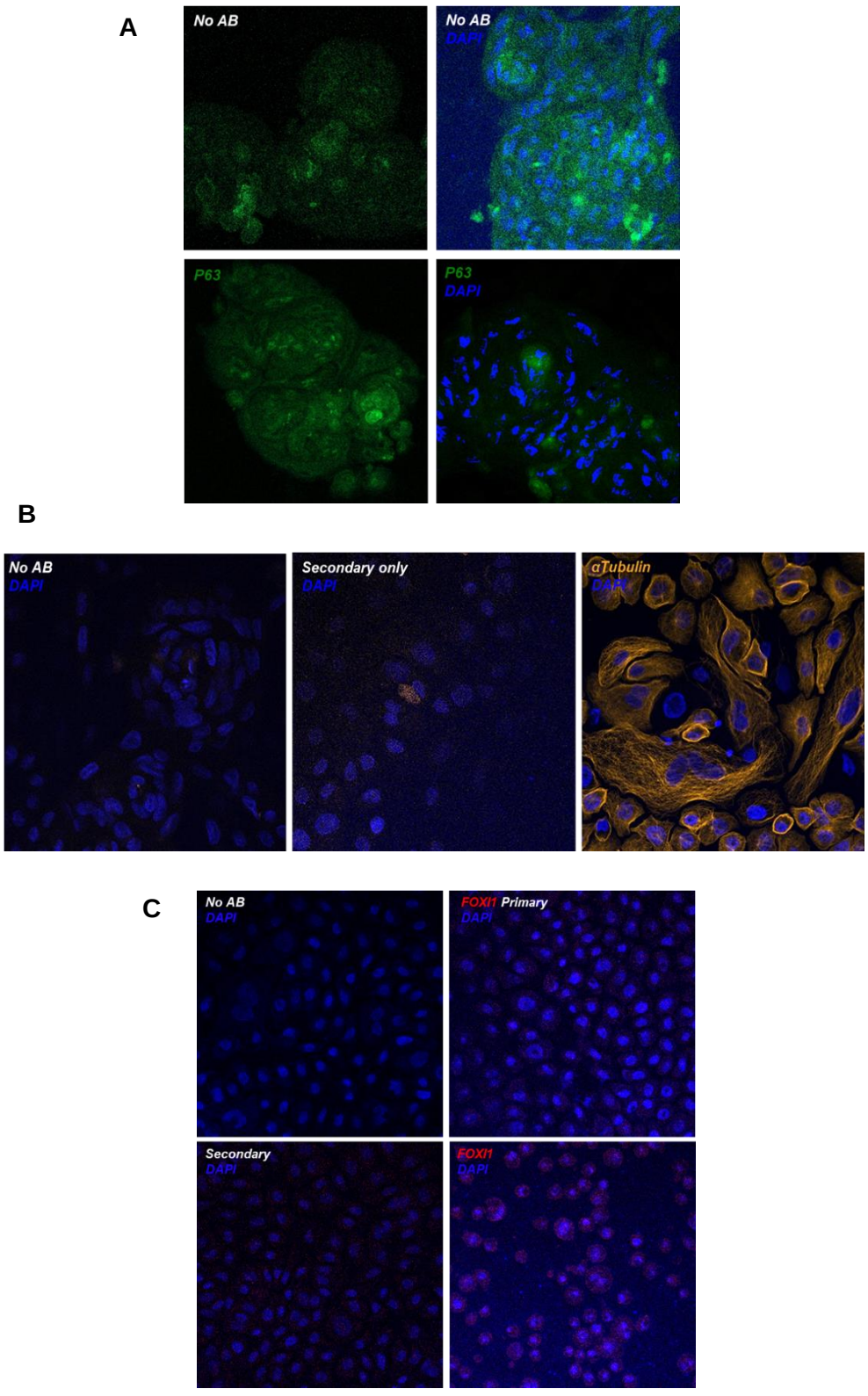


Figure 5.7 Visualisation of immunofluorescence of P63, αTubulin, and FOXI1 markers with Confocal Microscopy *previous samples were re-imaged with higher power confocal microscopy, to aid in confirmation of sample staining.*

5.3.3 Transepithelial/Transendothelial electrical resistance (TEER) of adapted cultures

Transepithelial/Transendothelial electrical resistance (TEER) readings were carried out on transwell cultures to aid in determination of layer development. Initial cultures were seeded onto standard PET membranes, with later adapted cultures seeded onto collagen coated membranes.

5.3.3.1 Collagen coated transwells comparative to non-collagen coated transwells

TEER readings were taken of both non-collagen coated and collagen coated transwell cultures; readings were taken at Day 14 post air lift (2 weeks) and Day 28 post air lift (4 weeks).

Regardless of condition, all transwell cultures displayed lower TEER readings than those seen in ALI literature; minimal to no difference could be observed between collagen and non-collagen samples. Despite overall lowered readings than expected of developed cultures, both collagen coated and non-collagen coated cultures displayed some small increase from Day 14 to Day 28 (Figure 5.8, A). all samples appeared higher than the blank transwell control at both timepoints.

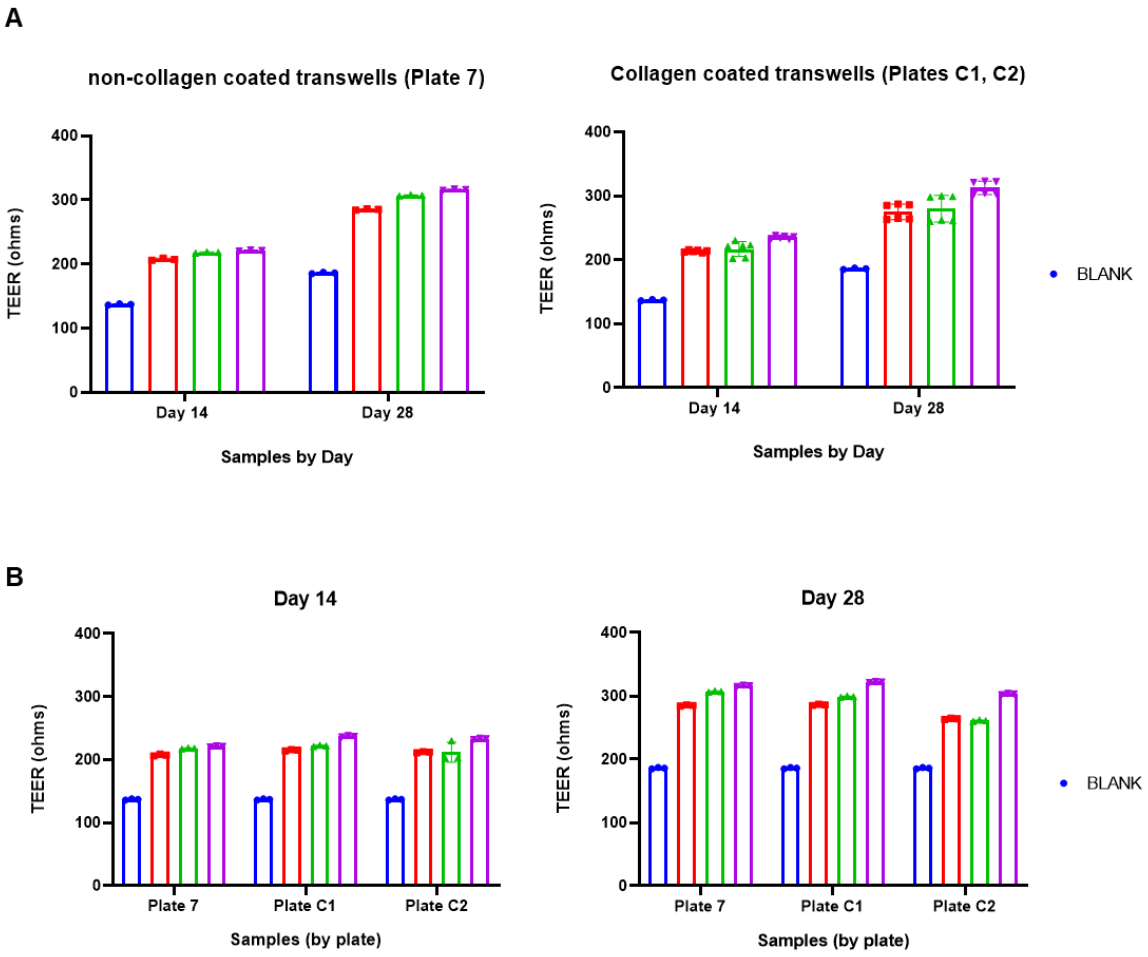


Figure 5.8 TEER readings of Transwell samples after introduction of collagen coated transwells and Air liquid Interface media system *(A) comparison of non-collagen transwells with collagen coated transwells by Day (B) comparison of non-collagen transwells with collagen coated transwells side by side (by plate). Minimal difference could be observed at each timepoint between either collagen or non-collagen transwells. Both transwell types demonstrated some increase from day 14 to day 28 in electrical resistance, with all samples higher than the unseeded transwell control (Blank). All experimental groups (n=3); all error bars represent the standard error (s.d.)*

5.3.4 Immunofluorescence of adapted cultures

Immunofluorescence was carried out on potentially differentiated layers at 4 weeks (Day 28). Markers for tight junctions (ZO-1) and mucin/mucus producing cells (MUC5AC) were used. Samples were imaged with confocal microscopy.

5.3.4.1 ZO-1 for Identification of Tight junction formation

ZO-1 immunofluorescent staining clearly highlighted the presence of tight junctions throughout the entire layer (Figure 5.9, ZO-1 in pink). DAPI only and ZO-1 only controls confirmed successful staining, with no bleed through observed and minimal to no background within both controls and the sample. DAPI staining helped to visualise each cell within the sample, however, web-like ZO-1 structure appeared to overlap directly with some individual nuclei. Tight junctions were observable, which is a potential indicator of layer development and differentiation.

5.3.4.2 MUC5AC for identification of Mucin secretion

MUC5AC immunofluorescent staining was also carried out, similarly to ZO-1 staining. Again, individual controls for DAPI only staining and MUC5AC only demonstrated minimal to no background, confirming successful staining. Within the sample, individual cells showed intense red fluorescence distinct from low level fluorescence. MUC5AC control also demonstrated

similar intense fluorescence within individual cells (Figure 5.10, MUC5AC in red). individual cells across the layer were positive for MUC5AC staining, potentially indicating some layer development and cell differentiation was occurring.

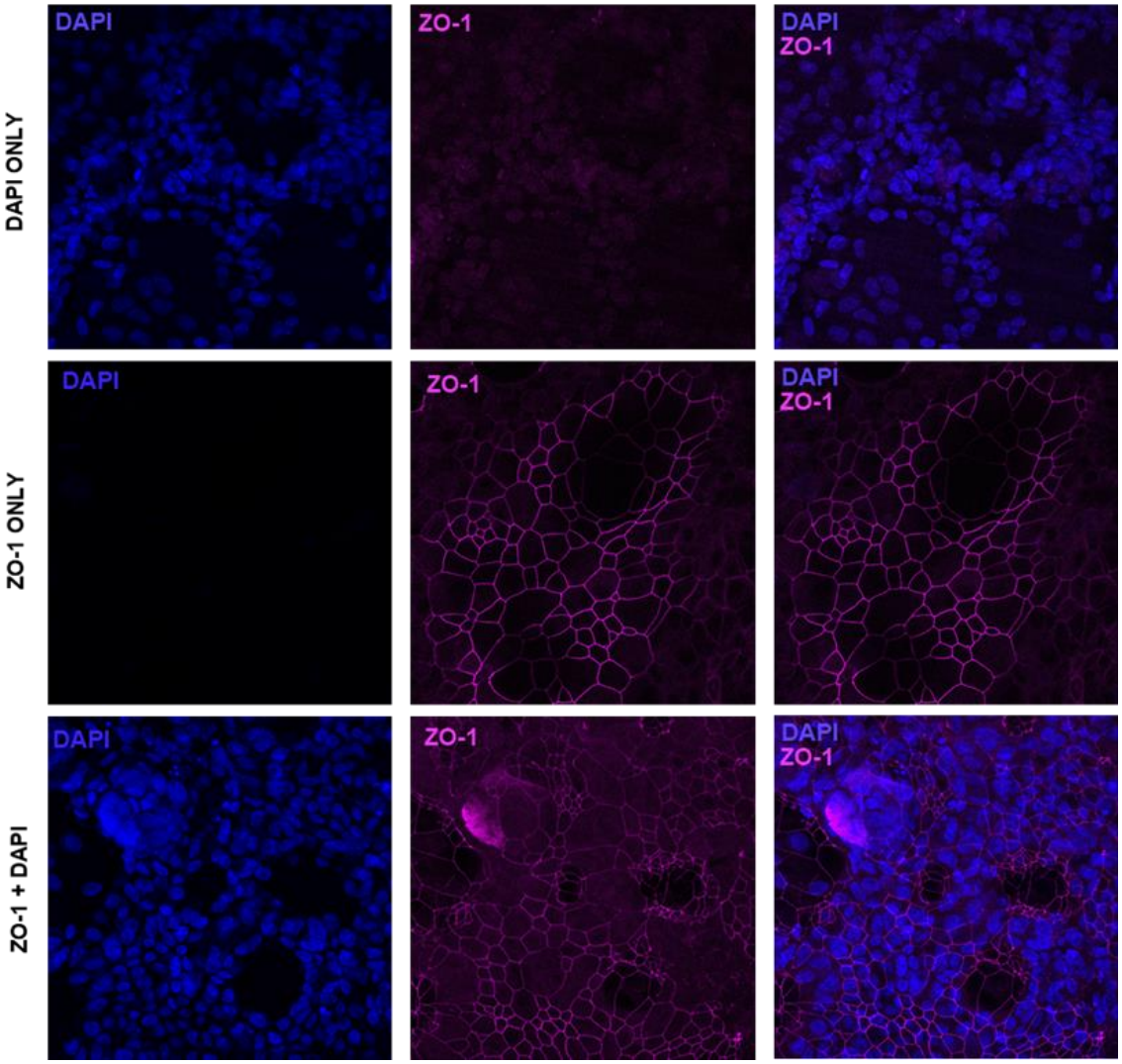


Figure 5.9 Immunofluorescence using ZO-1 Marker *Immunofluorescence of transwell cell layers at Day 28 (4 weeks at the air liquid interface) shows clear formation of tight junctions between cells. Primary conjugated fluorescent ZO-1 was used to identify tight junction formation, alongside DAPI to identify cell nuclei. 40x water Immersion.*

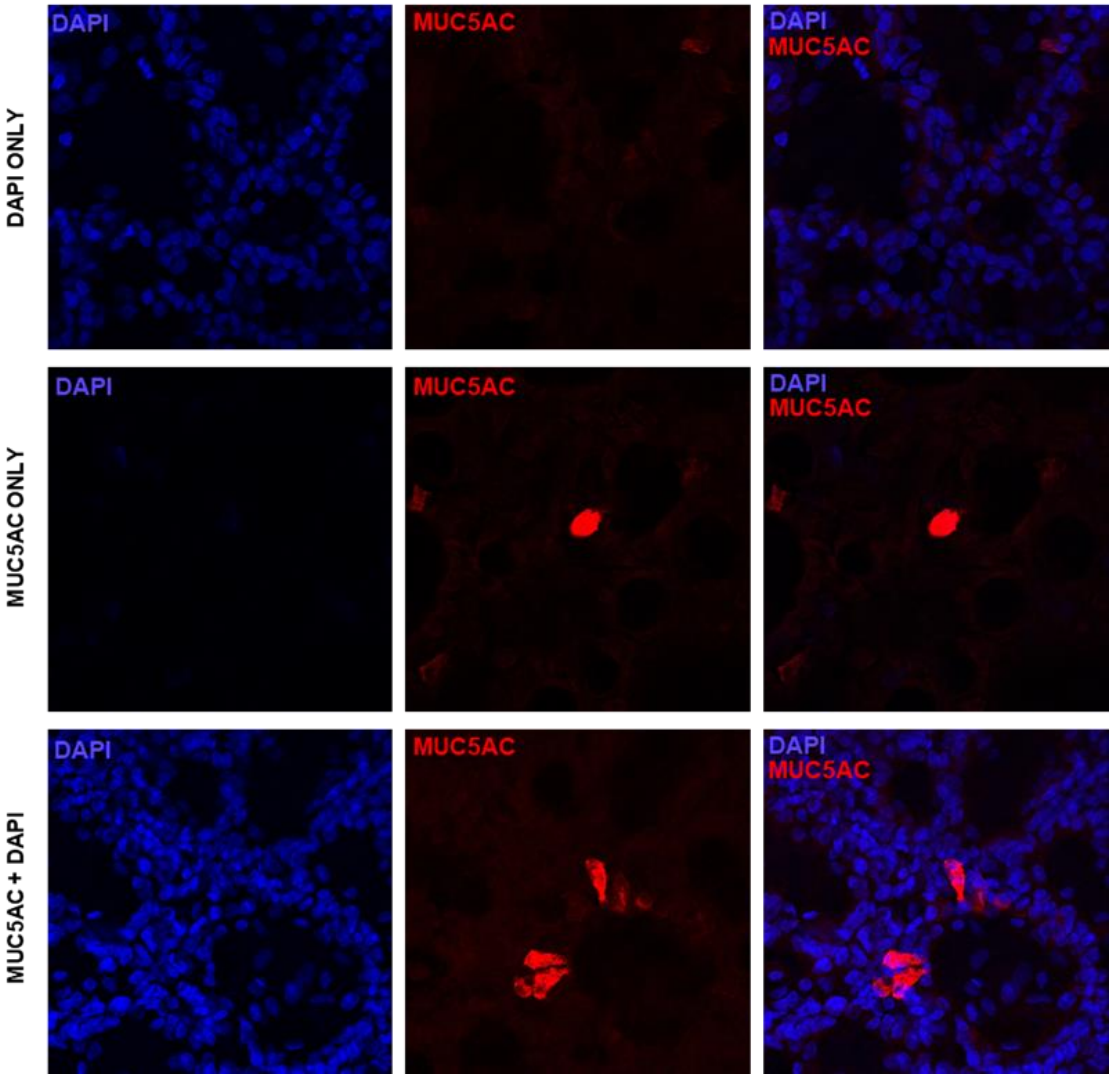


Figure 5.10 Immunofluorescence using MUC5AC Marker *Immunofluorescence of transwell cell layers at Day 28 (4 weeks at the air liquid interface) helps to identify cells secreting mucus. Primary conjugated fluorescent MUC5AC was used to identify any mucus producing/ goblet cells, alongside DAPI to identify cell nuclei. 40x water Immersion.*

5.4 Initial transfection of Transwell cultures

Initial transfection of potentially established ALI cultures was carried out to optimise peptide mediated delivery; initial transfection was delivered to the well below the transwell (the basal chamber), similarly to the standard method used for non-viral peptide mediated transfection. FLR44 peptide was used to deliver standard luciferase reporter plasmid (PMV-Gluc-2) and two enhanced luciferase plasmids (pGM206, pGM206SMAR) alongside an untransfected control. Transwell cultures were transfected after Day 28 post air lift (4 weeks at air liquid interface).

Initial expression appeared minimal to low in all conditions; around 10-fold difference was observed between enhanced vector pGM206SMAR and all other conditions, including the untransfected control (Figure 5.11). No significant difference could be observed between the untransfected control or any other condition, at Day 1, Day 3, or even a week (Day 7) post transfection. Despite some observable difference, expression from the enhanced vector pGM206SMAR did not demonstrate significant difference comparative to other conditions and may not represent true expression.

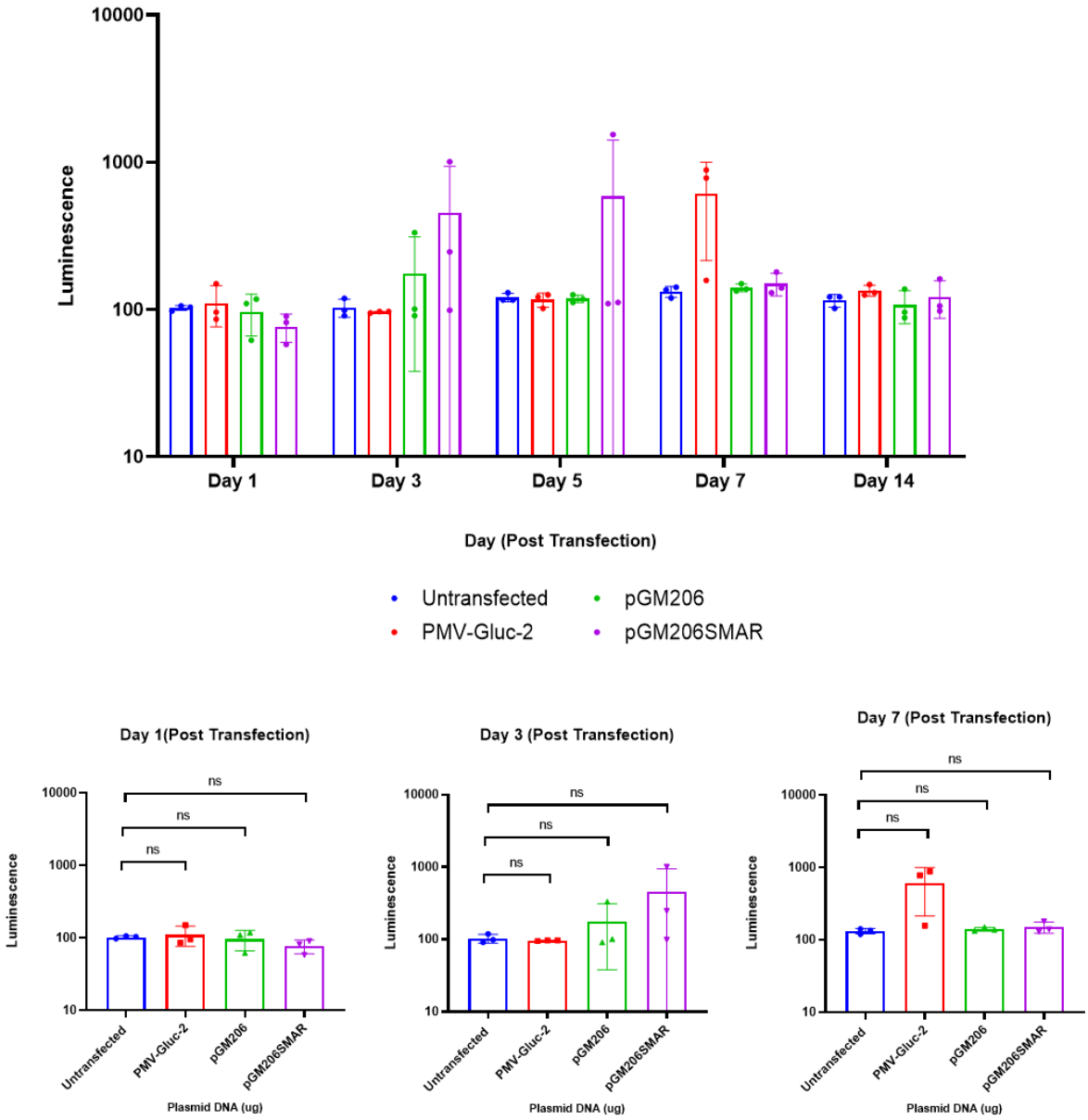


Figure 5.11 Initial Transfection attempt of iHBEC transwell cultures *initial transfection of post Day 28 transwell samples demonstrated minimal transfection, with no significant difference observed in expression at any day post transfection or any condition. All experimental groups (n=3); all error bars represent the standard error (s.d.).*

5.5 Discussion

Within this chapter, establishing Air Liquid Interface (ALI) cultures from human immortalised bronchial epithelial cell (iHBEC) populations was attempted, in order to differentiate cultures and achieve a phenotypical mucociliary layer on which to test GET non-viral peptide-based delivery. This model was chosen to follow on from precision cut lung slices as it was a more accurate *in vitro* model as it utilised human cells, as opposed to animal tissue, and incorporated air exposure of cultures which more accurately mimicked the *in vivo* environment, as opposed to using submerged lung cultures or tissue. Going forward with an *in vitro* model also aided in reducing overall animal use.

Significant optimisation was required to establish this model, with results unclear as to whether this objective had been fully achieved. Multiple experimental changes were made as optimisation continued, including utilisation of collagen coated plasticware and use of supplementation based specialised media, in an attempt to establish a mucociliary phenotype. Established confirmation methods such as TEER readings of layers and cell specific marker immunofluorescence was used to try and unanimously confirm developed layers. Initial experimentation was attempted on partially differentiated ALI cultures that presented both mucin positive cells and clear tight junction formation; transfection results showed minimal to no transfection, which may have been due to further optimisation needed when using GET peptide as the method of delivery.

5.5.1 Cell type and cell population age

Immortalised human bronchial epithelial cells (iHBEC) were utilised for all experimentation with transwell layer work. These cells were readily available and appeared to fit the specifications needed from a cell line for developing a mucociliary phenotype. after further review and optimisation, it was determined that although a robust cell type and initially fit for purpose, previous user passage number was perhaps too high for this type of work. The current literature gives a general recommendation of around passage 8 at the most, or earlier (Rayner, Makena, Prasad, & Cormet-Boyaka, 2019) so it appears newly established populations more easily give rise to the cell types required for a full mucociliary layer to successfully develop.

From previous research, it also appears primary cells are more likely to give rise to a fully developed layer (Rayner, Makena, Prasad, & Cormet-Boyaka, 2019); (Lee, Petris, Hynds, & O'Callaghan, 2020). As this particular iHBEC population would no longer be considered primary, this may also have impacted on experimentation and could explain difficulties during optimisation.

Storage of later stage passages could also have had an effect on culture and transwell optimisation; at certain stages during experimentation, cells were unable to be stored for the duration of storage time in liquid nitrogen, and thus for a period of time were stored at only -80^{o}C; this is not an optimum temperature to store cells long term (Kilbride, Meneghel, Fonseca, & Morris, 2021); (Kielberg, 2010) and thus could have had a detrimental effect on later passages of the iHBEC stocks.

Despite some optimisation issues, iHBECs performed well for the majority of experimentation and were easy to culture, with key markers later identifying indicators of successful layer development, such as tight junction formation and presence of mucin secreting cells.

Initially, iHBECs were seeded as monolayers and transfected using the GET system, to demonstrate that this cell type was transfectable and thus suitable to use for ALI model set up. Both FLR peptide and FLR:FLH in complex were used to deliver standard reporter plasmid (PMV-GLuc 2) and enhanced plasmid pGM206SMAR. Transfections were continued over time to observe any reduction in expression output.

Expression profiles were significantly higher in the iHBEC cell line than in any previous PCLS experimentation; initial expression at day 1 was around 1000000 for FLR conditions, and over time this demonstration slower decline than in PCLS. By Day 21, clear expression comparative to the untransfected control could still be observed (Figure 5.1).

When standard luciferase reporter plasmid was used, there was minimal difference in expression between delivery conditions, however this difference was more apparent when the enhanced vector pGM206 SMAR was used. Surprisingly, FLR only delivery appeared to give higher expression than the peptide complex. Overall, enhanced plasmid demonstrated slower decline in expression over time.

Once it was established that iHBECs were easily transfectable, they were utilised initial transwell experiments.

5.5.2 Initial transwell Iterations

Initial transwell work utilised iHBEC populations and upon recommendation, non-specialised media for initial set up and culture. These early cultures developed cell clusters on the layer surface from around day 7 post air liquid interface (ALI), with cluster continuing to be apparent in regular imaging. With weekly imaging, it was ascertained that the surface of the layer demonstrated no visual differences comparative to initial set up, as even at day 28, layers appeared flat except for the same large cell clusters forming (Figure 5.2). It was unclear why cell clusters were forming, but initial layers were considered to most likely be unsuccessful and thus further optimisation was needed to achieve fully developed layers.

Reagents and media currently used were investigated, and after review, it was difficult to find other research that used non-specialised media such as KSFM. A new specialised media system was utilised moving forward, and further experiments were cultured using Stemcell PneumaCult ALI media system.

5.5.3 TEER readings for confirmation of layer development

Initial attempts at TEER (Transepithelial/Transendothelial electrical resistance) was used to determine tight junction formation, a key indicator of epithelial layer development (Srinivasan, et al., 2015). TEER of initial experiments was taken of all currently active plates regardless of timepoint (Figure 5.3). these early samples showed some variation based on

timepoint, with a 2 week plate (Day 14) showing much lower TEER than a post 4 week plate (Day 40, 47). It was clear some difference could be observed over time and that TEER may be increasing, but overall numbers were distinctly lower than those recorded in the literature in developing layers, as developed layers can give readings of around 800 – 1000 ohms (Rayner, Makena, Prasad, & Cormet-Boyaka, 2019); (Kuek, et al., 2018); (Sakagami, 2006). Following experiments were recorded at 2 weeks ALI (Day 14), and 4 weeks ALI (Day 28). With the addition of a new media system when culturing, some improvement in TEER readings could be seen. Whilst still well below expected values, increase could be seen from the blank controls, and some increase was observed over time from 2 weeks to 4 weeks ALI.

5.5.3.1 Comparisons of non-coated and collagen coated plasticware

To further improve optimisation and establish a layer, collagen coated transwells were utilised and compared to previous non collagen transwells. Previous research has utilised collagen coated plasticware and transwells, with some reporting effectiveness (Michi & Proud, 2021); (Cozens, et al., 2018) with others noticing no difference in layer development (Leung, Wadsworth, Yang, & Dorscheid, 2020). Other research also demonstrates success of cultures on coated plasticware is both species specific and coating specific (Levardon, Yonker, Hurley, & Mou, 2018). To determine if collagen coated transwell could benefit layer development for this project, cells were seeded and cultured for up to 28 days on both collagen and non-

collagen membranes, with TEER readings carried out at day 14 and day 28. Three samples were read from each active plate, with repeats carried out for each sample (n=3).

Both collagen and non-collagen samples demonstrated some increase between Day 14 and Day 28, with all samples higher than the blank control (Figure 5.8 A). Individual samples from the collagen coated plates appeared to read higher than 300 ohms, the highest observed across all previous transwell TEER results. However, when all plate samples were aligned as collagen and non-collagen samples side by side at each timepoint (Figure 5.8 B), minimal difference could be observed across all samples. From initial results, collagen coating on membranes of transwells did not appear to have either detrimental or beneficial effect on development of layers, at least in the context of tight junction formation.

5.5.4 Choice of markers for immunofluorescence

Initial markers characterisation was attempted with included P63, acetylated alpha tubulin, and FOXI1. From an initial review of the literature and local guidance, it seemed these markers would be best for use to identify potentially differentiated cell types. P63 was used for basal cells, alpha tubulin for cilia or ciliated cells, and FOXI1 for the potential to identify pulmonary ionocytes; these cells make up only around 1% of the lung population and are linked to CFTR activity in the airway epithelium (Montoro, et al., 2018) .Concentration of initial markers was varied to optimise dose and improve characterisation. Samples were also fixed a multiple timepoints

to observe any changes in cell morphology and potentially identify development of layers over time.

Initial p63 Immunofluorescence was carried out on earlier initial ALI samples, before use of selective differentiation media (Figure 5.4). initial microscopy of these samples was post fixing at day 28. Interestingly, background fluorescence was more obvious at areas where cell clusters formed, alongside what may have been potential true staining. Some cell clusters appeared more intense than those around them, which could have been indication of the staining identifying basal cells. The fluorescence in some clusters also seemed to be further through the focal plane towards the transwell membrane and proved difficult to focus on, which, if the layer was developing and differentiated, basal cells would be more likely be located.

Similarly, initial alpha tubulin staining proved inconclusive (Figure 5.5). whilst cells outlines could be observed, alpha tubulin appeared to be throughout the majority of cells that could be seen, and despite magnification increase, it was difficult to discern exact localisation of true fluorescence comparative to potential background. Alpha tubulin staining was also carried out on samples fixed at weekly timepoints (Figure 5.6), and whilst some visual layer changes could be observed from initial seeding (Day 0) towards Day 14, staining appeared to be uniform throughout the cytoplasm of most if not all cells visible. There was the potential that this represented true staining, as cell outlines could be clearly identified in line with nuclei DAPI staining; however, staining did not seem to be specific and most likely was not identifying cilia or ciliated cells.

To confirm initial sample marker staining, all samples were taken for higher powered confocal microscopy to help identify any marker localisation from potential background, and aid in confirmation of cell types that may be present in developing layers (Figure 5.7 A). p63 staining proved difficult to identify; despite having controls in place where no antibody and/or no DAPI was used, cell clusters appeared to be similar in fluorescent intensity across all conditions. Potentially there was some intensity in particular areas of some clusters, but due to the similarity In fluorescence levels in all samples, even unstained, most likely any fluorescence observed was background and not representative of true staining.

Alpha tubulin staining displayed more observable differences when imaged with confocal microscopy (Figure 5.7 B). Both DAPI and alpha tubulin marker staining were distinct from unstained controls, with individual areas within each cell cytoplasm clearly identifiable. The staining process appeared to be successful and there were no issues with methodology, however, staining was not specific and appeared in the cytoplasm across most cells observed. This could be because Alpha tubulin is also found in the cell cytoplasm as a building block of microtubules that form part of the cytoskeleton (Eschun-Wilson, et al., 2019). Cilia are also a microtubule based organelle (Smith, Lake, & Johnson, 2020), however, due to the uniformly widespread amount of staining in these cells, most likely this staining was highlighting the microtubules present in the cytoplasm. Despite ciliated cells being a predominant cell type in the airway (Yaghi & Dolovich, 2016), This staining appeared to be fibrinous and tendril like within the cytoplasm when the layer

was viewed from above, further supporting that this was most likely cytoplasmic microtubule staining as opposed to cilial microtubule staining.

FOXI1 marker staining was also imaged with both fluorescent and confocal microscopy; even at the confocal level, it was apparent that majority of fluorescence observed was most likely background, as it appeared uniformly across unstained control samples (Figure 5.7 C). Overall, it would be unlikely to observe any FOXI1 staining if other cells such as basal cells could not be identified in the developing layer, as Ionocytes are both rare and specific cells only observed in fully differentiated mucociliary airways.

To improve identification of cells types in the potential layer, further optimisation was needed; based on further literature review, new markers were chosen based on specificity, and to improve characterisation of any differentiated cells present. ZO-1 was used to identify the extent of tight junctions forming in the developing within the layer, with MUC5AC chosen for specifically for identification of any mucus production and Goblet cells.

Samples stained for ZO-1 were imaged using confocal microscopy (Figure 5.9) with DAPI used to highlight cell nuclei. Overall, cells formed a circular pattern, with circular gaps in the layer where no staining was apparent. This was consistent across all samples, including controls. ZO-1 marker fluorescence was distinctly different from controls, evident as web-like structures across the cell layer. This confirmed successful staining and formation of tight junctions across the layer.

Samples stained for MUC5AC were also imaged using confocal microscopy (Figure 5.10). DAPI was also used to highlight cell nuclei. It was clear which

cells in the layer were positive for MUC5AC due to intense localised fluorescence. Individual cells appeared in MUC5AC only controls and MUC5AC + DAPI samples. These cells appeared intermittently throughout the layers. This confirmed that at least some cells in the layer were differentiating successfully into goblet cells.

Interestingly, the same circular patterns with ‘circular gaps’ were also apparent in these samples, as with ZO-1 staining (Figure 5.9). These ‘circular’ structures may have been further confirmation of layer formation and differentiation, as within *in vivo* lung, airways and alveolar would be tubular and spherical; a non- 3-dimensional cross section of such a structure would appear circular. This pattern was also similar to the appearance of a precision cut lung slice under a microscope, which, as a thin longitudinal piece of cut lung tissue, appeared to have many varying sized holes across its surface (Figures 3.3; 3.4; 4.1).

When viewed alongside other confirming protocols used to identify differentiation, such as TEER readings, it was still overall unclear if successful complete differentiation on the layer had occurred. Visual tight junction formation confirmed by positive ZO-1 staining is a regular key indicator of lung epithelial barrier function (Si, et al., 2021) however TEER reading of these samples should also have reflected this and been in line with those observed from other research. This could have been due to the type and origin of lung cells used, or potentially some differentiation was occurring, but the layer was not fully established and perhaps only ‘partially’ differentiated. Regardless, there was some evidence to suggest that the cells

in these transwell layers were being driven towards a mucociliary phenotype, as goblet cells and tight junctions were present at Day 28.

5.5.5 Initial GET peptide delivery to potentially established ALI cultures

The most recent 'potentially differentiated' Air liquid interface layers were utilised for peptide non-viral delivery optimisation. All 3 previously described luciferase vectors were delivered using FLR:FLH peptide in complex.

Initial results demonstrated minimal to no transfection efficiency; only enhanced vector pGM206SMAR and reporter PMV-Gluc-2 showed potential transfection that appeared around 10 fold higher than untransfected controls. Statistical analysis demonstrated no significant difference between untransfected controls and all vectors for Day 1, Day 3 and Day 7 timepoints, suggesting that what appeared to be initial transfection could not be fully confirmed.

Initial delivery demonstrated here was to the basal chamber only. Further optimisation would have aided in repeat experimentation and delivery via the apical chamber, which in hindsight would be the more accurate physical point of delivery due to the method in which such a potential therapy would be introduced to the lung *in vivo*; it would be most probable that delivery would be inhaled, and thus reach the epithelial/airway space before any other area of the lung.

6. Conclusions and Future Outlook

The overall aim of this project was to optimise and demonstrate the delivery capability of the non-viral based GET peptide system, and to demonstrate this within *in vitro* and *ex vivo* models for comparison and to highlight the benefits of using such model systems as opposed to *in vivo* work. The key was to showcase the potential of both non-viral mediated delivery and *in vitro* and *ex vivo* lung model systems in the context of gene therapy.

Non-viral delivery with the GET system has been demonstrated within murine PCLS (Chapter 3), and whilst not as efficient as in cell monolayers, this work does demonstrate the GET systems capability for delivery within an *ex vivo* lung model. As demonstrated within Chapter 3, viability post-delivery within this model does not appear to be reduced or affected by GET peptide usage, highlighting both the lack of toxicity of the delivery system and the robustness of the *ex vivo* model. Based on this, GET could also be utilised within other lung models and could be used in further work to deliver to a more translatable, accurate lung model such as air liquid interface culture. With more optimisation, it would be easy to demonstrate GET delivery capability within a fully differentiated human air liquid interface culture, to build on initial work demonstrated within chapter 5.

Further work to expand on the initial findings of this project could include optimisation of the delivery to air liquid interface layers; delivery should mimic the natural route into the lungs, and this would most likely be a top-down approach. A potential gene therapy product would most likely be designed for the inhalation route, hence it would reach the epithelial side of the airway before

other areas of the tissue. Future delivery studies would need to reflect this, and delivery should be added to the apical chamber of transwell experiments. Positive pressure or aerosolization could even be implemented to improve both delivery efficiency and *in vivo* mimicry within a static transwell model. The next step for such delivery studies could even be utilisation of a higher level *in vitro* model, such as airway or alveolar on chip.

Further confirmation of the efficacy of the GET peptide non-viral system could involve more comparisons with commercial agents (PEI, Lipofectamines etc.) within cell monolayers and fully established transwell cultures at the air liquid interface, to build on initial work demonstrated in Chapters 3 and 5. Future work could include direct comparison with an established viral based vector (Adenovirus, integrating or non-integrating lentivirus etc.) could also be beneficial in demonstrating its advantages and potential as a non-viral system specifically for gene therapy purposes.

Despite initial demonstration of non-viral delivery here, the GET peptide system, and the majority of non-viral vectors need further research to expand the knowledge base and improve their efficiency. Many viral vectors have made it to clinical trials and beyond, and whilst non-viral based vectors have proven some efficacy in *in vitro* settings and have the benefit of no immunogenicity. Another factor to consider is also cost; whilst expensive, some viral vectors are at a cost point where they are deliverable to individual patients in clinical trials and other treatment settings. Non-viral vectors will need to emerge as the most cost-effective option alongside the most demonstrable treatment efficacy if they are to surpass current viral vectors.

Another key area of this project to consider in future is animal use; Despite their overall utility and general cost effectiveness comparative to full scale animal models, tissue based *ex vivo* modelling such as precision cut lung slices still create some animal wastage, and does not always accurately model human disease or human response to delivery systems. Whilst transwells utilising human cells move a step towards reduction of animal use and improvement of accuracy of results in a more human context, their static nature makes them a cost effective midway point; next generation models that involve movement or stretch, such as organ on chips, present as *in vitro* models that may one day prove to be more accurate, ethical replacements for extensive animal research. Another key feature of such a model is the possibility of personalised medicine, as such a device could be seeded with any patients' cells, and potential gene therapies could be tailored and tested to determine their efficacy within that patient.

With the cost point of such specialised equipment reducing, and the research utilising such methods building a solid foundation of work within the last decade, this type of non- animal based human *in vitro* modelling is becoming more obtainable than ever before. There is demonstrable utility for investigation of drug efficacy, genetic therapy delivery, organ regeneration, and localised organ immune response in multiple contexts.

In part, this project demonstrates the potential of a non-viral peptide based delivery system for genetic delivery, within both the *ex vivo* model Precision cut lung slices (chapter 3), and its highlights its potential for expansion and testing within the *in vitro* human based static model Air liquid interface culture (Chapter

5). Potential model development was also briefly investigated, with an alternate perfusion material used for generating PCLS (Chapter 4).

Within chapter 3 of this work, it has been demonstrated that use of enhanced peptide formulations was key, particularly within PCLS; use of FLH with FLR appeared to improve transfection efficiency and by extension expression profiles within the model. In future, enhancing plasmid DNA may also be a way forward to improve delivery and prolong expression, as more the enhanced plasmid pGM206SMAR appeared to demonstrate some higher initial expression and reduced transience.

To build on the initial use of a human relevant ALI model (demonstrated in chapter 5), Further demonstration in a variety of models of this non-viral method would be required if it is to be taken further and considered as a potential gene therapy vector. It should be considered in the context of specific disease states with a single genetic mutated target, such as cystic fibrosis. Cystic fibrosis presents as a good disease candidate for gene editing, and thus development of a gene therapy, as targeted gene editing and site specific delivery can allow for insertion of a functional copy of CFTR.

Cystic fibrosis has presented challenges for gene therapy, including delivery of DNA and efficacy of treatment. In this respect, the GET non-viral peptide based delivery system shows the potential for a reduced transience treatment without host recognition issues of viral based delivery (Burney & Davies, 2012).

Within chapter 5 ,this work only focussed solely on a liquid based, as opposed to aerosolised based treatment. When dealing with the increased mucosal viscosity profile many CF patients present with, determination of the efficacy of

an aerosolised treatment in vector delivery is a significant issue (Duncan, Jung, Hanes, & Suk, 2016).

Despite showing efficacy for liquid based administration (Chapters3, 5), the GET system would also need further assessment to show cystic fibrosis gene therapy even intravenously. However, previous work with the GET peptide system has demonstrated PEGylation of DNA NPs can aid in delivery through CF mucus from patient sputum *ex vivo*, and deliver genetic cargo in both bronchial epithelial cells and murine PCLS (Osman, et al., 2018). This demonstrated the GET peptide systems mucosal infiltration when physical amendments were made to the system with PEGylation.

The GET peptide system demonstrates here that it has the potential to deliver pDNA in ex vivo modelling systems and at a cellular level. In future work, it could be utilised to investigate and target mutations in a monogenic disorder such as Cystic Fibrosis, if focus on mucosal transience of the peptide system and development of aerosolised delivery was prioritised.

7. References

Abashkin, V., Pedziwiatr-Werbicka, E., Gomez, R., de la Mata, F. J., Dzmitruk, V., Shcharbin, D., & Bryszewska, M. (2021). Prospects of Cationic Carbosilane Dendronized Gold Nanoparticles as Non-viral Vectors for Delivery of Anticancer siRNAs siBCL-xL and siMCL-1. *Pharmaceutics, 13*(10). doi:10.3390/pharmaceutics13101549

Abu-Awwad, H., Thiagarajan, L., & Dixon, J. (2017). Controlled release of GAG-binding enhanced transduction (GET) peptides for sustained and highly efficient intracellular delivery. *Acta Biomaterialia, 57*, 225-237. doi:10.1016/j.actbio.2017.04.028

Abu-Awwad, H., Thiagarajan, L., & Dixon, J. E. (2017). Controlled release of GAG-binding enhanced transduction (GET) peptides for sustained and highly efficient intracellular delivery. *Acta biomaterialia, 57*, 225–237. doi:10.1016/j.actbio.2017.04.028

Agarwal, A., Goss, J. A., Cho, A., McCain, M. L., & Parker, K. K. (2013). Microfluidic heart on a chip for higher throughput pharmacological studies. *Lab on a chip, 13*(18), 3599–3608. doi:10.1039/c3lc50350j

Aiuti, A. (2002). Correction of ADA-SCID by Stem Cell Gene Therapy Combined with Nonmyeloablative Conditioning. *Science, 296*(5577), pp.2410-2413.

Aiuti, A., Biasco, L., Scaramuzza, S., Ferrua, F., Cicalese, M. P., Baricordi, C., . . . Naldini, L. (2013). Lentiviral hematopoietic stem cell gene therapy in patients with Wiskott-Aldrich syndrome. *Science, 341*(6148), 1233151. doi:10.1126/science.1233151

Akram, K., Yates, L., Mongey, R., Rothery, S., Gaboriau, D., & Sanderson, J. (2019). Live imaging of alveologenesis in precision-cut lung slices reveals dynamic epithelial cell behaviour. *Nature Communications, 10*(1). doi:10.1038/s41467-019-090

Alabanza, L. M., Xiong, Y., Vu, B., Webster, B., Wu, B., Hu, P., . . . Schneider, D. (2022). Armored BCMA CAR T Cells Eliminate Multiple Myeloma and Are Resistant to the Suppressive Effects of TGF-β. *Frontiers in immunology, 13*(832645). doi:10.3389/fimmu.2022.832645

Almofti, M. R., Harashima, H., Shinohara, Y., Almofti, A., Baba, Y., & Kiwada, H. (2003). Cationic liposome-mediated gene delivery: biophysical study and mechanism of internalization. *Archives of biochemistry and biophysics, 410*(2), 246–253. doi:10.1016/s0003-9861(02)00725-7

Alsafadi, H., Staab-Weijnitz, C., Lehmann, M., Lindner, M., Peschel, B., Königshoff, M., & Wagner, D. (2017). An ex vivo model to induce early fibrosis-like changes in human precision-cut lung slices. *American Journal Of Physiology-Lung Cellular And Molecular Physiology, 316*(2), L896-L902. doi:10.1152/ajplung.00084.2017

Alton, E. F., Boyd, A. C., Cheung, S. H., Cunningham, S., Davies, J. C., & Gill, D. R. (2013). A randomised, double-blind, placebo-controlled phase IIB clinical trial

of repeated application of gene therapy in patients with cystic fibrosis. *Thorax, 68*, 1075 - 1077. doi:10.1136/thoraxjnl-2013-203309

Altube, M. J., Caimi, L. I., Huck-Iriart, C., Morilla, M. J., & Romero, E. L. (2021). Reparation of an Inflamed Air-Liquid Interface Cultured A549 Cells with Nebulized Nanocurcumin. *Pharmaceutics, 13*(9), 1331. doi:10.3390/pharmaceutics13091331

Apolonia, L., Waddington, S. N., Fernandes, C., Ward, N. J., Bouma, G., Blundell, M. P., . . . Philpott, N. J. (2007). Stable gene transfer to muscle using non-integrating lentiviral vectors. *Molecular therapy : the journal of the American Society of Gene Therapy, 15*(11), 1947–1954. doi:10.1038/sj.mt.6300281

Apostolou, A., Panchakshari, R. A., Banerjee, A., Manatakis, D. V., Paraskevopoulou, M. D., Luc, R., . . . Karalis, K. (2021). A Novel Microphysiological Colon Platform to Decipher Mechanisms Driving Human Intestinal Permeability. *Cellular and molecular gastroenterology and hepatology, 12*(5), 1719–1741. doi:10.1016/j.jcmgh.2021.07.004

Atchinson, R. W., Casto , B. C., & Hammon, M. (1965). Adenovirus-associated defective virus particles. *Science*(49), 754-756.

Ayub, A., & Wetting, S. (2022). An Overview of Nanotechnologies for Drug Delivery to the Brain. *Pharmaceutics, 14*(2). doi:10.3390/pharmaceutics14020224

Banerjee, S., Huckuntod, S., Mills, S., Kurten, R., & Pechous, R. (2019). Modeling Pneumonic Plague in Human Precision-Cut Lung Slices Highlights a Role for the Plasminogen Activator Protease in Facilitating Type 3 Secretion. *Infection And Immunity, 87*(8). doi:10.1128/iai.00175-19

Barde, I., Laurenti, E., Verp, S., Wiznerowicz, M., Offner, S., Viornery, A., . . . Trono, D. (2011). Lineage- and stage-restricted lentiviral vectors for the gene therapy of chronic granulomatous disease. *Gene therapy, 18*(11), 1087–1097. doi:10.1038/gt.2011.65

Barichello, J. M., Morishita, M., Takayama, K., & Nagai, T. (1999). Encapsulation of hydrophilic and lipophilic drugs in PLGA nanoparticles by the nanoprecipitation method. *Drug development and industrial pharmacy, 25*(4), 471–476. doi:10.1081/ddc-100102197

Basheeruddin Asdaq, S. M., Jomah, S., Rabbani, S. I., Alamri, A. M., Salem Alshammari, S. K., Duwaidi, B. S., . . . Imran, M. (2022). Insight into the Advances in Clinical Trials of SARS-CoV-2 Vaccines. *The Canadian journal of infectious diseases & medical microbiology, 6913772*. doi:10.1155/2022/6913772

Baum, C., Düllmann, J., Li, Z., Fehse, B., Meyer, J., Williams, D., & von Kalle, C. (2003). Side effects of retroviral gene transfer into hematopoietic stem cells. Blood. *Blood, 101*(6), 2099-2113. doi:10.1182/blood-2002-07-2314

Benam, K. H., Mazur, M., Choe, Y., Ferrante, T. C., Novak, R., & Ingber, D. E. (2017). Human Lung Small Airway-on-a-Chip Protocol. *Methods in molecular biology (Clifton, N.J.), 1612*, 345–365. doi:10.1007/978-1-4939-7021-6_25

Bepler, G., Jaques, G., Neumann, K., Aumuller, G., Gropp, C., & Havemann, K. (1987). Establishment, growth properties, and morphological Characteristics

of permanent human small cell lung cancer cell lines. *Journal of cancer research and clinical oncology, 1*, 31–40. doi:10.1007/BF00389964

Birzle, A. M., Martin , C., Yoshihara, L., Uhlig, S., & Wall, W. A. (2018). Experimental characterization and model identification of the nonlinear compressible material behavior of lung parenchyma. *Journal of the Mechanical Behavior of Biomedical Materials, 77*, 754-763. doi:doi.org/10.1016/j.jmbbm.2017.08.001

Blaese, R. W., Culver, K., Miller, A., & French Anderson, W. (1996). T lymphocyte-directed gene therapy for ADA-SCID: initial results after 4 years. *Trends in Genetics, 12*(1), p. 13.

Boucher, R., Knowles, M., Johnson, L., Olsen, J., Pickles, R., Wilson, J., . . . Grossman, M. (1994). Gene Therapy for Cystic Fibrosis Using E1-Deleted Adenovirus: A Phase I Trial in the Nasal Cavity. *Human Gene Therapy, 5*(5), 615-639. doi:10.1089/hum.1994.5.5-615

Bozzuto, G., & Molinari, A. (2015). Liposomes as nanomedical devices. *International Journal of Nanomedicine, 10*(1), 975-999. doi:10.2147/IJN.S68861

Brandenberger, C., Rothen-Rutishauser, B., Muhlfeld, C., Schmid, O., Ferron, G. A., Maier, K. L., . . . Lenz, A. G. (2010). Effects and uptake of gold nanoparticles deposited at the air-liquid interface of a human epithelial airway model. *Toxicology and applied pharmacology, 242*(1), 56–65. doi:10.1016/j.taap.2009.09.014

Breyer, B., Jiang, W., Cheng, H., Zhou, L., Paul, R., Feng, T., & He, T. (2001). Adenoviral Vector-Mediated Gene Transfer for Human Gene Therapy. *Current Gene Therapy, 1*(2), 149-162. doi:10.2174/1566523013348689

Brown, B., Venneri, M., Zingale, A., Sergi, L., & Naldini, L. (2006). Endogenous microRNA regulation suppresses transgene expression in hematopoietic lineages and enables stable gene transfer. *Nature Medicine, 12*(5), pp.585-591.

Bryson, K. J., Garrido, D., Esposito, M., Mclachlan, G., Digard, P., Schouler, C., . . . Vervelde, L. (2020). Precision cut lung slices: a novel versatile tool to examine host–pathogen interaction in the chicken lung. *Veterinary Research, 51*(2). doi:https://doi.org/10.1186/s13567-019-0733-0

Burney, T. J., & Davies, J. C. (2012). Gene therapy for the treatment of cystic fibrosis. *The application of clinical genetics, 5*, 29-36. doi:10.2147/TACG.S8873

Cao, X., Muskhelishvili, L., Latendresse, J., Richter, P., & Heflich, R. H. (2017). Evaluating the Toxicity of Cigarette Whole Smoke Solutions in an Air-Liquid-Interface Human In Vitro Airway Tissue Model. *Toxicological sciences : an official journal of the Society of Toxicology, 156*(1), 14–24. doi:10.1093/toxsci/kfw239

Carey, J. L., Remmers, A. E., & Flanigan, D. C. (2020). Use of MACI (Autologous Cultured Chondrocytes on Porcine Collagen Membrane) in the United States: Preliminary Experience. *Orthopaedic journal of sports medicine, 8*(8). doi:10.1177/2325967120941816

Cavazzana-Calvo, M. (2000). Gene Therapy of Human Severe Combined Immunodeficiency (SCID)-X1 Disease. *Science, 288*(5466), pp.669-672.

Cavazzana-Calvo, M., Payen, E., Negre, O., Wang, G., Hehir, K., Fusil, F., . . . Leboulch, P. (2010). Transfusion independence and HMGA2 activation after gene therapy of human β-thalassaemia. , . *Nature, 467*(7313), pp.318-322.

Cevc, G., & Richardsen, H. (1999). Lipid vesicles and membrane fusion. *Advanced drug delivery reviews, 38*(3), 207–232. doi:10.1016/s0169-409x(99)00030-7

Chan, C. L., Majzoub, R. N., Shirazi, R. S., Ewert, K. K., Chen, Y. J., Liang, K. S., & Safinya, C. R. (2012). Endosomal escape and transfection efficiency of PEGylated cationic liposome-DNA complexes prepared with an acid-labile PEG-lipid. *Biomaterials, 33* (19), 4928–4935. doi:10.1016/j.biomaterials.2012.03.038

Choe, M. M., Tomei, A. A., & Swartz, M. A. (2006). Physiological 3D tissue model of the airway wall and mucosa. *Nature protocols, 1*(1), 357–362. doi:10.1038/nprot.2006.54

Choi, S. W., & Kim, J. H. (2007). Design of surface-modified poly(D,L-lactide-co-glycolide) nanoparticles for targeted drug delivery to bone. *Journal of controlled release : official journal of the Controlled Release Society, 122*(1), 24–30. doi:10.1016/j.jconrel.2007.06.003

Chu, W., & Pavan-Langston, E. (1979). Ocular Surface Manifestations of the Major Viruses. *International Ophthalmology Clinics, 19*(2), 135-168. doi:10.1097/00004397-197901920-00010

Cidem, A., Bradbury, P., Traini, D., & Ong, H. X. (2020). Modifying and Integrating in vitro and ex vivo Respiratory Models for Inhalation Drug Screening. ,. *Frontiers in bioengineering and biotechnology, 8*(581995). doi:10.3389/fbioe.2020.581995

ClinicalTrials.gov Identifier: NCT04436471. (2020). An Open Study of the Safety, Tolerability and Immunogenicity of the Drug "Gam-COVID-Vac" Vaccine Against COVID-19. *Gamaleya Research Institute of Epidemiology and Microbiology, Health Ministry of the Russian Federation, Acellena Contract Drug Research and Development*, https://clinicaltrials.gov/ct2/show/NCT04436471.

Cockrell, A. S., & Kafri, T. (2007). Gene delivery by lentivirus vectors. *Molecular biotechnology, 36*(3), 184–204. doi:10.1007/s12033-007-0010-8

Cohen, A. D., Parekh, S., Santomasso, B. D., Perez-Larraya, J. G., van de Donk, N., Arnulf, B., . . . Jagannath, S. (2022). Incidence and management of CAR-T neurotoxicity in patients with multiple myeloma treated with ciltacabtagene autoleucel in CARTITUDE studies. *Blood cancer journal, 12*(2), 32. doi:10.1038/s41408-022-00629-1

Cores, J., Dinh, P. C., Hensley, T., Adler, K. B., Lobo, L. J., & Cheng, K. (2020). A pre-investigational new drug study of lung spheroid cell therapy for treating pulmonary fibrosis. *Stem cells translational medicine, 7*, 786–798. doi:10.1002/sctm.19-0167

Cozens, D., Grahame, E., Sutherland, E., Taylor, G., Berry, C. C., & Davies, R. L. (2018). Development and optimization of a differentiated airway epithelial cell model of the bovine respiratory tract. *Scientific reports, 8*(1), 853. doi:10.1038/s41598-017-19079-y

Crystal, R. (2014). Adenovirus: The First Effective In Vivo Gene Delivery Vector. *Human Gene Therapy, 25*(1), 3-11. doi:10.1089/hum.2013.2527

Cunniff, B., Druso, J. E., & van der Velden, J. L. (2021). Lung organoids: advances in generation and 3D-visualization. *Histochemistry and cell biology, 155*(2), 301–308. doi:10.1007/s00418-020-01955-w

Delgado, D., Gascon, A. R., Del Pozo-Rodriguez, A., Echevarria, E., Ruiz de Garibay, A. P., Rodriguez, J. M., & Solinis, M. A. (2012). Dextran-protamine-solid lipid nanoparticles as a non-viral vector for gene therapy: in vitro characterization and in vivo transfection after intravenous administration to mice. *International journal of pharmaceutics, 425*((1-2)), 35–43. doi:10.1016/j.ijpharm.2011.12.052

Derakhshankhah, H., & Jafari, S. (2018). Cell penetrating peptides: A concise review with emphasis on biomedical applications. *Biomedicine & pharmacotherapy = Biomedecine & pharmacotherapie, 108*, 1090–1096. doi:10.1016/j.biopha.2018.09.097

Deshayes, S., Gerbal-Chaloin, S., Morris, M. C., Aldrian-Herrada, G., Charnet, P., Divita, G., & Heitz, F. (2004). On the mechanism of non-endosomial peptide-mediated cellular delivery of nucleic acids. *Biochimica et biophysica acta, 1667*(2), 141–147. doi:10.1016/j.bbamem.2004.09.010

Diallo, J., Roy, D., Abdelbary, H., De Silva, N., & Bell, J. (2011). Ex Vivo Infection of Live Tissue with Oncolytic Viruses. *Journal Of Visualized Experiments*(52). doi:10.3791/2854

Dimmock, N., Easton, A., & Leppard, K. (2016). Introduction to Modern Virology. Wiley Blackwell.

Ding, R., Chao, C. C., & Gao, Q. (2022). High-efficiency of genetic modification using CRISPR/Cpf1 system for engineered CAR-T cell therapy. *Methods in cell biology, 167*, 1–14. doi:10.1016/bs.mcb.2021.08.001

Dinh, P. C., Paudel, D., Brochu, H., Popowski, K. D., Gracieux, M. C., Cores, J., . . . Cheng, K. (2020). Inhalation of lung spheroid cell secretome and exosomes promotes lung repair in pulmonary fibrosis. *Nature communications, 11*(1), 1064. doi:10.1038/s41467-020-14344-7

Dixon, J., Osman, G., Morris, G., Markides, H., Rotherham, M., & Bayoussef, Z. (2016). Highly efficient delivery of functional cargoes by the synergistic effect of GAG binding motifs and cell-penetrating peptides. *Proceedings Of The National Academy Of Sciences , 113*(3), E291-E299. doi:10.1073/pnas.1518634113

Douple, E. B., Cate, C. C., Curphey, T. J., Pettengill, O. S., Sorenson, G. D., & Maurer, L. H. (1895). Evaluation of drug efficacy in vitro using human small cell carcinoma of the lung spheroids. *Cancer, 56*(8), 1918–1925.

doi:10.1002/1097-0142(19851015)56:8<1918::aid-cncr2820560804>3.0.co;2-e

Duchardt, F., Fotin-Mleczek, M., Schwarz, H., Fischer, R., & Brock, R. (2007). A comprehensive model for the cellular uptake of cationic cell-penetrating peptides. *Traffic (Copenhagen, Denmark), 8*(7), 848–866. doi:10.1111/j.1600-0854.2007.00572.x

Duffney, P. F., McCarthy, C. E., Nogales, A., Thatcher, T. H., Martinez-Sobrido, L., Phipps, R. P., & Sime, P. J. (2018). Cigarette smoke dampens antiviral signaling in small airway epithelial cells by disrupting TLR3 cleavage. *American journal of physiology. Lung cellular and molecular physiology, 314*(3), L505–L513. doi:10.1152/ajplung.00406.2017

Duncan, G. A., Jung, J., Hanes, J., & Suk, J. S. (2016). The Mucus Barrier to Inhaled Gene Therapy. *Molecular therapy : the journal of the American Society of Gene Therapy, 24*(12), 2043-2053. doi:10.1038/mt.2016.182

Editas Medicine, Inc. (2019). *https://clinicaltrials.gov/ct2/show/record/NCT03872479*. Retrieved from Clinicaltrials.gov.

Eenjes, E., van Riet, S., Kroon, A. A., Slats, A. M., Khedoe, P., Boerema-de Munck, A., . . . Hiemstra, P. S. (2021). Disease modelling following organoid-based expansion of airway epithelial cells. *American journal of physiology. Lung cellular and molecular physiology*. doi:doi.org/10.1152/ajplung.00234.2020

Engelman, A., Englund, G., Orenstein, J. M., Martin, M. A., Craigie, R., & , . (1995). Multiple effects of mutations in human immunodeficiency virus type 1 integrase on viral replication. *Journal of virology, 69*(5), 2729–2736. doi:10.1128/JVI.69.5.2729–2736.1995

Eschun-Wilson, L., Zhang, R., Portran, D., Nachbury, M. V., Toso, D. B., Löhr, T., . . . Nogales, E. (2019). Effects of α-tubulin acetylation on microtubule structure and stability. *Proceedings of the National Academy of Sciences of the United States of America, 116*(21), 10366–10371. doi:10.1073/pnas.1900441116

Evans, K. V., & Lee, J. H. (2020). Alveolar wars: The rise of in vitro models to understand human lung alveolar maintenance, regeneration, and disease. *Stem cells translational medicine, 9*(8), 867–881. doi:10.1002/sctm.19-0433

Eyquem, J., Mansilla-Soto, J., Giavridis, T., van der Stegen, S. J., Hamieh, M., & Cunanan, K. M. (2017). Targeting a CAR to the TRAC locus with CRISPR/Cas9 enhances tumour rejection. *Nature, 543*(7643), 113-117. doi:10.1038/nature21405

Fay, F., Hansen, L., Hectors, S., Sanchez-Gaytan, B. L., Zhao, Y., Tang, J., . . . Mulder, W. (2017). Investigating the Cellular Specificity in Tumors of a Surface-Converting Nanoparticle by Multimodal Imaging. *Bioconjugate chemistry, 28*(5), 1413–1421. doi:10.1021/acs.bioconjchem.7b00086

FDA. (2021, June 30). *https://www.fda.gov/vaccines-blood-biologics/cellular-gene-therapy-products/maci-autologous-cultured-chondrocytes-porcine-collagen-membrane*. Retrieved from https://www.fda.gov/vaccines-blood-biologics/cellular-gene-therapy-products/approved-cellular-and-gene-therapy-

products: https://www.fda.gov/vaccines-blood-biologics/cellular-gene-therapy-products/approved-cellular-and-gene-therapy-products

FDA. (2022, June 09). *https://www.fda.gov/vaccines-blood-biologics/cellular-gene-therapy-products/luxturna*. Retrieved from https://www.fda.gov/vaccines-blood-biologics/cellular-gene-therapy-products/approved-cellular-and-gene-therapy-products: https://www.fda.gov/vaccines-blood-biologics/cellular-gene-therapy-products/luxturna

Fjellbirkeland, L., Bjerkvig, R., & Laerum, O. D. (1998). Non-small-cell lung carcinoma cells invade human bronchial mucosa in vitro. *In vitro cellular & developmental biology, 34*(4), 333–340. doi:10.1007/s11626-998-0010-4

Flotte, T. R., Cataltepe, O., Puri, A., Batista, A. R., Moser, R., Mckenna-Yasek, D., . . . Sena-Esteves, M. (2022). AAV gene therapy for Tay-Sachs disease. *Nature medicine, 28*(2), 251–259. doi:10.1038/s41591-021-01664-4

Flynn, R. P., Zacharias, J., Zhou, X., Cannon, M. L., & Philpott, N. J. (2011). Non-integrating lentiviral vectors for specific killing of Epstein-Barr virus nuclear antigen 1-positive B cell lymphoma cells. *The journal of gene medicine, 13*(9), 487–496. doi:10.1002/jgm.1601

Folegatti, P. M., Ewer, K. J., Aley, P. K., Angus, B., Becker, S., Belij-Rammerstorfer, S., & Oxford COVID Vaccine Trial Group. (2020). Safety and immunogenicity of the ChAdOx1 nCoV-19 vaccine against SARS-CoV-2: a preliminary report of a phase 1/2, single-blind, randomised controlled trial. *Lancet, 396*(10249), 467–478. doi:10.1016/S0140-6736(20)31604-4

Freidmann, T., & Roblin, R. (1972). Gene Therapy for Human Genetic Disease. *Science, 175*(4025), pp.949-955.

Gonzalo, T., Clemente, M. I., Chonco, L., Weber, N. D., Diaz, L., Serramia, M. J., . . . Jimenez, J. L. (2010). Gene therapy in HIV-infected cells to decrease viral impact by using an alternative delivery method. *ChemMedChem, 5*(6), 921–929. doi:10.1002/cmdc.201000029

Gras, D., Petit, A., Charriot, J., Knabe, L., Alagha, K., Gamez, A. S., . . . Vachier, I. (2017). Epithelial ciliated beating cells essential for ex vivo ALI culture growth. *BMC pulmonary medicine, 17*(1). doi:10.1186/s12890-017-0423-5

Gurumoorthy, N., Nordin, F., Tye, G. J., Wan Kamarul Zaman, W. S., Ng, M. H., & , . (2022). Non-Integrating Lentiviral Vectors in Clinical Applications: A Glance Through. *Biomedicines, 10*(1). doi:10.3390/biomedicines10010107

Hacein-Bey-Abina, S. (2003). LMO2-Associated Clonal T Cell Proliferation in Two Patients after Gene Therapy for SCID-X1. *Science, 302*(5644), pp.415-419.

Hadianamrei, R., & Zhao, X. (2022). Current state of the art in peptide-based gene delivery. *Journal of controlled release : official journal of the Controlled Release Society, 343*, 600–619. doi:10.1016/j.jconrel.2022.02.010

Han, S., Gheorghiu, D. B., Li, S., Kang, H. R., & Koeberl, D. (2022). Minimum Effective Dose to Achieve Biochemical Correction With AAV Vector-Mediated Gene Therapy in Mice With Pompe Disease. *Human gene therapy*. doi:10.1089/hum.2021.252

Han, Y. Y.-P. (2020).

Hassan, A. O., Kafai, N. M., Dmitriev, I. P., Fox, J. M., Smith, B. K., Harvey, I. B., . . . Diamond, M. S. (2020). A Single-Dose Intranasal ChAd Vaccine Protects Upper and Lower Respiratory Tracts against SARS-CoV-2. *Cell, 183*(1), 169–184.e13. doi:10.1016/j.cell.2020.08.026

Hatakeyama, H., Akita, H., Kogure, K., Oishi, M., Nagasaki, Y., Kihira, Y., . . . Harashima, H. (2007). Development of a novel systemic gene delivery system for cancer therapy with a tumor-specific cleavable PEG-lipid. *Gene therapy, 14*(1), 68–77. doi:10.1038/sj.gt.3302843

Hayes, M. E., Drummond, D. C., Kirpotin, D. B., Zheng, W. W., Noble, C. O., Park, J. W., . . . Hong, K. (2006). Genospheres: self-assembling nucleic acid-lipid nanoparticles suitable for targeted gene delivery. *Gene therapy, 13*(7), 646–651. doi:10.1038/sj.gt.3302699

Held, H., Martin, C., & Uhlig, S. (1999). Characterization of airway and vascular responses in murine lungs. *British Journal Of Pharmacology, 126*(5), 1191-1199. doi:10.1038/sj.bjp.0702394

Henjakovic, M., Sewald, K., Switalla, S., Kaiser, D., Müller, M., & Veres, T. (2008). Ex vivo testing of immune responses in precision-cut lung slices. *Toxicology And Applied Pharmacology, 231*(1), 68-76. doi:10.1016/j.taap.2008.04.003

Herzog, F., Loza, K., Balog, S., Clift, M., Epple, M., Gehr, P., . . . Rothen-Rutishauser, B. (2014). Mimicking exposures to acute and lifetime concentrations of inhaled silver nanoparticles by two different in vitro approaches. *Beilstein journal of nanotechnology, 5*, 1357–1370. doi:10.3762/bjnano.5.149

Hill, D. B., & Button, B. (2012). Establishment of respiratory air-liquid interface cultures and their use in studying mucin production, secretion, and function. *Methods in molecular biology (Clifton, N.J.), 842*, 245–258. doi:10.1007/978-1-61779-513-8_15

Hirn, S., Haberi, N., Loza, K., Epple, M., Kreyling, W. G., Rothen-Rutishauser, B., . . . Krombach, F. (2014). Proinflammatory and cytotoxic response to nanoparticles in precision-cut lung slices. *Beilstein Journal of Nanotechnology, 5*, 2440 - 2448. doi:doi:10.3762/bjnano.5.253

Hosseinkhani, H., Azzam, T., Tabata, Y., & Domb, A. J. (2004). Dextran-spermine polycation: an efficient nonviral vector for in vitro and in vivo gene transfection. *Gene therapy, 11*(2), 194–203.

Howard-Varona, C., Hargreaves, K., Abedon, S., & Sullivan, M. (2017). Lysogeny in nature: mechanisms, impact and ecology of temperate phages. *The ISME Journal, 11*(7), 1511-1520. doi:10.1038/ismej.2017.16

Hu, Y., & Patel, S. (2016). Thermodynamics of cell-penetrating HIV1 TAT peptide insertion into PC/PS/CHOL model bilayers through transmembrane pores: the roles of cholesterol and anionic lipids. *Soft matter, 12*(32), 6716–6727. doi:10.1039/c5sm01696g

Hu, Y., & Patel, S. (2016). Thermodynamics of cell-penetrating HIV1 TAT peptide insertion into PC/PS/CHOL model bilayers through transmembrane pores: the

roles of cholesterol and anionic lipids. *Soft matter, 12*(32), 6716–6727. doi:10.1039/c5sm01696g

Hu, Y., Sheng, Y., Ji, X., Liu , P., Tang, L., Chen, G., & Chen, G. (2020). Comparative anti-inflammatory effect of curcumin at air-liquid interface and submerged conditions using lipopolysaccharide stimulated human lung epithelial A549 cells. *Pulmonary Pharmocology and Therapeutics, 63*(101939). doi:10.1016/j.pupt.2020.101939

Hu, Y., Sinha, S. K., & Patel, S. (2015). Investigating Hydrophilic Pores in Model Lipid Bilayers Using Molecular Simulations: Correlating Bilayer Properties with Pore-Formation Thermodynamics. *Langmuir : the ACS journal of surfaces and colloids, 31*(24), 6615–6631. doi:10.1021/la504049q

Hu, Y., Yang, L., Duan, X., Duan, F., Nilsson-Payant, B. E., Yaron, T. M., . . . Chen, S. (2020). Identification of Candidate COVID-19 Therapeutics using hPSC-derived Lung Organoids. *bioRxiv : the preprint server for biology*. doi:10.1101/2020.05.05.079095

Huang, S., Boda, B., Vernaz, J., Ferreira, E., Wiszniewski, L., & Constant, S. (2017). Establishment and characterization of an in vitro human small airway model (SmallAir™). *European journal of pharmaceutics and biopharmaceutics : official journal of Arbeitsgemeinschaft fur Pharmazeutische Verfahrenstechnik, 118*, 68–72. doi:10.1016/j.ejpb.2016.12.006

Huckaby, J. T., Landoni, E., Jacobs, T. M., Savoldo, B., Dotti, G., & Lai, S. K. (2021). Bispecific binder redirected lentiviral vector enables in vivo engineering of CAR-T cells. *Journal for immunotherapy of cancer, 9*(9). doi:10.1136/jitc-2021-002737

Huh, D., Matthews, B. D., Mammoto, A., Montoya-Zavala, M., Hsin, H. Y., & Ingber, D. E. (2010). Reconstituting organ-level lung functions on a chip. *Science, 328*(5986), 1662–1668. doi:10.1126/science.1188302

Iravaidya, K., & Shuler, M. L. (2004). Incorporation of 3T3-L1 cells to mimic bioaccumulation in a microscale cell culture analog device for toxicity studies. *Biotechnology progress, 20*(2), 590–597. doi:10.1021/bp034238d

Irigoyen, C., Amenabar Alonso, A., Sanchez-Molina, J., Rodríguez-Hidalgo, M., Lara-López, A., & Ruiz-Ederra, J. (2022). Subretinal Injection Techniques for Retinal Disease: A Review. *Journal of clinical medicine, 11*(16), 4717. doi:10.3390/jcm11164717

Ishikawa, S., & Ito, S. (2017). Repeated whole cigarette smoke exposure alters cell differentiation and augments secretion of inflammatory mediators in air-liquid interface three-dimensional co-culture model of human bronchial tissue. *oxicology in vitro : an international journal published in association with BIBRA, 38*, 170–178. doi:10.1016/j.tiv.2016.09.004

Jacoby, E., Bielorai, B., Hutt, D., Itzhaki, O., Adam, E., Bar, D., . . . Toren, A. (2022). Parameters of long-term response with CD28-based CD19 chimaeric antigen receptor-modified T cells in children and young adults with B-acute lymphoblastic leukaemia. *British journal of haematology*. doi:10.1111/bjh.18105

Jain, A., Barrile, R., van der Meer, A. D., Mammoto, A., Mammoto, T., De Ceunynck, K., . . . Ingber, D. E. (2018). Primary Human Lung Alveolus-on-a-chip Model of Intravascular Thrombosis for Assessment of Therapeutics. *Clinical pharmacology and therapeutics, 103*(2), 332–340. doi:10.1002/cpt.742

Jang, K. J., & Suh, K. Y. (2010). A multi-layer microfluidic device for efficient culture and analysis of renal tubular cells. *Lab on a Chip, 10*(1), 36 - 42. doi:10.1039/b907515a

Jiang, D., Schaefer, N., & Chu, H. (2018). Air–Liquid Interface Culture of Human and Mouse Airway Epithelial Cells Methods and Protocols. In *Lung Innate Immunity and Inflammation.* (Vol. 1809, pp. 91 - 109). New York, NY, United States of America: Humana Press. doi:https://doi.org/10.1007/978-1-4939-8570-8_8

Jin, C., Fotaki, G., Ramachandran, M., Nilsson, B., Essand, M., & Yu, D. (2016). Safe engineering of CAR T cells for adoptive cell therapy of cancer using long-term episomal gene transfer. *EMBO molecular medicine, 8*(7), 702–711. doi:10.15252/emmm.201505869

Jones, C. H., Chen, C. K., Ravikrishnan, A., Rane, S., & Pfeifer, B. A. (2013). Overcoming nonviral gene delivery barriers: perspective and future. *Molecular pharmaceutics, 10*(11), 4082–4098. doi:10.1021/mp400467x

Jones, M., Harrach, B., Ganac, R., Gozum, M., dela Cruz, W., Riedel, B., . . . Schnurr, D. (2007). New Adenovirus Species Found in a Patient Presenting with Gastroenteritis. *Journal Of Virology, 81*(11), 5978-5984. doi:10.1128/jvi.02650-06

Junquera, E., & Aicart, E. (2016). Recent progress in gene therapy to deliver nucleic acids with multivalent cationic vectors. *Advances in colloid and interface science, 233*, 161–175. doi:10.1016/j.cis.2015.07.003

Kalos, M., Levine, B. L., Porter, D. L., Katz, S., Grupp, S. A., Bagg, A., & June, C. H. (2011). T cells with chimeric antigen receptors have potent antitumor effects and can establish memory in patients with advanced leukemia. *Science translational medicine, 3*(95). doi:10.1126/scitranslmed.3002842

Kampik, D., Basche, M., Luhmann, U., Nishiguchi, K. M., Williams, J., Greenwood, J., . . . Ali, R. R. (2017). In situ regeneration of retinal pigment epithelium by gene transfer of E2F2: a potential strategy for treatment of macular degenerations. *Gene therapy, 24*(12), 810–818. doi:10.1038/gt.2017.89

Kannan, S., Dai, H., Navath, R. S., Balakrishnan, B., Jyoti, A., Janisse, J., . . . Kannan, R. M. (2012). Dendrimer-based postnatal therapy for neuroinflammation and cerebral palsy in a rabbit model. *Science translational medicine, 4*(130), 130ra46. doi:10.1126/scitranslmed.3003162

Keeler, A. M., ElMallah, M. K., & Flotte, T. R. (2017). Gene Therapy 2017: Progress and Future Directions. *Clinical and Translational Science, 10*, 242 - 248. doi:10.1111/cts.12466

Kerns, S. J., Belgur, C., Petropolis, D., Kanellias, M., Barrile, R., Sam, J., . . . Cabon, L. (2021). Human immunocompetent Organ-on-Chip platforms allow safety

profiling of tumor-targeted T-cell bispecific antibodies. *eLife, 10*, e67106. doi:10.7554/eLife.67106

Khanna, P., Ong, C., Bay, B. H., & Baeg, G. H. (2015). Nanotoxicity: An Interplay of Oxidative Stress, Inflammation and Cell Death. *Nanomaterials, 5*(3), 1163–1180. doi:10.3390/nano5031163

Kielberg, V. (2010). *Cryopreservation of Mammalian Cells - Protocols.* Retrieved from www.ThermoScientific.com: https://assets.fishersci.com/TFS-Assets/LSG/Application-Notes/D19575.pdf

Kilbride, P., Meneghel, J., Fonseca, F., & Morris, J. (2021). The transfer temperature from slow cooling to cryogenic storage is critical for optimal recovery of cryopreserved mammalian cells. *PloS one, 16*(11), e0259571. doi:10.1371/journal.pone.0259571

Kim, H. J., & Ingber, D. E. (2013). Gut-on-a-Chip microenvironment induces human intestinal cells to undergo villus differentiation. *Integrative biology : quantitative biosciences from nano to macro, 5*(9), 1130–1140. doi:10.1039/c3ib40126

Kim, H., Kim, Y., Park, S., Bae, B., Kang, H., & Cho, S. (2015). Airway Smooth Muscle Sensitivity to Methacholine in Precision-Cut Lung Slices (PCLS) from Ovalbumin-induced Asthmatic Mice. *The Korean Journal Of Physiology & Pharmacology, 19*(1), 65. doi:10.4196/kjpp.2015.19.1.65

Klimek, L., Novak, N., Hamelmann, E., Werfel, T., Wagenmann, M., Taube, C., . . . Worm, M. (2021). Severe allergic reactions after COVID-19 vaccination with the Pfizer/BioNTech vaccine in Great Britain and USA: Position statement of the German Allergy Societies: Medical Association of German Allergologists (AeDA)... *Allergo journal international, 30*(2), 51–55. doi:10.1007/s40629-020-00160-4

Kochenderfer, J. N., Wilson, W. H., Janik, J. E., Dudley, M. E., Stetler-Stevenson, M., Feldman, S. A., . . . Rosenberg, S. A. (2010). Eradication of B-lineage cells and regression of lymphoma in a patient treated with autologous T cells genetically engineered to recognize CD19. *Blood, 116*(20), 4099–4102. doi:10.1182/blood-2010-04-281931

Kolbe, U., Yi, B., Poth , T., Saunders, A., Boutin, S., & Dalpke, A. H. (2020). Early Cytokine Induction Upon Pseudomonas aeruginosa Infection in Murine Precision Cut Lung Slices Depends on Sensing of Bacterial Viability. ,. *Frontiers in immunology, 11*(598636). doi:doi.org/10.3389/fimmu.2020.598636

Komáromy, A., Alexander, J., Rowlan, J., Garcia, M., Chiodo, V., Kaya, A., . . . Aguirre, G. (2010). Gene therapy rescues cone function in congenital achromatopsia. *Human Molecular Genetics, 19*(13), pp.2581-2593.

Kotin, R. M., Siniscalo, M., Samulski, R. J., Zhu, X. D., Hunter, L., Laughlin, C. A., . . . Berns, K. I. (1990). Site-specific integration by adeno-associated virus. *Proceedings of the National Academy of Sciences, 87*(6), 2211–2215. doi:10.1073/pnas.87.6.2211

Krabbe, J., Esser, A., Kanzler, S., Braunschweig, T., Kintsler, S., & Spillner, J. (2018). The effects of zinc- and copper-containing welding fumes on murine, rat and human precision-cut lung slices. *Journal Of Trace Elements In Medicine And Biology, 49*, 192-201. doi:10.1016/j.jtemb.2018.03.008

Krimmling, T., & Schwegmann-Weßels, C. (2017). Comparison of mono- and co-infection by swine influenza A viruses and porcine respiratory coronavirus in porcine precision-cut lung slices. *Research In Veterinary Science, 115*, 470-477. doi:10.1016/j.rvsc

Kuek, L. E., Griffin, P., Martinello, P., Graham, A. N., Kalitsis, P., Robinson, P. J., & Mackay, G. A. (2018). Identification of an Immortalized Human Airway Epithelial Cell Line with Dyskinetic Cilia. *American journal of respiratory cell and molecular biology, 59*(3), 375–382. doi:10.1165/rcmb.2017-0188OC

Kuwana, Y., Asakura, Y., Utsunomiya, N., Nakanishi, M., Arata, Y., Itoh, S., . . . Kurosawa, Y. (1987). Expression of chimeric receptor composed of immunoglobulin-derived V resions and T-cell receptor-derived C regions. *Biochemical and Biophysical Research Communications, 149*(3), 960-968. doi:10.1016/0006-291X(87)90502-X

Lambermont, V., Schlepütz, M., Dassow, C., König, P., Zimmermann, L., & Ulhig, S. (2014). Comparison of Airway Responses in Sheep of Different Age in Precision-Cut Lung Slices (PCLS). *Plos ONE, 9*(9). doi:10.1371/journal.pone.0097610

Lauenstein, L., Switalla, S., Prenzler, F., Seehase, S., Pfennig, O., & Förster, C. (2014). Assessment of immunotoxicity induced by chemicals in human precision-cut lung slices (PCLS). *Toxicology In Vitro, 28*(4), 588-599. doi:10.1016/j.tiv.2013

Lee, D. W., Kochenderfer, J. N., Stetler-Stevenson, M., Cui, Y. K., Delbrook, C., Feldman, S. A., . . . Mackall, C. L. (2015). T cells expressing CD19 chimeric antigen receptors for acute lymphoblastic leukaemia in children and young adults: a phase 1 dose-escalation trial. *Lancet, 385*(9967), 517–528. doi:10.1016/S0140-6736(14)61403-3

Lee, D., Petris, A., Hynds, R. E., & O'Callaghan, C. (2020). Ciliated Epithelial Cell Differentiation at Air-Liquid Interface Using Commercially Available Culture Media. *Methods in molecular biology (Clifton, N.J.), 2109*, 275–291. doi:10.1007/7651_2019_269

Lee, M. K., Lim, S. J., & Kim, C. K. (2007). Preparation, characterization and in vitro cytotoxicity of paclitaxel-loaded sterically stabilized solid lipid nanoparticles. *Biomaterials, 28*(12), 2137–2146. doi:10.1016/j.biomaterials.2007.01.014

Lenz, A. G., Karg, E., Lentner, B., Dittrich, V., Brandenberger, C., Rothen-Rutishauser, B., . . . Schmid, O. (2009). A dose-controlled system for air-liquid interface cell exposure and application to zinc oxide nanoparticles. *Particle and Fibre Toxicology, 6*(32). doi:10.1186/1743-8977-6-32

Lenz, A., Stoeger, T., Cei, D., Schmidmeir, M., Semren, N., Burgstaller, G., . . . Schmid, O. (2014). Efficient bioactive delivery of aerosolized drugs to human pulmonary epithelial cells cultured in air-liquid interface conditions. *American*

journal of respiratory cell and molecular biology, 51(4), 526–535. doi:doi.org/10.1165/rcmb.2013-0479OC

Leung, C., Wadsworth, S. J., Yang, S. J., & Dorscheid, D. R. (2020). Structural and functional variations in human bronchial epithelial cells cultured in air-liquid interface using different growth media. *American journal of physiology. Lung cellular and molecular physiology, 318*(5), L1063–L1073. doi:10.1152/ajplung.00190.2019

Levardon, H., Yonker, L. M., Hurley, B. P., & Mou, H. (2018). Expansion of Airway Basal Cells and Generation of Polarized Epithelium. *Bio-protocol, 8*(11). doi:10.21769/BioProtoc.2877

Levine, B., Humeau, L., Boyer, J., MacGregor, R., Rebello, T., Lu, X., . . . June, C. (2006). Gene transfer in humans using a conditionally replicating lentiviral vector. *Proceedings of the National Academy of Sciences, 103*(46), pp.17372-17377.

Li, G., Cohen, J. A., Martines, C., Ram-Mohan, S., Brain, J. D., Krishnan, R., . . . Bai, Y. (2020). Preserving Airway Smooth Muscle Contraction in Precision-Cut Lung Slices. *Scientific Reports, 10*(6480). doi:https://doi.org/10.1038/s41598-020-63225-y

Lim, S. J., & Kim, C. K. (2002). Formulation parameters determining the physicochemical characteristics of solid lipid nanoparticles loaded with all-trans retinoic acid. *International journal of pharmaceutics, 243*(1-2), 135–146. doi:10.1016/s0378-5173(02)00269-7

Lim, W. A., & June, C. H. (2017). The Principles of Engineering Immune Cells to Treat Cancer. *Cell, 168*(4), 724–740. doi:10.1016/j.cell.2017.01.016

Liu, C., Zhang, L., Zhu, W., Guo, R., Sun, H., Chen, X., & Deng, N. (2020). Barriers and Strategies of Cationic Liposomes for Cancer Gene Therapy. Molecular therapy. *Methods & clinical development, 18*, 751–764. doi:10.1016/j.omtm.2020.07.015

Liu, R., An, L., Liu, G., Li, X., Tang, W., & Chen, X. (2015). Mouse lung slices: An ex vivo model for the evaluation of antiviral and anti-inflammatory agents against influenza viruses. *Antiviral Research, 120*, 101-111. doi:10.1016/j.antiviral.2015.05.008

Lu, T., Cao, Y., Zhao, P., Shen, S., & Xi, Y. (2021). Organoid: a powerful tool to study lung regeneration and disease. *Cell regeneration (London, England), 10*(1), 21. doi:10.1186/s13619-021-00082-8

Lundin, P., Johansson, H., Guterstam, P., Holm, T., Hansen, M., Langel, U., & EL Andaloussi, S. (2008). Distinct uptake routes of cell-penetrating peptide conjugates. *Bioconjugate chemistry, 19*(12), 2535–2542. doi:10.1021/bc800212

Lungwitz, U., Breunig, M., Blunk, T., & Göpferich, A. (2005). Polyethylenimine-based non-viral gene delivery systems. *European Journal Of Pharmaceutics And Biopharmaceutics, 60*(2), 247-266. doi:10.1016/j.ejpb.2004.11.011

Luni, C., Serena, E., & Elvassore, N. (2014). Human-on-chip for therapy development and fundamental science. *Current opinion in biotechnology, 25*, 45 - 50. doi:10.1016/j.copbio.2013.08.015

Maarsingh, H., Bidan, C., Brook , C., Zuidhof, A., Elzinga, C., & Smit, M. (2019). Small airway hyperresponsiveness in COPD: relationship between structure and function in lung slices. . *American Journal Of Physiology-Lung Cellular And Molecular Physiology, 316*(3), L537-L546. doi:10.1152/ajplung.00325.2018

Madani, F., Lindberg, S., Langel, U., Futaki, S., & Graslund, A. (2011). Mechanisms of cellular uptake of cell-penetrating peptides. *Journal of biophysics (Hindawi Publishing Corporation : Online), 414729*. doi:10.1155/2011/414729

Magdolenova, Z., Drlickova, M., Henjum, K., Runden-Pran, E., Tulinska, J., Bilanicova, D., . . . Dusinska, M. (2015). Coating-dependent induction of cytotoxicity and genotoxicity of iron oxide nanoparticles. *Nanotoxicology*, 44–56. doi:10.3109/17435390.2013.847505

Mainardi, A., Occhetta, P., & Rasponi, M. (2022). Mechanical Induction of Osteoarthritis Traits in a Cartilage-on-a-Chip Model. *Methods in molecular biology, 2373*, 231–251. doi:10.1007/978-1-0716-1693-2_14

Makadia, H. K., & Siegel, S. J. (2011). Poly Lactic-co-Glycolic Acid (PLGA) as Biodegradable Controlled Drug Delivery Carrier. *Polymers, 3*(3), 1377–1397. doi:10.3390/polym3031377

Makita, S., Yoshimura, K., & Tobinai, K. (2017). Clinical development of anti-CD19 chimeric antigen receptor T-cell therapy for B-cell non-Hodgkin lymphoma. *Cancer science, 108*(6), 1109–1118. doi:10.1111/cas.13239

Mali, S. (2013). Delivery systems for gene therapy. *Indian journal of human genetics, 19*(1), 3–8. doi:10.4103/0971-6866.112870

Mancuso, K., Hauswirth, W., Li, Q., Connor, T., Kuchenbecker, J., Mauck, M., . . . Neitz, M. (2009). Gene therapy for red–green colour blindness in adult primates. *Nature, 461*(7265), pp.784-787.

Marktel, S., Scaramuzza, S., Cicalese, M. P., Giglio, F., Galimberti, S., Lidonnici, M. R., . . . Ferrari, G. (2019). Intrabone hematopoietic stem cell gene therapy for adult and pediatric patients affected by transfusion-dependent ß-thalassemia. *Nature medicine, 25*(2), 234–241. doi:10.1038/s41591-018-0301-6

Martinez, E. C., Li, J., Ataam, J. A., Tokarski, K., Thakur, H., Karakikes, I., . . . Kapiloff, M. S. (2022). Targeting mAKAPβ expression as a therapeutic approach for ischemic cardiomyopathy. *Gene therapy*. doi:10.1038/s41434-022-00321-w

Martinez-Fong, D., Navarro-Quiroga, I., Ochoa, I., Alvarez-Maya, I., Meraz, M. A., Luna, J., & Arias-Montaño, J. A. (1999). Neurotensin-SPDP-poly-L-lysine conjugate: a nonviral vector for targeted gene delivery to neural cells. *Brain research. Molecular brain research, 69*(2), 249–262. doi:10.1016/s0169-328x(99)00114-x

Mastorakos, P., Kambhampati, S. P., Mishra, M. K., Wu, T., Song, E., Hanes, J., & Kannan, R. M. (2015). Hydroxyl PAMAM dendrimer-based gene vectors for

transgene delivery to human retinal pigment epithelial cells. *Nanoscale, 7*(9), 3845–3856. doi:10.1039/c4nr04284k

Masuda, T., Akita, H., Niikura, K., Nishio, T., Ukawa, M., Enoto, K., . . . Harashima, H. (2009). Envelope-type lipid nanoparticles incorporating a short PEG-lipid conjugate for improved control of intracellular trafficking and transgene transcription. *Biomaterials, 30*(27), 4806–4814. doi:10.1016/j.biomaterials.2009.05.036

Maude, S. L., Frey, N., Shaw, P. A., Aplenc, R., Barrett, D. M., Bunin, N. J., . . . Grupp, S. A. (2014). Chimeric antigen receptor T cells for sustained remissions in leukemia. *The New England journal of medicine, 371*(16), 1507–1517. doi:10.1056/NEJMoa1407222

Mayor, S., & Pagano, R. (2007). Pathways of clathrin-independent endocytosis. *Nature Reviews Molecular Cell Biology, 8*, 603–612. doi:10.1038/nrm2216

McGarrity, G. J., Hoyah, G., Winemiller, A., Andre, K., Stein, D., Blick, G., . . . Rebello , T. (2013). Patient monitoring and follow-up in lentiviral clinical trials. *The journal of gene medicine, 15*(2), 78–82. doi:10.1002/jgm.2691

Merril, C., Geier, M., & Petricciani, J. (1971). Bacterial Virus Gene Expression in Human Cells. *Nature, 233*(5319), pp.398-400.

Mhaidly, R., & Verhoeyen, E. (2019). The Future: In Vivo CAR T Cell Gene Therapy. *Molecular therapy : the journal of the American Society of Gene Therapy, 27*(4), 707–709. doi:10.1016/j.ymthe.2019.03.012

Michi, A. N., & Proud, D. (2021). A toolbox for studying respiratory viral infections using air-liquid interface cultures of human airway epithelial cells. *American journal of physiology. Lung cellular and molecular physiology, 321*(1), L263–L280. doi:10.1152/ajplung.00141.2021

Midoux, P., Breuzard, G., Gomez, J. P., & Pichon, C. (2008). Polymer-based gene delivery: a current review on the uptake and intracellular trafficking of polyplexes. *Current gene therapy, 8*(5), 335–352. doi:10.2174/156652308786071014

Miller, A. J., & Spence, J. R. (2017). In Vitro Models to Study Human Lung Development, Disease and Homeostasis. *Physiology (Bethesda, Md.), 32*(3), 246–260. doi:10.1152/physiol.00041.2016

Milletti , F. (2012). Cell-penetrating peptides: classes, origin, and current landscape. *Drug discovery today, 17*((15-16)), 850–860. doi:10.1016/j.drudis.2012.03.002

Milone, M. C., & O'Doherty, U. (2018). Clinical use of lentiviral vectors. *Leukemia, 32*, 1529–1541. doi:10.1038/s41375-018-0106-0

Mishra, M. K., Beaty, C. A., Lesniak, W. G., Kambhampati, S. P., Zhang, F., Wilson, M. A., . . . Kannan, R. M. (2014). Dendrimer brain uptake and targeted therapy for brain injury in a large animal model of hypothermic circulatory arrest. *ACS nano, 8*(3), 2134–2147. doi:10.1021/nn404872e

Montana, G., Bondi, M. L., Carrotta, R., Picone, P., Craparo, E. F., San Biagio, P. L., . . . Di Carlo, M. (2007). Employment of cationic solid-lipid nanoparticles as

RNA carriers. *Bioconjugate chemistry, 18*(2), 302–308. doi:10.1021/bc0601166

Montoro, D. T., Haber, A. L., Biton, M., Vinarsky, V., Lin, B., Birket, S. E., . . . Rajagopal, J. (2018). A revised airway epithelial hierarchy includes CFTR-expressing ionocytes. *Nature, 560*(7718), 319–324. doi:10.1038/s41586-018-0393-7

Moore, N. M., Sheppard, C. L., & Sakiyama-Elbert, S. E. (2009). Characterization of a multifunctional PEG-based gene delivery system containing nuclear localization signals and endosomal escape peptides. *Acta biomaterialia, 5*(3), 854–864. doi:10.1016/j.actbio.2008.09.009

Moreno, E. L., Hachi, S., Hemmer, K., Trietsch, S. J., Baumuratov, A. S., Hankmeier, T., . . . Fleming, R. M. (2015). Differentiation of neuroepithelial stem cells into functional dopaminergic neurons in 3D microfluidic cell culture. *Lab on a chip, 15*(11), 2419–2428. doi:10.1039/c5lc00180c

Morgan, R., Dudley, M., Wunderlich, J., Hughes, M., Yang, J., Sherry, R., . . . Rosenberg, S. (2006). Cancer Regression in Patients After Transfer of Genetically Engineered Lymphocytes. *Science, 314*(5796), pp.126-129.

Mougiakakos, D., Krönke, G., Völkl, S., Kretschmann, S., Aigner, M., Kharboutli, S., . . . Schett, G. (2021). CD19-Targeted CAR T Cells in Refractory Systemic Lupus Erythematosus. *The New England journal of medicine, 385*(6), 567–569. doi:10.1056/NEJMc2107725

Munis, A. M., Hyde, S. C., & Gill, D. R. (2020). A human surfactant B deficiency air-liquid interface cell culture model suitable for gene therapy applications. *Molecular Therapy Methods and Clinical Development, 20*, 237 - 246. doi:doi.org/10.1016/j.omtm.2020.11.013

Munyon, W., Kraiselburd, E., Davis, D., & Mann, J. (1971). Transfer of Thymidine Kinase to Thymidine Kinaseless L Cells by Infection with Ultraviolet-Irradiated Herpes Simplex Virus. *Journal of Virology, 7*(6), pp.813-820.

Murrah, K., Turner, R., Pang , B., Perez, A., Reimche, J., King, L., . . . Ornelles, D. (2015). Replication of type 5 adenovirus promotes middle ear infection by Streptococcus pneumoniae in the chinchilla model of otitis media. *Pathogens and Disease, 73*(2), 1-8.

Nance, E., Kambhampati, S. P., Smith, E. S., Zhang, Z., Zhang, F., Singh, S., . . . Kannan, S. (2017). Dendrimer-mediated delivery of N-acetyl cysteine to microglia in a mouse model of Rett syndrome. *Journal of neuroinflammation, 14*(1), 252. doi:10.1186/s12974-017-1004-5

Naso, M. F., Tomkowicz, B., Perry, W. L., & Strohl, W. (2017). Adeno-Associated Virus (AAV) as a Vector for Gene Therapy. *Biodrugs*(31), 317-334. doi:10.1007/s40259-017-0234-5

Nassimi, M., Schleh, C., Lauenstein, H., Hussein, R., Hoymann, H., & Koch, W. (2010). A toxicological evaluation of inhaled solid lipid nanoparticles used as a potential drug delivery system for the lung. *European Journal Of Pharmaceutics And Biopharmaceutics, 75*(2), 107-116. doi:10.1016/j.ejpb.2010.02.014

Nathwani, A., Tuddenham, E., Rangarajan, S., Rosales, C., McIntosh, J., Linch, D., . . . Davidoff, A. (2011). Adenovirus-Associated Virus Vector–Mediated Gene Transfer in Hemophilia B. *New England Journal of Medicine, 365*(25), pp.2357-2365.

Nayerossadat, N., Maedeh, T., & Ali, P. A. (2012). Viral and nonviral delivery systems for gene delivery. *Advanced biomedical research, 1*(27). doi:10.4103/2277-9175.98152

Neuhaus, V., Danov, O., Konzok, S., Obernolte, H., Dehmel, S., Braubach, P., . . . Sewald, K. (2018). Assessment of the Cytotoxic and Immunomodulatory Effects of Substances in Human Precision-cut Lung Slices. *Journal Of Visualised Experiments, 57042*(135). doi:https://doi.org/10.3791/57042

Neuhaus, V., Schaudien, D., Golovina, T., Temann, U., Thompson, C., & Lippmann, T. (2017). Assessment of long-term cultivated human precision-cut lung slices as an ex vivo system for evaluation of chronic cytotoxicity and functionality. *Journal Of Occupational Medicine And Toxicology, 12*(1). doi:10.1186/s12995-017-0158-5

Neves, A. R., Albuquerque, T., Faria, R., Paul, M., Biswas, S., Sousa, A., & Costa, D. (2021). Development of Tailor-Made Dendrimer Ternary Complexes for Drug/Gene Co-Delivery in Cancer. *Pharmaceutics, 13*(8), 1256. doi:10.3390/pharmaceutics130

Nichols, J. E., Niles, J. A., Vega, S. P., & Cortiella, J. (2013). Novel in vitro respiratory models to study lung development, physiology, pathology and toxicology. *Stem cell research & therapy, 4 Suppl 1(Suppl 1)*(S7). doi:10.1186/scrt368

Oh, T. K., Li, M. Z., & Kim, S. T. (2006). Gene therapy for diabetes mellitus in rats by intramuscular injection of lentivirus containing insulin gene. *Diabetes research and clinical practice, 71*(3), 233–240. doi:10.1016/j.diabres.2005.08.005

Ong, H. X., Jackson, C. L., Cole, J. L., Lackie, P. M., Traini, D., Young, P. M., . . . Conway, J. (2016). Primary Air-Liquid Interface Culture of Nasal Epithelium for Nasal Drug Delivery. *Molecular pharmaceutics, 13*(7), 2242–2252. doi:10.1021/acs.molpharmaceut.5b00852

Opalinska, J., & Gewirtz, A. (2002). Nucleic-acid therapeutics: basic principles and recent applications. *Nature Reviews Drug Discovery, 1*, 503–514. doi:10.1038/nrd837

Osman, G., Rodriguez, J., Chan, S., Chisolm, J., Duncan, G., Kim, N., . . . Dixon, J. (2018). PEGylated enhanced cell penetrating peptide nanoparticles for lung gene therapy. *Journal Of Controlled Release, 285*, 35-45. doi:10.1016/j.jconrel.2018.07.001

Paolicelli, G., Luca, A., Jose, S. S., Antonini, M., Teloni, I., Fric, J., & Zelante, T. (2019). Using Lung Organoids to Investigate Epithelial Barrier Complexity and IL-17 Signaling During Respiratory Infection. *Frontiers in immunology, 10*(323). doi:10.3389/fimmu.2019.00323

Parayath, N. N., Stephan, S. B., Koehne, A. L., Nelson, P. S., & Stephan, M. T. (2020). In vitro-transcribed antigen receptor mRNA nanocarriers for transient

expression in circulating T cells in vivo. *Nature communications, 11*(1). doi:10.1038/s41467-020-19486-2

Pawliuk, R. (2001). Correction of Sickle Cell Disease in Transgenic Mouse Models by Gene Therapy. *Science, 294*(5550), pp.2368-2371.

Pedersen, N., Hansen, S., Heydenreich, A. V., Kristensen, H. G., & Poulsen, H. S. (2006). Solid lipid nanoparticles can effectively bind DNA, streptavidin and biotinylated ligands. *European journal of pharmaceutics and biopharmaceutics, 62*(2), 155–162. doi:10.1016/j.ejpb.2005.09.003

Perry, L., Penny-Dimri, J., Aslam, A., Lee, T., & Southern, K. (2017). Topical cystic fibrosis transmembrane conductance regulator gene replacement for cystic fibrosis-related lung disease. *Paediatric Respiratory Reviews, 22*, pp.47-49.

Petrosyan, A., Cravedi, P., & Villani, V. (2019). A glomerulus-on-a-chip to recapitulate the human glomerular filtration barrier. *Nature Communications, 10*(3656). doi:10.1038/s41467-019-11577-z

Piao, L., Li, H., Teng, L., Yung, B. C., Sugimoto, Y., Brueggemeier, R. W., & Lee, R. J. (2013). Human serum albumin-coated lipid nanoparticles for delivery of siRNA to breast cancer. *Nanomedicine : nanotechnology, biology, and medicine, 9*(1), 122–129. doi:10.1016/j.nano.2012.03.008

Plebani, R., Potla, R., Soong, M., Bai, H., Izadifar, Z., Jiang, A., . . . Ingber, D. E. (2021). Modeling pulmonary cystic fibrosis in a human lung airway-on-a-chip: Cystic fibrosis airway chip. *Journal of cystic fibrosis : official journal of the European Cystic Fibrosis Society*, S1569-1993(21)02106-8. doi:10.1016/j.jcf.2021.10.004

Plénat, T., DeShayes, S., Boichot, S., Milhiet, P. E., Cole, R. B., Heitz, F., & Le Grimellec, C. (2004). Interaction of primary amphipathic cell-penetrating peptides with phospholipid-supported monolayers. *Langmuir : the ACS journal of surfaces and colloids, 20*(21), 9255–9261. doi:10.1021/la048622b

Porter, D., Levine, B., Kalos, M., Bagg, A., & June, C. (2011). Chimeric Antigen Receptor–Modified T Cells in Chronic Lymphoid Leukemia. *New England Journal of Medicine, 365*(8), pp.725-733.

Power, R. N., Cavanagh, B. L., Dixon, J. E., Curtin, C. M., & O'Brien, F. J. (2022). Development of a Gene-Activated Scaffold Incorporating Multifunctional Cell-Penetrating Peptides for pSDF-1α Delivery for Enhanced Angiogenesis in Tissue Engineering Applications. *International journal of molecular sciences, 23*(3). doi:10.3390/ijms23031460

Prulière-Escabasse, V., Fanen, P., Dazy, A. C., Lechapt-Zalcman, E., Rideau, D., Edelman, A., . . . Coste, A. (2005). TGF-beta 1 downregulates CFTR expression and function in nasal polyps of non-CF patients. *American journal of physiology. Lung cellular and molecular physiology, 288*(1). doi:10.1152/ajplung.00048.2004

Raemy, D. O., Grass, R. N., Stark, W. J., Schumacher, C. M., Clift, M. J., Gehr, P., & Rothen-Rutishauser, B. (2012). Effects of flame made zinc oxide particles in human lung cells - a comparison of aerosol and suspension exposures. *Particle and fibre toxicology, 9*(33). doi:doi.org/10.1186/1743-8977-9-33

Rai, R., Alwani, S., & Badea, I. (2019). Polymeric Nanoparticles in Gene Therapy: New Avenues of Design and Optimization for Delivery Applications. *Polymers, 11*(4). doi:10.3390/polym11040745

Ramishetti, S., Kedmi, R., Goldsmith, M., Leonard, F., Sprague, A. G., Godin, B., . . . Peer, D. (2015). Systemic Gene Silencing in Primary T Lymphocytes Using Targeted Lipid Nanoparticles. *ACS nano, 9*(7), 6706–6716. doi:10.1021/acsnano.5b02796

Rancan, F., Papakostas, D., Hadam, S., Hackbarth, S., Delair, T., Primard, C., . . . Vogt, A. (2009). Investigation of polylactic acid (PLA) nanoparticles as drug delivery systems for local dermatotherapy. *Pharmaceutical research, 26*(8), 2027–2036. doi:10.1007/s11095-009-9919-x

Rayner, R. E., Makena, P., Prasad, G. L., & Cormet-Boyaka, E. (2019). Optimization of Normal Human Bronchial Epithelial (NHBE) Cell 3D Cultures for in vitro Lung Model Studies. *Scientific Reports, 9*(500). doi:10.1038/s41598-018-36735-z

Reddy, V., Natchiar, S., Stewart, P., & Nemerow, G. (2010). Crystal Structure of Human Adenovirus at 3.5 A Resolution. *Science, 329*(5995), 1071-1075. doi:10.1126/science.1187292

Reissmann, S. (2014). Cell penetration: scope and limitations by the application of cell-penetrating peptides. *Journal of peptide science : an official publication of the European Peptide Society, 20*(10), 760–784. doi:10.1002/psc.2672

Ressmeyer, A., Larsson, A., Vollmer, E., Dahlen, S., Ulhig, S., & Martin, C. (2006). Characterisation of guinea pig precision-cut lung slices: comparison with human tissues. *European Respiratory Journal, 28*(3), 603-611. doi:10.1183/09031936.06.0000420

Rizvi, S., & Saleh, A. M. (2018). Applications of nanoparticle systems in drug delivery technology. *Saudi pharmaceutical journal : SPJ : the official publication of the Saudi Pharmaceutical Society, 26*(1), 64–70. doi:10.1016/j.jsps.2017.10.012

Rosales Gerpe, M., Van Vloten, J., Santry, L., De Jong, J., Mould, R., & Pelin, A. (2018). Use of Precision-Cut Lung Slices as an Ex Vivo Tool for Evaluating Viruses and Viral Vectors for Gene and Oncolytic Therapy. *Molecular Therapy - Methods & Clinical Development, 10*, 245-256. doi:10.1016/j.omtm.2018.07.010

Rosner, S. R., Ram-Mohan, S., Paez-Cortez, J. R., Lavoie, T. L., Dowell, M. L., Yuan, L., . . . Krishnan, R. (2014). Airway Contractility in the Precision-Cut Lung Slice after Cryopreservation. *American Journal of Respiratory Cell and Molecular Biology, 50*(5), 876 - 881. doi:doi:10.1165/rcmb.2013-0166MA

Rowe, W., Huebner, R., Gilmore, L., Parrott, R., & Ward, T. (1953). Isolation of a Cytopathogenic Agent from Human Adenoids Undergoing Spontaneous Degeneration in Tissue Culture. *Experimental Biology And Medicine, 84*(3), 570-573. doi:10.3181/00379727-84-20714

Roybal, J. L., Endo, M., Radu, A., Zoltick, P. W., & Flake, A. W. (2011). Early gestational gene transfer of IL-10 by systemic administration of lentiviral

vector can prevent arthritis in a murine model. *Gene therapy, 18*(7), 719–726. doi:10.1038/gt.2011.23

Rudolph, C., Lausier, J., Naundorf, S., Muller, R. H., & Rosenecker, J. (2000). In vivo gene delivery to the lung using polyethylenimine and fractured polyamidoamine dendrimers. *The journal of gene medicine, 2*(4), 269–278. doi:10.1002/1521-2254(200007/08)2:4<269::AID-JGM112>3.0.CO;2-F

Ruuskanen, O., Mertsola, J., & Meurman, O. (1988). Adenovirus infection in families. *Archives Of Disease In Childhood, 63*(10), 1250-1253. doi:10.1136/adc.63.10.1250

Sadoff, J., Struyf, F., & Douoguih, M. (2021). A plain language summary of how well the single-dose Janssen vaccine works and how safe it is. *Future virology, 16*(11), 725–739. doi:10.2217/fvl-2021-0199

Sainz-Ramos, M., Gallego, I., Villate-Beitia, I., Zarate, J., Maldonado, I., Puras, G., & Pedraz, J. L. (2021). How Far Are Non-Viral Vectors to Come of Age and Reach Clinical Translation in Gene Therapy? *International journal of molecular sciences, 22*(14), 7545. doi:10.3390/ijms22147545

Sakagami, M. (2006). In vivo, in vitro and ex vivo models to assess pulmonary absorption and disposition of inhaled therapeutics for systemic delivery. *Advanced drug delivery reviews, 58*(9-10), 1030–1060. doi:10.1016/j.addr.2006.07.012

Sakalem, M. E., De Sibio, M. T., da Costa, F., & de Oliveira, M. (2021). Historical evolution of spheroids and organoids, and possibilities of use in life sciences and medicine. *Biotechnology journal, 16*(5), e2000463. doi:10.1002/biot.202000463

Salahudeen, A. A., Choi, S. S., Rustagi, A., Zhu, J., de la, O. S., Flynn, R. A., . . . Kuo, C. J. (2020). Progenitor identification and SARS-CoV-2 infection in long-term human distal lung organoid cultures. *bioRxiv : the preprint server for biology*. doi:2020.07.27.212076

Salgueiro, L., Kummer, S., Sonntag-Buck, V., Weiß, A., Schneider, M. A., Kräusslich, H. G., & Sotillo, R. (2022). Generation of Human Lung Organoid Cultures from Healthy and Tumor Tissue to Study Infectious Diseases. *Journal of virology*. doi:10.1128/jvi.00098-22

Samulski, R. J., Zhu, X., Xiao, X., Brook, J. E., Housman, D. E., Epstein, N., & Hunter, L. A. (1992). Targeted integration of adeno-associated virus (AAV) into human chromosome 19. *The EMBO Journal, 10*(12), 3941–3950.

Sanderson, M. (2011). Exploring lung physiology in health and disease with lung slices. *Pulmonary Pharmacology & Therapeutics, 24*(5), 452-465. doi:10.1016/j.pupt.2011.05.001

Sangamo Therapeutics. (2017). *https://clinicaltrials.gov/ct2/show/NCT03041324.* Retrieved from Clinicaltrials.gov.

Santos-Carballal, B., Fernández Fernández, E., & Goycoolea, F. (2018). Chitosan in Non-Viral Gene Delivery: Role of Structure, Characterization Methods, and Insights in Cancer and Rare Diseases Therapies. *Polymers, 10*(4), 444. doi:10.3390/polym10040444

Schlimgen, R., Howard, J., Wooley, D., Thompson, M., Baden, L. R., Yang, O. O., . . . Vyas, J. M. (2016). Risks Associated With Lentiviral Vector Exposures and Prevention Strategies. *Journal of occupational and environmental medicine, 58*(12), 1159–1166. doi:10.1097/JOM.0000000000000879

Schmid, O., Jud, C., Umehara, Y., Mueller, D., Bucholski, A., Gruber, F., . . . Rothen-Rutishauser, B. (2017). Biokinetics of Aerosolized Liposomal Ciclosporin A in Human Lung Cells In Vitro Using an Air-Liquid Cell Interface Exposure System. *Journal of aerosol medicine and pulmonary drug delivery, 30*(6), 411–424. doi:0.1089/jamp.2016.1361

Seehase, S., Lauenstein, H., Schlumbohm, C., Switalla, S., Neuhaus, V., & Förster, C. (2012). LPS-Induced Lung Inflammation in Marmoset Monkeys – An Acute Model for Anti-Inflammatory Drug Testing. *Plos ONE, 7*(8). doi:10.1371/journal.pon

Sessa, M., Lorioli, L., Fumagalli, F., Acquati, S., Redaelli, D., Baldoli, C., . . . Biffi, A. (2016). Lentiviral haemopoietic stem-cell gene therapy in early-onset metachromatic leukodystrophy: an ad-hoc analysis of a non-randomised, open-label, phase 1/2 trial. *Lancet, 388*(10043), 476–487. doi:10.1016/S0140-6736(16)30374-9

Severino, P., Szymanski, M., Favaro, M., Azzoni, A. R., Chaud, M. V., Santana, M. H., . . . Souto, E. B. (2015). Development and characterization of a cationic lipid nanocarrier as non-viral vector for gene therapy. *European journal of pharmaceutical sciences : official journal of the European Federation for Pharmaceutical Sciences, 66*, 78–82. doi:10.1016/j.ejps.2014.09.021

Shabalina, E. Y., Skorova, E. Y., Chudakova, D. A., Anikin, V. B., Reshetov, I. V., Mynbaev, O. A., & Petersen, E. V. (2021). The matrix-dependent 3D spheroid model of the migration of non-small cell lung cancer: a step towards a rapid automated screening. *Frontiers in Molecular Biosciences, 8*. doi:10.3389/fmolb.2021.610407

Shah, N. N., Johnson, B. D., Schneider, D., Zhu, F., Szabo, A., Keever-Taylor, C. A., . . . Hari, P. (2020). Bispecific anti-CD20, anti-CD19 CAR T cells for relapsed B cell malignancies: a phase 1 dose escalation and expansion trial. *Nature medicine, 26*(10), 1569–1575. doi:10.1038/s41591-020-1081-3

Shi, Q., Wilcox, D. A., Fahs, S. A., Fang, J., Johnson, B. D., DU, L. M., . . . Montgomery, R. R. (2007). Lentivirus-mediated platelet-derived factor VIII gene therapy in murine haemophilia A. *Journal of thrombosis and haemostasis, 5*(2), 352–361. doi:10.1111/j.1538-7836.2007.02346.x

Si, L., Bai, H., Rodas, M., Cao, W., Oh, C. Y., Jiang, A., . . . Ingber, D. E. (2021). A human-airway-on-a-chip for the rapid identification of candidate antiviral therapeutics and prophylactics. *Nature Biomedical Engineering, 5*, 815–829. doi:10.1038/s41551-021-00718-9

Si, L., Bai, H., Rodas, M., Cao, W., Oh, C. Y., Jiang, A., . . . Ingber, D. E. (2021). A human-airway-on-a-chip for the rapid identification of candidate antiviral therapeutics and prophylactics. *Nature biomedical engineering, 5*(8), 815–829. doi:10.1038/s41551-021-00718-9

Sia, K. C., Gan, S. U., Mohd Rodhi, S. H., Fu, Z. Y., Kopchick, J. J., Waters, M. J., & Lee, K. O. (2022). First use of gene therapy to treat growth hormone resistant dwarfism in a mouse model. *Gene therapy*. doi:10.1038/s41434-022-00313-w

Simonelli, F., Maguire, A., Testa, F., Pierce, E., Mingozzi, F., Bennicelli, J., . . . Auricchio, A. (2010). Gene Therapy for Leber's Congenital Amaurosis is Safe and Effective through 1.5 Years after Vector Administration. *Molecular Therapy, 18*(3), pp.643-650.

Singh, B. N., Prateeksha, , Gupta, V. K., Chen, J., & Atanasov, A. G. (2017). Organic Nanoparticle-Based Combinatory Approaches for Gene Therapy. *Trends in biotechnology, 35*(12), 1121–1124. doi:10.1016/j.tibtech.2017.07.010

Sirianni, Q., Wang, T., Borecki, A., Deng, Z., Ronald, J. A., & Gillies, E. R. (2022). Self-immolative polyplexes for DNA delivery. *Biomaterials science*. doi:10.1039/d1bm01684a

Slepushkin, V. A., Staber, P. D., Wang, G., McCray, P. B., & Davidson, B. L. (2001). Infection of human airway epithelia with H1N1, H2N2, and H3N2 influenza A virus strains. *Molecular therapy : the journal of the American Society of Gene Therapy, 3*(3). doi:doi.org/10.1006/mthe.2001.0277

Slita, A., Egorova, A., Casals, E., Kiselev, A., & Rosenholm, J. M. (2018). Characterization of modified mesoporous silica nanoparticles as vectors for siRNA delivery. *Asian journal of pharmaceutical sciences, 13*(6), 592–599. doi:10.1016/j.ajps.2018.01.006

Smith, C., Lake, A., & Johnson, C. A. (2020). Primary Cilia, Ciliogenesis and the Actin Cytoskeleton: A Little Less Resorption, A Little More Actin Please. *Frontiers in cell and developmental biology, 8*. doi:10.3389/fcell.2020.622822

Song, H., Wang, G., He, B., Li, L., Li, C., Lai, Y., . . . Gu, Z. (2012). Cationic lipid-coated PEI/DNA polyplexes with improved efficiency and reduced cytotoxicity for gene delivery into mesenchymal stem cells. *International journal of nanomedicine, 7*, 4637–4648. doi:10.2147/IJN.S33923

Song, M. J., Davidovich, N., Lawrence, G. G., & Margulies, S. S. (2016). Superoxide mediates tight junction complex dissociation in cyclically stretched lung slices. *Journal of biomechanics, 49*(8), 1330–1335. doi:doi.org/10.1016/j.jbiomech.2015.10.032

Souer, M., Woulters, A., de Saint-Georges, A., Content, J., & Depierreux, M. (1991). Meningoencephalitis and meningitis due to an adenovirus type 5 in two immunocompetent adults. *Acta Neurologica Belgica, 91*(3), 141 - 150.

Sousa de Almeida, M., Taladriz-Blanco, P., Drasler, B., Balog, S., Yajan, P., Petri-Fink, A., & Rothen-Rutishauser, B. (2022). Cellular Uptake of Silica and Gold Nanoparticles Induces Early Activation of Nuclear Receptor NR4A1. *Nanomaterials, 12*(4). doi:10.3390/nano12040690

Srinivasan, B., Kolli, A. R., Esch, M. B., Abaci, H. E., Schuler, M. L., & Hickman, J. J. (2015). TEER measurement techniques for in vitro barrier model systems. *Journal of laboratory automation, 20*(2), 107–126. doi:10.1177/2211068214561025

Straussberg, R., Harel, L., Levy, Y., & Amir, J. (2001). A Syndrome of Transient Encephalopathy Associated With Adenovirus Infection. *Pediatrics, 107*(5). doi:10.1542/peds.107.5.e69

Stucki, J. D., Hobi, N., Galimov, A., Stucki, A. O., Schneider-Daum, N., Lehr, C. M., . . . Guenat, O. T. (2018). Medium throughput breathing human primary cell alveolus-on-chip model. *Scientific reports, 8*(1). doi:10.1038/s41598-018-32523-x

Switalla, S., Knebel, J., Ritter, D., Krug, N., Braun, A., & Sewald, K. (2010). Effects of acute in vitro exposure of murine precision-cut lung slices to gaseous nitrogen dioxide and ozone in an air–liquid interface (ALI) culture. *Toxicology Letters, 196*(2), 117-124. doi:10.1016/j.toxlet.2010.04.004

Tabernero, J., Shapiro, G. I., LoRusso, P. M., Cervantes, A., Schwartz, G. K., Weiss, G. J., . . . Burris, H. A. (2013). First-in-humans trial of an RNA interference therapeutic targeting VEGF and KSP in cancer patients with liver involvement. *Cancer discovery, 3*(4), 406–417. doi:10.1158/2159-8290.CD-12-0429

Tajer, P., Pike-Overzet, K., Sagrario, A., Havenga, M., & Staal, F. J. (2019). Ex Vivo Expansion of Hematopoietic Stem Cells for Therapeutic Purposes: Lessons from Development and the Niche. *Cells, 8*(169). doi:10.3390/cells8020169

Tan, Q., Choi, K. M., Sicard, D., & Tschumperlin, D. J. (2017). Human airway organoid engineering as a step toward lung regeneration and disease modelling. *Biomaterials, 113*, 118–132. doi:10.1016/j.biomaterials.2016.10.046

Tarahovsky, Y. S., Koynova, R., & MacDonald, R. C. (2004). DNA release from lipoplexes by anionic lipids: correlation with lipid mesomorphism, interfacial curvature, and membrane fusion. *Biophysical journal, 87*(2), 1054–1064. doi:10.1529/biophysj.104.042895

Temann, A., Golovina, T., Neuhaus, V., Thompson, C., Chicester, J. A., Braun, A., & Yusibov, V. (2017). Evaluation of inflammatory and immune resposnse in long -term cultured human precison-cut lung slices. *Human Vaccines and Immunotherapeutics, 13*(2), 351 - 258. doi:dx.doi.org/10.1080/21645515.2017.1264794

Themis, M., Waddington, S. N., Schmidt, M., von Kalle, C., Wang, Y., Al-Allaf, F., . . . Thrasher, A. (2005). Oncogenesis following delivery of a nonprimate lentiviral gene therapy vector to fetal and neonatal mice. *Molecular therapy : the journal of the American Society of Gene Therapy, 12*(4), 763–771. doi:10.1016/j.ymthe.2005.07.358

Thomas, C., Ehrhardt, A., & Kay, M. (2003). Progress and problems with the use of viral vectors for gene therapy. *Nature Reviews Genetics, 4*(5), 346-358. doi:10.1038/nrg1066

Thompson, A. A., Walters, M. C., Kwiatkowski, J., Rasko, J., Ribeil, J. A., Hongeng, S., . . . Cavazzana, M. (2018). Gene Therapy in Patients with Transfusion-Dependent β-Thalassemia. *The New England journal of medicine, 378*(16), 1479–1493. doi:10.1056/NEJMoa1705342

Tindle, C., Fuller, M., Fonseca, A., Taheri, S., Ibeawuchi, S. R., Beutler, N., . . . Das, S. (2021). Adult Stem Cell-derived Complete Lung Organoid Models Emulate Lung Disease in COVID-19. *bioRxiv : the preprint server for biology*. doi:10.1101/2020.10.17.344002

Trabulo, S., Cardoso, A. L., Mano, M., & De Lima, M. C. (2010). Cell-Penetrating Peptides-Mechanisms of Cellular Uptake and Generation of Delivery Systems. *Pharmaceuticals (Basel, Switzerland), 3*(4), 961–993. doi:10.3390/ph3040961

Troelnikov, A., Perkins, G., Yuson, C., Ahamdie, A., Balouch, S., Hurtado, P. R., & Hissaria, P. (2021). Basophil reactivity to BNT162b2 is mediated by PEGylated lipid nanoparticles in patients with PEG allergy. *The Journal of allergy and clinical immunology, 148*(1), 91–95. doi:10.1016/j.jaci.2021.04.032

Trojan, J., Johnson, T., Rudin, S., Ilan, J., & Tykocinski, M. (1993). Treatment and prevention of rat glioblastoma by immunogenic C6 cells expressing antisense insulin-like growth factor I RNA. *Science, 259*(5091), pp.94-97.

Trojan, J., Pan, Y., Wei , M., Ly, A., Shevelev, A., Bierwagen, M., . . . Alvarez, A. (2012). Methodology for Anti-Gene Anti-IGF-I Therapy of Malignant Tumours. *Chemotherapy Research and Practice*, pp.1-12.

Trubetskoy, V. S., Torchilin, V. P., Kennel, S. J., & Huang, L. (1992). Use of N-terminal modified poly(L-lysine)-antibody conjugate as a carrier for targeted gene delivery in mouse lung endothelial cells. *Bioconjugate chemistry, 3*(4), 323–327. doi:10.1021/bc00016a011

Tünnemann, G., Martin, R. M., Haupt, S., Patsch, C., Edenhofer, F., & Cardoso, M. C. (2006). Cargo-dependent mode of uptake and bioavailability of TAT-containing proteins and peptides in living cells. *FASEB journal : official publication of the Federation of American Societies for Experimental Biology, 20*(11), 1775–1784. doi:10.1096/fj.05-5523com

U.S. Congress, Office of Technology Assessment. (1984). *Human gene therapy – A background paper (OTA-BP-BA-32).* Washington, DC.

Uchida, N., Drysdale, C. M., Nassehi, T., Gamer, J., Yapundich, M., DiNicola, J., . . . Tisdale, J. F. (2021). Cas9 protein delivery non-integrating lentiviral vectors for gene correction in sickle cell disease. *Molecular therapy. Methods & clinical development, 21*, 121–132. doi:10.1016/j.omtm.2021.02.022

Upadhyay, S., & Palmberg, L. (2018). Air-Liquid Interface: Relevant In Vitro Models for Investigating Air Pollutant-Induced Pulmonary Toxicity. *Toxicological sciences : an official journal of the Society of Toxicology, 164*(1), 21–30. doi:doi.org/10.1093/toxsci/kfy053

Vander, J. (2009). Safety and Efficacy of Gene Transfer for Leber's Congenital Amaurosis. *Yearbook of Ophthalmology*, pp.136-137.

Verghese, S. C., Goloviznina, N. A., Skinner, A. M., Lipps, H. J., & Kurre, P. (2014). S/MAR sequence confers long-term mitotic stability on non-integrating lentiviral vector episomes without selection. *Nucleic acids research, 42*(7). doi:10.1093/nar/gku082

Viana, F., O'Kane, C. M., & Schroeder, G. N. (2021). Precision-cut lung slices: A powerful ex vivo model to investigate respiratory infectious diseases. *Molecular microbiology*. doi:10.1111/mmi.14817

Vitor, M. T., Bergami-Santos, P. C., Barbuto, J. A., & de la Torre, L. G. (2013). Cationic liposomes as non-viral vector for RNA delivery in cancer immunotherapy. *Recent patents on drug delivery & formulation, 7*(2), 99–110. doi:10.2174/18722113113079990010

Vives, E., Brodin, P., & Lebleu, B. (1997). A truncated HIV-1 Tat protein basic domain rapidly translocates through the plasma membrane and accumulates in the cell nucleus. *The Journal of biological chemistry, 272*(25), 16010–16017. doi:10.1074/jbc.272.25.16010

Vogel, A. B., Kanevsky, I., Che, Y., Swanson, K. A., Muik, A., Vormehr, M., . . . Sahin, U. (2021). BNT162b vaccines protect rhesus macaques from SARS-CoV-2. *Nature, 592*(7853), 283–289. doi:10.1038/s41586-021-03275-y

Wan, T., Pan, Q., Liu, C., Guo, J., Li, B., Yan, X., . . . Ping, Y. (2021). A Duplex CRISPR-Cas9 Ribonucleoprotein Nanomedicine for Colorectal Cancer Gene Therapy. *Nano letters, 21*(22), 9761–9771. doi:10.1021/acs.nanolett.1c03708

Wang, J., Zhao, L., Gu, X., Xue, Y., Wang, S., Xiao, R., . . . Li, H. (2022). Efficient delivery of adeno-associated virus (AAV) into inner ear in vivo via trans-stapes route in adult guinea pig. *Human gene therapy*. doi:10.1089/hum.2021.236

Wang, T., Larcher, L. M., Ma, L., & Veedu, R. N. (2018). Systematic Screening of Commonly Used Commercial Transfection Reagents towards Efficient Transfection of Single-Stranded Oligonucleotides. *Molecules, 23*(10), 2564. doi:10.3390/molecules23102564

Weber, N., Ortega, P., Clemente, M. I., Shcharbin, D., Bryszewska, M., de la Mata, F. J., . . . Munoz-Fernandez, M. A. (2008). Characterization of carbosilane dendrimers as effective carriers of siRNA to HIV-infected lymphocytes. *Journal of controlled release, 132*(1), 55–64. doi:10.1016/j.jconrel.2008.07.035

Wold, W., & Toth, K. (2014). Adenovirus Vectors for Gene Therapy, Vaccination and Cancer Gene Therapy. *Current Gene Therapy, 13*(6), 421-433. doi:10.2174/1566523213666131125095046

Wong, J., Mohseni, R., Hamidieh, A. A., MacLaren, R. E., Habib, N., & Seifalian, A. M. (2017). Limitations in Clinical Translation of Nanoparticle-Based Gene Therapy. *Trends in biotechnology, 35*(12), 1124–1125. doi:10.1016/j.tibtech.2017.07.009

Wong, K., Sung, G., Zhang, X., Dai, H., Liu, Y., He, C., & Leong, K. W. (2006). PEI-g-chitosan, a novel gene delivery system with transfection efficiency comparable to polyethylenimine in vitro and after liver administration in vivo. *Bioconjugate chemistry, 17*(1), 152–158. doi:10.1021/bc0501597

Wood, K. C., Azarin, S. M., Arap, W., Pasqualini, R., Langer, R., & Hammond, P. T. (n.d.). Tumor-targeted gene delivery using molecularly engineered hybrid

polymers functionalized with a tumor-homing peptide. *Bioconjugate chemistry, 19*(2), 403–405. doi:10.1021/bc700408r

Wu, N., Li, M., Chen, Z. T., Zhang, X. B., Liu, H. Z., Li, Z., . . . Yang, S. M. (2013). In vivo delivery of Atoh1 gene to rat cochlea using a dendrimer-based nanocarrier. *Journal of biomedical nanotechnology, 9*(10), 1736–1745. doi:10.1166/jbn.2013.1684

Wu, S. Y., & McMillan, N. A. (2009). Lipidic systems for in vivo siRNA delivery. *The AAPS journal, 11*(4), 639–652. doi:10.1208/s12248-009-9140-1

Wu, W., Booth, J., Duggan, E., Wu, S., Patel, K., Coggeshall, K., & Metcalf, J. (2010). Innate immune response to H3N2 and H1N1 influenza virus infection in a human lung organ culture model. *Virology, 396*(2), 178-188. doi:10.1016/j.virol.2009.10.016

Wu, X., Van Dijk, E., Bos, I., Kistemaker, L., & Gosens, R. (2019). Mouse Lung Tissue Slice Culture. *Methods In Molecular Biology,*, 297-311. doi:10.1007/978-1-4939-9086-3_21

Wu, Z., Yang, H., & Colosi, P. (2010). Effect of Genome Size on AAV Vector Packaging. *Molecular Therapy, 18*(1), 80-86. doi:10.1038/mt.2009.255

Xiao, S., Castro, R., Rodrigues, J., Shi, X., & Tomas, H. (2015). PAMAM Dendrimer/pDNA Functionalized-Magnetic Iron Oxide Nanoparticles for Gene Delivery. *Journal of biomedical nanotechnology, 11*(8), 1370–1384. doi:10.1166/jbn.2015.2101

Xin, T., Cheng, L., Zhou, C., Zhao, Y., Hu, Z., & Wu, X. (2022). In-Vivo Induced CAR-T Cell for the Potential Breakthrough to Overcome the Barriers of Current CAR-T Cell Therapy. *Frontiers in oncology, 12*(809754). doi:10.3389/fonc.2022.809754

Xu, Q., Boylan, N. J., Cai, S., Miao, B., Patel, H., & Hanes, J. (2013). Scalable method to produce biodegradable nanoparticles that rapidly penetrate human mucus. *Journal of controlled release : official journal of the Controlled Release Society, 170*(2), 279–286. doi:10.1016/j.jconrel.2013.05.035

Xu, Z., Chen, F., Zhang, L., Lu, J., Xu, P., Liu, G., . . . Liu, D. (2016). Non-integrating lentiviral vectors based on the minimal S/MAR sequence retain transgene expression in dividing cells. *Science China. Life sciences, 59*(10), 1024–1033. doi:10.1007/s11427-016-0067-0

Yaghi, A., & Dolovich, M. B. (2016). Airway Epithelial Cell Cilia and Obstructive Lung Disease. *Cells, 5*(4). doi:10.3390/cells5040040

Yamashita, M., & Emerman, M. (2004). Capsid is a dominant determinant of retrovirus infectivity in nondividing cells. *Journal of virology, 78*(11), 5670–5678. doi:10.1128/JVI.78.11.5670-5678.2004

Yu, W., Liu, C., Liu, Y., Zhang, N., & Xu, W. (2010). Mannan-modified solid lipid nanoparticles for targeted gene delivery to alveolar macrophages. *Pharmaceutical research, 27*(8), 1584–1596. doi:10.1007/s11095-010-0149-z

Yu, Z., Zeng, Z., Zhang, J., Pan, Y., Chen, M., Guo, Y., . . . Zhang, Q. (2016). Fatal Community-acquired Pneumonia in Children Caused by Re-emergent Human

Adenovirus 7d Associated with Higher Severity of Illness and Fatality Rate. *Scientific Reports, 6*(1). doi:10.1038/srep37216

Zhang, C., Zhao, Z., Abdul Rahim, N. A., van Noort, D., & Yu, H. (2009). Towards a human-on-chip: culturing multiple cell types on a chip with compartmentalized microenvironments. *Lab on a chip, 9*(22), 3185–3192. doi:10.1039/b915147h

Zhang, H., Zhao, P., & Huang, H. (2020). Engineering better chimeric antigen receptor T cells. *Experimental Hematology and Oncology, 9*(34). doi:10.1186/s40164-020-00190-2

Zhang, K. X., Moussavi, M., Kim, C., Chow, E., Chen, I. S., Fazli, L., . . . Rennie, P. S. (2009). Lentiviruses with trastuzumab bound to their envelopes can target and kill prostate cancer cells. *Cancer gene therapy, 16*(11), 820–831. doi:10.1038/cgt.2009.28

Zhang, Y., Boado, R., & Pardridge, W. (2003). In vivo knockdown of gene expression in brain cancer with intravenous RNAi in adult rats. *The Journal of Gene Medicine, 5*(12), pp.1039-1045.

Zhao, M. D., Cheng, J. L., Yan, J. J., Chen, F. Y., Sheng, J. Z., Sun, D. L., . . . Huang, H. F. (2016). Hyaluronic acid reagent functional chitosan-PEI conjugate with AQP2-siRNA suppressed endometriotic lesion formation. *International journal of nanomedicine, 11*, 1323–1336. doi:10.2147/IJN.S99692

Zhu, K., Dobard, C., & Chow, S. A. (2004). Requirement for integrase during reverse transcription of human immunodeficiency virus type 1 and the effect of cysteine mutations of integrase on its interactions with reverse transcriptase. *Journal of virology, 78*(10), 5045–5055. doi:10.1128/jvi.78.10.5045-5055.2004

Zhu, Y., Yue, M., Guo, T., Li, F., Li, Z., Yang, D., & Lin, M. (2021). PEI-PEG-Coated Mesoporous Silica Nanoparticles Enhance the Antitumor Activity of Tanshinone IIA and Serve as a Gene Transfer Vector. *Evidence-based complementary and alternative medicine : eCAM, 6756763*. doi:10.1155/2021/6756763